NOTICE

AVIS

The quality of this microform is heavily dependent upon the quality of the original thesis submitted for microfilming. Every effort has been made to ensure the highest quality of reproduction possible.

La qualité de cette microforme dépend grandement de la qualité de la thèse soumise au microfilmage. Nous avons tout fait pour assurer une qualité supérieure de reproduction.

If pages are missing, contact the university which granted the degree.

S'il manque des pages, veuillez communiquer avec l'université qui a conféré le grade.

Some pages may have indistinct print especially if the original pages were typed with a poor typewriter ribbon or if the university sent us an inferior photocopy.

La qualité d'impression de certaines pages peut laisser à désirer, surtout si les pages originales ont été dactylographiées à l'aide d'un ruban usé ou si l'université nous a fait parvenir une photocopie de qualité inférieure.

Canada

HORIZONTAL WELL TESTING IN COMPOSITE RESERVOIRS

BY

KHANI GHAFFARI   ©

A THESIS

SUBMITTED TO THE FACULTY OF GRADUATE STUDIES AND RESEARCH IN

PARTIAL FULFILMENT OF THE REQUIREMENTS FOR THE DEGREE OF

MASTER OF SCIENCE

IN

PETROLEUM ENGINEERING

DEPARTMENT OF MINING, METALLURGICAL AND PETROLEUM

ENGINEERING

EDMONTON, ALBERTA

SPRING, 1995

ISBN 0-612-01608-0

Canada

UNIVERSITY OF ALBERTA

RELEASE FORM

NAME OF AUTHOR: Khani Ghaffari

TITLE OF THESIS: Horizontal Well Testing in Composite
                                    Reservoirs

DEGREE FOR WHICH THESIS WAS PRESENTED: MASTER OF SCIENCE

YEAR THE DEGREE WAS GRANTED: SPRING, 1995

Permission is hereby granted to THE UNIVERSITY OF ALBERTA LIBRARY to
reproduce single copies of this thesis and to lend or sell such copies for private, scholarly
or scientific research purposes only.

The author reserves publication rights, and neither the thesis nor extensive extracts from it
may be printed or otherwise reproduced without the author's written permission.

(SIGNED)-

PERMANENT ADDRESS:

Bikhak, Jarough

Kazeroon, IRAN

DATED: November 24, 1994

THE UNIVERSITY OF ALBERTA

FACULTY OF GRADUATE STUDIES AND RESEARCH
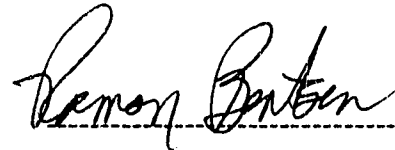
The undersigned certify that they have read, and recommend to the Faculty of Graduate Studies and Research for acceptance, a thesis entitled "HORIZONTAL WELL TESTING IN COMPOSITE RESERVOIRS" submitted by KHANI GHAFFARI in partial fulfillment of the requirements for the degree of MASTER OF SCIENCE in PETROLEUM ENGINEERING.
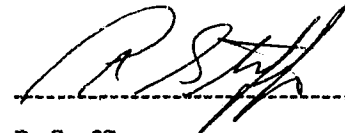
A. K. Ambastha (Supervisor)

K. Barron

R. G. Bentsen

P. Steffler

DATED: November 17, 1994

DEDICATION

This thesis is dedicated to the memory of those political prisoners in Iran who lost their lives during the **"National Tragedy"** in 1988. It is also dedicated to those political prisoners who were incarcerated and tortured because they spoke up against the intolerant policies implemented by the fundamentalist regime, currently governing Iran.

ABSTRACT

Horizontal wells are becoming popular for primary and enhanced oil recovery operations because of their unique advantages over vertical wells. Some of these advantages are improved sweep efficiency, effective use of gravity drainage, less severe coning problems and higher productivity. Steam injection through horizontal wells has also been attempted at several places to improve heavy oil recovery. However, well test analysis for horizontal wells under steam injection is still in its infancy. For a horizontal well undergoing steam injection, a steam chamber containing high mobility steam is established. This steam chamber is surrounded by low mobility reservoir fluids. Such reservoir situations where a high mobility fluid is surrounded by a low mobility fluid are referred to as composite reservoirs.

To evaluate the applicability and accuracy of the pseudosteady-state method in the estimation of swept volume, to have a better understanding of horizontal well testing in composite reservoirs, and to have a good knowledge of the growth of the steam chamber volume with time, a computer program was developed to simulate single-phase flow around a horizontal well in three dimensions (x-, y-, and z-). The model is a closed, box-shaped reservoir with a horizontal well. This research considers the pressure behaviour analysis of two-region and multi-region composite reservoirs with horizontal wells, with emphasis on the two-region composite reservoir situations.

The pseudosteady-state method has been used to estimate the swept volume. During the pseudosteady-state period, a straight line on a Cartesian graph of pressure versus time is expected whose slope is inversely proportional to the swept volume. The effects of grid size, well location in different directions, swept region shape, mobility ratio, storativity ratio and the number of regions on the swept volume estimation have been studied. None

of the above mentioned parameters appear to have a significant effect on the swept volume estimation and the expected constant value of the Cartesian derivative. Results of this study show that the pseudosteady-state method may be used to estimate the swept volume for steam injection through a horizontal well. However, the swept volume may be overestimated by up to 30 percent. A theoretical expression for the Cartesian pressure derivative constant value during the pseudosteady-state period for rectangular reservoirs has been developed. By comparing this value with simulated values for different tests, the error percentages are obtained. Analysis of the well test data shows that the steam chamber mobility can be accurately estimated from pressure responses of horizontal wells.

ACKNOWLEDGEMENTS

TABLE OF CONTENTS

LIST OF TABLES

LIST OF FIGURES

NOMENCLATURE

a $\quad$ = Reservoir length, ft (m)

A $\quad$ = Area, ft^2 (m^2)

a_s $\quad$ = Swept-region length, ft (m)

a_{sD} $\quad$ = Dimensionless swept-region length

A_x $\quad$ = Cross-sectional area of grid block perpendicular to x-axis, ft^2 (m^2)

A_y $\quad$ = Cross-sectional area of grid block perpendicular to y-axis, ft^2 (m^2)

A_z $\quad$ = Cross-sectional area of grid block perpendicular to z- axis, ft^2 (m^2)

b $\quad$ = Reservoir width, ft (m)

b_s $\quad$ = Swept-region width, ft (m)

b_{sD} $\quad$ = Dimensionless swept-region width

c $\quad$ = Compressibility, 1/psia (1/pa)

c_t $\quad$ = Total compressibility, 1/psia (1/pa)

E $\quad$ = Pressure-drop coefficient in the current grid in Eq. 4.23

F $\quad$ = Storativity ratio

F $\quad$ = Pressure-drop coefficient in the following grid in the x-direction in Eq. 4.24

F_{sli} $\quad$ = Storativity ratio for a multi-region system, $(\phi c_t)_1/(\phi c_t)_i$

h $\quad$ = Reservoir thickness, ft (m)

H $\quad$ = Pressure-drop coefficient in the following grid in the y-direction in Eq. 4.25

h_s $\quad$ = Swept-region thickness, ft (m)

h_{sD} $\quad$ = Dimensionless swept-region thickness

I_w $\quad$ = Well index, Eq. 4.36

k $\quad$ = Permeability, md (m^2)

k_x $\quad$ = Permeability in x-direction, md (m^2)

k_y $\quad$ = Permeability in y-direction, md (m^2)

k_z $\quad$ = Permeability in z-direction, md (m^2)

k_{x1} = Permeability in x-direction for swept region, md (m^2)

k_{y1} = Permeability in y-direction for swept region, md (m^2)

k_{z1} = Permeability in z-direction for swept region, md (m^2)

k_{x2} = Permeability in x-direction for unswept region, md (m^2)

k_{y2} = Permeability in y-direction for unswept region, md (m^2)

k_{z2} = Permeability in z-direction for unswept region, md (m^2)

L = pressure drop coefficient in the preceding grid in the x-direction in Eq. 4.22

L = Well length, ft (m)

L_D = Dimensionless well length

M = Mobility ratio

m_c = Cartesian slope corresponding to pseudosteady-state flow, psia/hr (pa/s)

m_{sl} = Semi-log slope corresponding to early radial flow, psia/cycle (pa/cycle)

m_{tr} = Transition-region slope for multi-region systems as defined by Acosta (1994)

N = Number of equations in matrix

p = Pressure, psia (pa)

p_D = Dimensionless pressure, Eq. 4.30

p_i = Initial pressure, psia (pa)

p_o = Grid-block pressure, psia (pa)

p_{wf} = Wellbore flowing pressure, psia (pa)

p_{wD} = Dimesionless wellbore pressure, Eq. 4.30

$\bar{p}_{wf}$ = Average wellbore pressure, psia (pa)

q = Flow rate, STB/d (m^3/s)

q* = Production rate, STB/d (m^3/s)

$q_{i,j,k}$ = Right-hand side of Eq. 4.19, bbl/d (m^3/s)

R = Radius, ft (m)

R = Regression, Figures 5.6 and 5.7

R_D = Dimensionless radius, R/r_w

R_{D1} = Dimensionless radius of region 1, R_1/r_w

R_{Dn-1} = Dimensionless radius of region n-1, R_{n-1}/r_w

r_{eD} = Dimesionless outer-region radius, r_e/r_w

r_o = Block radius, ft (m), Eq. 4.37

r_w = Wellbore radius, ft (m)

r_{wD} = Dimensionless wellbore radius

$(r_w)_{eq}$ = Equivalent wellbore radius, ft (m), Eq. 4.38

S = Pressure-drop coefficient in the following grid in the z-direction in Eq. 26

t = Time, hr (s)

T = Transmisibility Eq. 4.10

t_D = dimensionless time, Eq. 4.28

t_{DA} = dimensionless time based on area

t_{Dc} = dimensionless time based on R as defined by Ambastha (1988)

t_{RD} = dimensionless time based on R as defined by Ambastha and Ramey (1989)

U = Pressure-drop coefficient in the preceding grid in the y-direction in Eq. 4.21

v_b = Reservoir bulk pore volume, ft^3 (m^3)

v_s = Swept pore volume, ft^3 (m^3)

W = Pressure-drop coefficient in the preceding grid in the z-direction in Eq. 4.20

x_o = Well location with respect to x-axis, ft (m)

x_{soD} = Dimensionless well location with respect to the x-axis in the swept region

Y_1 = The starting point of the well along the y-axis, ft (m)

Y_2 = The ending point of the well along the y-axis, ft (m)

Y_{1D} = Dimensionless starting point of the well

Y_{2D} = Dimensionless ending point of the well

Y_{s1D} = Dimensionless starting point of the well in the swept region

Y_{s2D} = Dimensionless ending point of the well in the swept region

z_o = Well location with respect to the z-axis, ft (m)

z_{soD} = Dimensionless well location with respect to the z-axis in the swept region

Δp = Pressure drop, psi (pa)

Δt = Time interval, hr (s)

ΔX = Block size in the x-direction, ft (m)

ΔY = Block size in the y-direction, ft (m)

ΔZ = Block size in The z-direction, ft (m)

Greek Symbols

α = $3790.85\phi\mu c_t$, hr

β = Formation volume factor, RB/STB (m^3/sm^3)

μ = Viscosity, cp (pa.s)

ϕ = Porosity, fraction

Subscripts

b = Block, bulk

eq = Equivalent

i = Initial

i = Grid index in the x-direction

J = Grid index in the y-direction

k = Grid index in the z-direction

t = total

w = Well

wf = Wellbore flowing

x = x-direction

y = y-direction

z   = z-direction

Superscripts

−   = Average

n   = Known time level

n+1   = Unknown time level

1. INTRODUCTION

In the past several years, there has been a lot of interest in the use of horizontal wells for the purpose of increasing productivity and reducing water and gas coning problems. Horizontal wells have been widely and successfully used in different parts of the world such as: Prudhoe Bay, Alaska, Empire Abo Unit in New Mexico, France and off-shore Italy (Joshi, 1986). It has been reported that horizontal wells can produce at rates two to five times that of unstimulated vertical wells (Joshi, 1986). In addition, horizontal wells can be drilled to intersect vertical fractures to improve production.

The use of horizontal wells is reviving heavy oil production in Saskatchewan and Alberta by making primary production profitable, even under unfavorable conditions. Over 300 horizontal wells have been drilled in Saskatchewan. Nearly all of the horizontal wells are being used for primary production. Some 60% of them are considered to be economical (Farouq Ali et al., 1993).

Horizontal wells are becoming popular for primary and enhanced oil recovery because of unique advantages in comparison to those for vertical wells (Economides et al., 1991). The main advantages of horizontal wells over vertical wells are: (1) they offer a greater area of contact with the formation that makes them suitable for the efficient recovery of oil, especially from thin reservoirs. (2) for a similar flow rate, the pressure gradient at the periphery of horizontal wells is smaller than that for vertical wells. Small pressure gradients result in less severe coning (or cresting) problems. Therefore, horizontal wells perform significantly better than vertical wells in reservoirs with a gas cap and/or bottom water. (3) Due to the possibility of intersection of a multitude of natural fractures by horizontal wells, horizontal wells can be more effective in naturally fractured reservoirs (Ozkan et al., 1989). (4) In Steam-Assisted Gravity Drainage (SAGD) processes used for

both the production of bitumens and for the production of conventional heavy oils, the use of horizontal production wells provides a large contact with the reservoir and this allows operation at economic rates without the bypassing of steam (Butler, 1994).

However, due to excessive drilling costs and competition with hydraulic fracturing, the development of horizontal wells has been slow. The drilling costs of horizontal wells are 1.4 to 2.0 times greater than those of vertical wells (Joshi, 1986). In addition to this, as reported by Joshi (1986), horizontal wells are not very effective in thick (150-180 m) reservoirs with low vertical permeability.

In many reservoirs, the vertical permeability is less than the horizontal permeability. For a horizontal well, a decrease in vertical permeability results in an increase in vertical-flow resistance and a decrease in oil production rates. Field experience (Joshi, 1986) indicates that horizontal wells not only increase oil production, but also reduce gas and water coning tendencies.

The pseudosteady-state method, first proposed by Eggenschwiler et al. (1980), has proven to be quite successful in estimating the swept volume from pressure falloff tests on vertical steam injection wells. Eggenschwiler et al. (1980) showed that, for a falloff test, if the mobility and storativity contrasts between the inner and outer regions of a composite system are large enough, the inner (swept) region could behave like a closed system for a short period of time following the end of the first semi-log straight line corresponding to infinite-acting radial flow in the inner region. This results in a pseudosteady-state type flow regime, during which pressure is a linear function of time. The slope of a straight line on a Cartesian graph of pressure versus time during the pseudosteady-state flow regime is inversely proportional to the swept volume.

It has been reported that the pseudosteady-state method may be used to estimate the swept volume for steam injection through a horizontal well. However, the swept volume may be overestimated by 5 to 60 percent (Issaka, 1991, and Issaka and Ambastha, 1992b). The estimates of the swept volume as well as the steam chamber mobility are sensitive to the choice of appropriate straight lines. It has been reported that the steam swept volume overestimation may have been caused ʰy steam-assisted gravity drainage and/or location of the producer and irregular swept region shape (Issaka, 1991).

The research conducted in this study investigates an application of the pseudosteady-state method for a horizontal well located in a composite reservoir. By using a numerical soluricr, the effects of grid pattern, grid size, well location, shape of the swept region, mobility ratio, storativity ratio and the number of regions in a multi-region system on the pseudosteady-state method are evaluated. In this study, the reservoir is considered as two distinct regions. Reservoir and fluid properties are uniform for each region. Each region is assumed to be homogeneous and anisotropic. The fluid flowing into the reservoir is assumed to be single-phase and slightly compressible. The reservoir has an uniform initial pressure. All of the outer bounda ᵃ are closed.

To evaluate the accuracy and applicability of the pseudosteady-state method in the estimation of the swept volume for steam injection through a horizontal well, a simplified approach to evaluate the problems involved in horizontal well testing under steam injection is undertaken. For this purpose, a single-phase, 3-D reservoir simulator is developed. The numericaı model simulates the pressure response during the test by recording the wellbore gridblock pressure with time, for a specified reservoir swept volume. Chapter 2 presents the literature survey conducted for the current study. The statement of the problem is presented in Chapter 3. Chapter 4 contains the development of the numerical model and its validation. Chapter 5 presents a detailed study of the transient pressure behaviour of a

horizontal well in a composite reservoir. Finally, Chapter 6 presents the conclusions drawn from this study and recommendations for future investigations.

2. LITERATURE REVIEW

2.1 Well Testing in Composite Reservoirs

A composite reservoir, consisting of a zone surrounding the well in which rock and/or fluid properties are different from the properties of the rest of the reservoir, represents a wide variety of reservoir configurations of practical interest. Figures 2.1 and 2.2 schematically illustrate rectangular reservoir models for the two- and multi-region composite reservoirs considered in this study. The terms swept-region, and altered zone, have the same meaning in the context of composite reservoirs. For pressure transient analysis in a composite reservoir situation, one ...ds to answer the following questions:

1. What is the size of the altered zone in order to perform accurate graphical analysis to achieve reliable estimates of altered zone parameters?

2. What is the duration and nature of the transition period between the pressure data which represent the altered zone and those which represent the unaltered zone?

3. What influence do the wellbore effects of skin and storage have upon the pressure transient response of a composite reservoir?

Brown (1985) presented equations for calculating mobility in the altered and unaltered zones, and for calculating the radius of the altered zone by extending the model of a composite reservoir previously developed by Eggenschwiler et al. (1980) to determine the characteristics of a composite reservoir pressure transient response. He reformulated the Eggenschwiler et al. (1980) model using unaltered zone properties as the model basis.
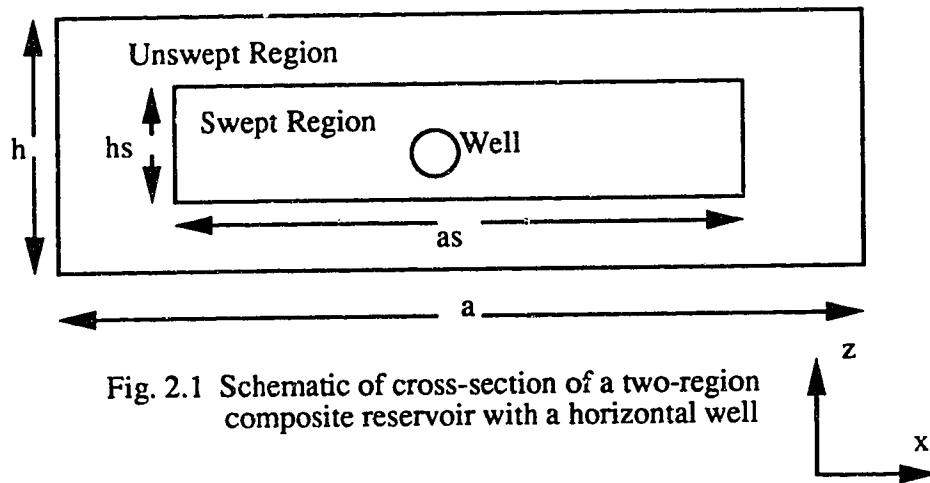
Fig. 2.1 Schematic of cross-section of a two-region
composite reservoir with a horizontal well
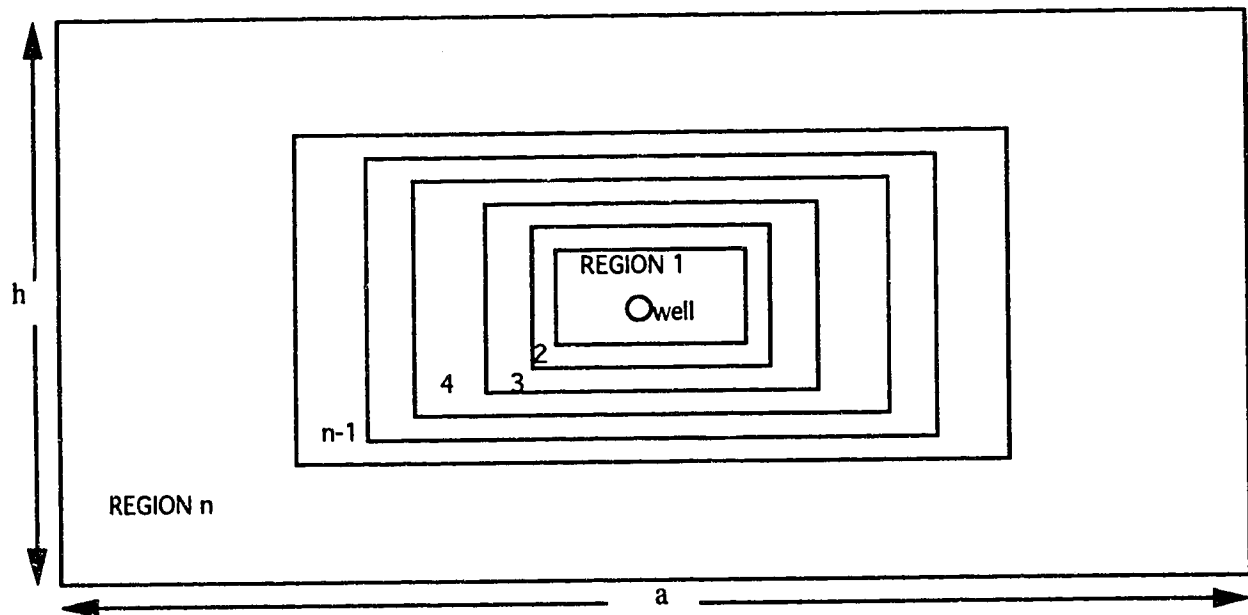
Fig. 2.2 Schematic of cross-section of a multi-region
composite reservoir with a horizontal well

His model shows that, in the absence of wellbore storage effects, pressure data appear as two semi-log straight lines, representing the mobilities in the swept and unswept zones, respectively. The slope of the semi-log straight line representing the unaltered zone is independent of the storativity ratio. He also shows that the storativity ratio influences the timing and shape of the transition region between the two semi-log straight lines and does not influence the slopes of these lines. He concluded that the characteristic shape of the transition region depends upon the mobility ratio and the storativity ratio between the altered and the unaltered zones.

Ambastha and Ramey (1989) investigated the pressure-derivative behaviour of a well in a two-zone, radial, infinite or finite composite reservoir. Their study shows that the dimensionless time to the end of the first semi-log line, based on the front radius, is a constant. They also show that the correlations developed for the end of the pseudosteady-state behaviour of the swept region can help select the correct Cartesian line to calculate the swept volume. They also presented derivative type curves applicable for all front radii, with mobility and storativity ratios as parameters, for infinitely large composite reservoirs. For closed and constant pressure outer boundaries, the ratio of the outer boundary to the front radius is the third parameter.

Ambastha and Ramey (1989) describe different methods to calculate the front radius, such as (1) deviation-time method, (2) intersection-time method, (3) type-curve matching method and (4) pseudosteady-state method. They plotted $dp_{wD}/dlogt_D$ versus t_{RD} to correlate pressure responses for all front radii. They investigated the effect of mobility and storativity ratios on the semi-log pressure derivative behaviour. During the transition period, the pressure derivative goes through a maximum above the slope of the second semi-log line corresponding to the outer-region mobility, if the mobility ratio or the

storativity ratio or both are greater than unity. Ambastha and Ramey (1989) concluded that the deviation-time method and the intersection-time method are not suitable for thermal recovery well test analysis. This is because wellbore storage may mask the first semi-log line for both methods. Also, well tests are seldom run long enough to observe a second semi-log line and outer boundary effects likely dominate the response before the establishment of the second semi-log line. They have also provided guidelines for sufficient test data collection to ensure reliable type-curve matching. If a pseudosteady Cartesian line develops, the pseudosteady-state method should yield a correct volume and average front radius for irregularly-shaped swept regions.

Ambastha and Ramey (1990) studied the injection-time effects on falloff responses for a well in a two-region composite reservoir. They pointed out that all of the swept volume estimation methods may produce an inaccurate estimate for swept volume, if injection time is short.

Eggenschwiler et al. (1980) investigated the drawdown responses from composite reservoirs through an analytical model. They developed an analytic pressure solution using the Laplace transformation with numerical inversion using the Stehfest (1970) algorithm. They made the following observations for large mobility and storativity contrasts between the two regions:

1.   The initial wellbore-storage effects vanish quickly and a semi-log straight line corresponding to the inner region mobility develops almost immediately.

2.   The first semi-log straight line corresponding to the inner-region mobility is followed by a pseudosteady Cartesian straight line characteristic of the inner swept volume. They demonstrated that a pseudosteady-state pressure response occurs

after the end of the swept region semi-log straight line, if a large mobility contrast between the swept and the unswept regions exists. The slope of this line may be used to calculate the inner swept volume, v_s:

$$v_s = q\beta/(m_c c_t) \tag{2.1}$$

Equation 2.1 is written in SI units.

3. A second semi-log straight line corresponding to the outer region mobility may appear after a long transition period.

Messner and Williams (1982) studied the application of pressure transient analysis in steam injection wells to determine the swept volume, so that important steamflood characteristics such as cumulative heat losses and sweep efficiencies could be calculated. To gain a further understanding of pressure falloff behaviour, they initiated a numerical study using a multi-phase, fully-implicit thermal simulator. After injecting steam for a certain period of time, the well was shut-in and the pressure was computed as a function of time. Both transient and pseudosteady periods corresponding to the steam swept zone were apparent, and from these data the steam permeability and the swept zone volume were calculated.

Messner and Williams (1982) concluded that the pressure falloff curves were characterized by a period of wellbore storage and damage domination, followed by a short transient and a pseudosteady period corresponding to the steam-swept zone. The end of the pseudosteady period usually occurred in a reasonable range of time after shut-in.

2.1.1 Well Testing in Multi-Region Composite Reservoirs

Acosta (1994) utilized a multi-region, composite reservoir to study the effect of various trends of mobility and storativity variations, within the swept region, on well tests for composite reservoirs. He designed his study to address analytically the problem of multi-region composite reservoirs by using the Laplace transformation technique. He defined his model with three zones: the swept zone with the highest mobility and/or storativity, the transition zone with continuously changing mobility and/or storativity, and the unswept zone with the lowest values for mobility and/or storativity. He investigated how representing these models by a different number of regions affects the pressure behaviour analysis. His study presents an evaluation of the applicability, utility and accuracy of the pseudosteady-state method to estimate the swept volume in a steam injection project analytically modeled as a multi-region composite reservoir.

By analyzing the drawdown response of multi-region composite reservoirs, he concluded that:

1. The transient pressure derivative behaviour corresponding to transition zone effects is affected by the number of regions representing the transient zone.

2. Representing the transition zone by one region may generate transient pressure derivative responses which may appear to be due to a higher mobility or storativity contrast than what actually exists. Using several regions to represent the transition zone allows a more realistic representation of property variation in the transition region.

3.   For a high mobility or storativity contrast between the swept and the transition regions, the pseudosteady-state method may yield a good estimate for the first discontinuity radius. However, for a low mobility contrast, the pseudosteady-state method may yield an overestimated value for the discontinuity radius.

4.   Using the pseudosteady-state method to estimate the last discontinuity radius R_{Dn-1} will normally yield overestimated values and, in some cases, it may be impossible to use the method due to insignificant flattening of the Cartesian pressure derivative.

5.   A mobility contrast yields a larger and better defined Cartesian pressure derivative flattening than a storativity contrast of the same magnitude. In other words, large mobility contrasts are more likely to yield a pseudosteady-state flow period than large storativity contrasts.

2.2   Transient Pressure Behaviour of Horizontal Wells

2.2.1   Drawdown Response

The use of horizontal wells in the oil industry began in the 1940's (Goode and Thambyanayagam, 1987). Although the development of horizontal wells has been slow, due to excessive costs of drilling and also competition with hydraulic fracturing for a significant period of time, recent advances in technology have lowered drilling costs considerably. Laboratory and field studies have demonstrated the unique advantages of horizontal wells in situations such as:

1.   naturally fractured reservoirs,

2.   reservoirs with gas and/or water coning problems,

3.   thin reservoirs and

4.   reservoirs with high vertical permeabilities.

Kuchuk et al. (1991) presented an analytical solution in real time and in Laplace space for horizontal wells producing at a constant rate without wellbore storage and skin effects. Their solution includes the effect of a gas cap and/or aquifer. They studied an anisotropic reservoir filled with a slightly compressible fluid of constant compressibility and viscosity. Kuchuk et al. (1991) treated the horizontal well as a uniform-flux line source. To compute the response for an infinite-conductivity horizontal well, they averaged the pressure along the well length, instead of using an equivalent pressure point.

Kuchuk et al. (1991) identified the correct equivalent wellbore radius to be used in the case of an anisotopic formation. They also identified new flow periods and simple equations and existence criteria for flow periods that can occur during the transient test. Kuchuk et al. (1991) concluded that the fact that an intermediate time radial flow period may not develop in a reasonable testing time makes interpretation difficult. They also mentioned that a large anisotropy ratio and the existence of multiple boundaries with unknown distances to the wellbore increases the complexity of the interpretation problem.

Goode and Kuchuk (1991) studied the general inflow performance of a horizontal well. They presented a solution for the pseudosteady-state pressure drop of a horizontal well producing from a rectangular region of uniform thickness, bounded above and below by no-flow boundaries. They argued that, when the steady- or pseudosteady-state pressure drop is normalized with respect to the horizontal well flow rate, it provides a measure of the pressure drawdown needed to flow a unit of volume per unit time.

Ozkan et al. (1989) presented an analysis of the pressure transient behaviour of a horizontal well or a drainhole. They developed analytical expressions and correlations for the pseudo-skin factor, and developed new methods of analysis to determine formation properties and well characteristics. They discussed new applications of the derivative approach such as the normalized pressure procedure.

Ozkan et al. (1989) considered the flow of a slightly compressible fluid to a horizontal line-source well of length L in a reservoir of height h. The vertical and horizontal permeabilities were assumed to be different, and gravity effects were negligible. Two boundary conditions on the well surface were considered: infinite-conductivity and uniform-flux. They concluded that:

1. Horizontal well pressure responses are functions of the dimensionless well length, L_D, and the dimensionless well radius, r_{wD}.

2. For a horizontal well or a drainhole, the infinite-conductivity idealization is the only viable boundary condition.

3. The pressure response of horizontal wells and pseudo-skin factors are, for all practical purposes, insensitive to the well location in the vertical plane of the reservoir.

Karcher and Giger (1986) studied the expected productivity improvement from vertical fractures. They used a numerical finite-difference model to solve the pseudosteady-state flow equations for wells and fractures located in a closed area. They reported that because of linear flow, instead of radial flow, around the well, the productivity of a fracture with

the same length as the horizontal well and full vertical penetration will always be larger than the productivity of a horizontal well.

Clonts and Ramey (1986) presented an analytical solution for the transient pressure response of a uniform flux horizontal drainhole in an anisotropic reservoir of finite thickness. In their work, a set of log-log type curves of dimensionless pressure versus dimensionless time for different drainhole radii is presented, which can be used to determine reservoir characteristics. They also presented conditions under which horizontal drainholes may yield a greater productivity than vertical wells or hydraulic fractures. Their solution, which applies for a reservoir with multiple drainholes in a vertical array, showed the possible occurrence of two transient flow types:

1.   For a short drainhole relative to the reservoir height, an initial radial flow perpendicular to the drainhole axis occurs, which is then followed by a transition to pseudo-radial flow.

2.   For a long drainhole, the initial radial flow ends rapidly and linear flow identical to that for a of uniform-flux vertical fracture appears.

Odeh and Babu (1990) provide equations for analyzing drawdown and buildup data obtained on a horizontal well. The equations are derived using a closed drainage volume, with arbitrary anisotropy, location and length of the well. They point out that the infinite or semi-infinite extension assumption of the reservoir in the x-y plane could lead to the occurrence or non-occurrence of some of the transient flow periods. They assume that the reservoir is sealed on all three sides. They identified four possible transient flow periods for a horizontal well in a closed, box-shaped reservoir model. They present simplified equations describing the pressure-time relations during each flow period as well as the duration of the periods. They also illustrated, using examples, the method of analyzing

data, obtained from testing the well, to determine permeability anisotropy in the drainage volume as well as the skin factor.

Issaka and Ambastha (1992a) presented a study of the numerical evaluation of an analytical solution for the transient pressure response of a horizontal well located in a closed, box-shaped, anisotropic reservoir. They concluded that this numerical evaluation is in reasonable agreement with the analytical evaluation. They have shown that the time criteria, based on the semi-log pressure derivative response, generally suggest shorter flow period durations than those corresponding to the time criteria based on the pressure response.

Goode and Thambyanayagam (1987) presented an analytical solution for the pressure response during drawdown and buildup of a horizontal well. The physical model considered in their analysis consists of an infinite conductivity horizontal well located in a semi-infinite homogeneous and anisotropic medium of uniform thickness and width. A slightly compressible fluid of constant compressibility is produced through the horizontal well. Their model results from solving the three-dimensional diffusivity equation. To develop the solution as a first approximation, they replaced the horizontal well with a thin strip. During the drawdown period, they assumed uniform flux along the length of the well. They demonstrated different flow regimes for both drawdown and buildup tests. They presented examples to calculate the directional permeabilities, average pressure and mechanical skin factors.

Kamal et al. (1993) presented pressure transient analysis for a well with multiple horizontal sections. They have shown how the values of horizontal permeability, vertical permeability and skin are affected by analyzing numerically simulated tests from wells that are only partially open to flow in the horizontal section. They presented an analytical solution that

allows for a well to consist of a number of arbitrary lengths, strengths and skin. They reported the appearance of a new radial flow regime from the results of the segmented horizontal well model. It results in a flat pressure derivative at a value of 0.5 divided by the number of producing segments.

In their (Kamal et al., 1993) work, analysis of numerous transient tests from horizontal wells, which were drilled normal to the maximum permeability direction, resulted in a horizontal permeability in the well direction (k_x) greater than or equal to that in the direction normal to the well (k_y). They conducted an investigation to understand the reason(s) behind this observation and to determine appropriate analysis methods for tests in horizontal wells. As a result of this investigation, they identified the need for a new interpretation model that accounts for the fact that flow in a horizontal well occurs only through some intervals, not the entire length of the well. They (Kamal et al., 1993) developed a segmented horizontal well model and used it in analyzing several field tests. They have concluded that the effective well length may be, and usually is, less than the length of the drilled and completed horizontal segment. They believe that the effective length should be estimated and used in analyzing pressure transient tests. They have also mentioned that the results of analyzing numerically generated and field data show that the segmented horizontal well model produces better estimates of the reservoir parameters than does a contiguous model.

2.3 Transient Pressure Behaviour of Horizontal Wells in Composite Reservoirs

Issaka (1991) used a thermal numerical simulator to generate the pressure falloff data to evaluate the accuracy and applicability of the pseudosteady-state method in estimating the swept volume for steam injection through a horizontal well. Results of his study show that

the pseudosteady-state method may be used to estimate the swept volume for steam injection through a horizontal well with an overestimation of 10 to 60 percent. Injection time and swept region shape effects on the estimated volume were also studied. His investigation showed that a longer injection time prior to shut-in appears to have an adverse effect on the estimated swept volume because of a more irregular swept region shape for longer injection-time cases. He reported that an irregular swept region shape does not appear to have a noticeable effect on the early time well test data.

2.4   Estimating Swept Volume

The literature reports several attempts to determine swept volume from pressure falloff data on vertical wells in both steam injection and in-situ combustion processes. All of these studies treated the reservoir undergoing thermal recovery as a composite system consisting of two zones with different rock and fluid properties. Therefore, determining the swept volume is analogous to finding the volume of the inner region.

A significant amount of work has been reported in the literature to estimate the swept or burned volume from pressure falloff data for vertical wells. Many authors have applied different methods, such as the deviation time, the intersection time, the type curve matching and the pseudosteady-state methods. In the following, discussions related to the pseudosteady-state method appear. Other methods are not used in this study and, therefore, are not discussed further.

2.4.1 Pseudosteady-state Method

The pseudosteady-state method was proposed by Eggenschwiler et al. (1980). A Cartesian plot of pressure versus time during the pseudosteady-state period yields a straight line

whose slope is inversely related to the swept volume. Eggenschwiler et al. (1980) tested their method by using two field cases published by Van Poollen (1965) and Kazemi (1966). They reported a close agreement in the results.

Walsh et al. (1981) used the information from the field studies to validate their method of swept volume determination from pressure transient tests at an injection well. In their study, they noted that in order that the swept volume may be calculated from the slope of the Cartesian straight line, the average reservoir pressure and temperature in the swept zone must be estimated. The average pressure can be approximated from the early-time flattening of the pressure curve on a semi-log graph. The average temperature can be estimated from the pressure for steam injection, but requires calculation for in-situ combustion cases. They mentioned that the wellbore storage effect ceases rapidly and a semi-log straight line develops immediately, indicating the mobility of the swept zone. Due to the high mobility contrast, the front behaves like an impermeable boundary. They reported that a long transition zone between the two semi-log straight lines for the swept and unswept regions contains an approximate pseudosteady-state region based on the swept volume.

Onyekonwu et al. (1984) studied the determination of the swept volume and the average temperature to use for interpretation of combustion falloff data using the pseudosteady-state concept in a one-dimensional radial reservoir. Their study was based on the fact that, because of the very large contrast between the mobility of the gas in the swept volume and the mobility of fluids in the unswept volume, the falloff data in the transition period forms a straight line on a Cartesian graph whose slope is related to the swept volume. Onyekonwu et al. reported that the correct interpretation of pressure falloff data depends on analyzing the correct portions of the data, because the pseudosteady-state behaviour has a limited duration, and often is difficult to identify. Their results obtained from the analysis of

simulated data showed good agreement between calculated swept volume and actual swept volume. However, they reported that the swept volume included both the burned and the high gas saturation zone ahead of the combustion front.

Da Prat et al. (1985) applied the pseudosteady-state method to locate the burning front in an in-situ combustion project in Eastern Venezuela. They conducted two falloff tests. To find the location of the burning front under the assumptions of the composite system, they used the fact that the pore volume of the swept zone is related to the slope of the pseudosteady-state straight line. They reported that the slope of the Cartesian straight line was almost the same for both tests, indicating the calculated value for the swept volume and front radius was reliable.

Fassihi (1988) presented a study to evaluate the applicability of the pseudosteady-state method for estimating the swept volume from thermal pressure falloff tests in heterogeneous systems. He used a numerical simulator to simulate falloff tests of steamflood and in-situ combustion processes. Fassihi (1988) investigated the effects of parameters such as wellbore grid size, non-uniform permeability, layering and oil vaporization on the estimated swept volume. He reported that the presence of gas-saturated oil or flowing non-condensable gas ahead of the steam front causes a long transition between the end of the infinite-acting period and the start of the pseudosteady-state period. For very heterogeneous reservoirs, the transition period is so long that it may mask the pseudosteady-state data. Fassihi (1988) found that, for in-situ combustion, the onset of the pseudosteady-state period depends strongly on gas mobility at the front. For high gas mobility, the estimated swept volume from an analysis of falloff data was found to be highly overestimated compared to the simulated swept volume. However, it approaches the simulated volume as the gas mobility decreases.

Ziegler (1990) presented a study on pressure falloff and step-rate injectivity tests for a light oil steamflood at the Buena Vista Hills field, CA. He describes two pressure falloff tests and an intermediate step-rate injectivity test conducted at a steam-injection well. The objectives of these tests were to determine reservoir properties in the vicinity of the injection well and to identify the reservoir fracture pressure. He plotted the pseudo-pressure change and the derivative of the pseudo-pressure change versus time for the falloff test. Both data sets show the presence of a boundary after a period of time. The slope of the derivative curve after this period of time was unity. This implies that there exists a pseudosteady-state flow regime and the corresponding boundary is the steam front. Analysis of the pressure data from the pseudosteady-state period indicated that the steam zone adjacent to the injection well was small in volume and in thickness. He concluded that falloff testing of steam injection wells is an effective method for estimating swept volumes.

A great amount of work has been devoted to the application of the pseudosteady-state method to determine the swept volume in thermal recovery processes for vertical wells in the literature. Most of the investigations in this area of interest have met a good degree of success. However, the literature does not contain a considerable amount of study on an application of the pseudosteady-state method to horizontal wells under steam injection and this field of study is still in its infancy. To the best of my knowledge, there is only one reference to the application of the pseudosteady-state method to horizontal wells under steam injection available in the literature survey conducted by Issaka (1991).

3. STATEMENT OF THE PROBLEM

The transient pressure behaviour of a horizontal well can be quite different from that of a vertical well. Due to the potential occurrence of four or more different transient flow periods in contrast to the occurrence of essentially one flow period for vertical wells, horizontal well testing is more complex than vertical well testing. For a vertical well in a homogeneous and unfractured reservoir, flow is radial in the horizontal direction, assuming infinite horizontal extension of the reservoir. For a horizontal well, transient pressure data may not necessarily appear as a semi-log straight line during the time period controlled by the swept region mobility.

The pseudosteady-state method has been used to estimate the swept volume for vertical wells from pressure falloff and pressure drawdown testing with a good degree of success. For a horizontal well in a homogeneous and anisotropic reservoir, the swept volume is ellipsoidal in shape (Issaka, 1991). The behaviour of composite reservoirs has attracted considerable attention, and many studies have appeared on this subject. However, these studies have concentrated on vertical wells. The main objectives of this study are:

1. To investigate the application of pseudosteady-state analysis to compute the steam chamber volume.

2. To investigate the effect of steam chamber shape and well location on pressure transient tests.

3. To improve the understanding of horizontal well testing in composite reservoirs.

To achieve the preceding objectives, a numerical simulation study of the pressure falloff behaviour of a horizontal well undergoing steam injection in a closed reservoir with anisotropy is conducted. For this purpose, a computer program has been developed to simulate single-phase flow around a horizontal well in three dimensions (x-y-z). A steam chamber containing high mobility steam is represented by blocks of large effective permeability, large compressibility and/or small viscosity in the simulator. Similarly, a low mobility fluid surrounding the steam chamber is represented by blocks of small effective permeability, small compressibility and/or large viscosity.

4. NUMERICAL MODEL FOR A COMPOSITE RESERVOIR WITH A HORIZONTAL WELL

This chapter considers the development of the numerical model. This chapter also describes the validation of the numerical solution against various studies presented in the literature such as those of Odeh and Babu (1990), Issaka and Ambastha (1992a), Ambastha (1988) and Acosta (1994).

4.1 Model Description

The box shaped reservoir is assumed to be of length a, width b, and thickness h. Figure 4.1 shows a schematic of the model. A horizontal well is drilled in a box-shaped drainage volume, with all six faces closed to flow. The well is located along the y-direction extending from Y_1 to Y_2 at (X_0, Y_0) and has a radius of r_w. The well can be fully or partially penetrating, and it produces at a constant flow rate of q from an anisotropic reservoir with permeabilities of k_x k_y and k_z in the x-, y-, and z-directions, respectively. The fluid flowing in the reservoir has slight, but constant, compressibility and the reservoir pressure is initially at p_i. Attempts have been made to refine the grids in the neighbourhood of the well in the x- and z- directions to improve the accuracy of the simulated pressure transient results. In the current research, the gravity effect is neglected.

For reservoirs undergoing steam injection, the mobility and storativity ratios are defined as follows:

$$M = \frac{\left(\frac{kh}{\mu}\right)_1}{\left(\frac{kh}{\mu}\right)_2}$$ (4.1)
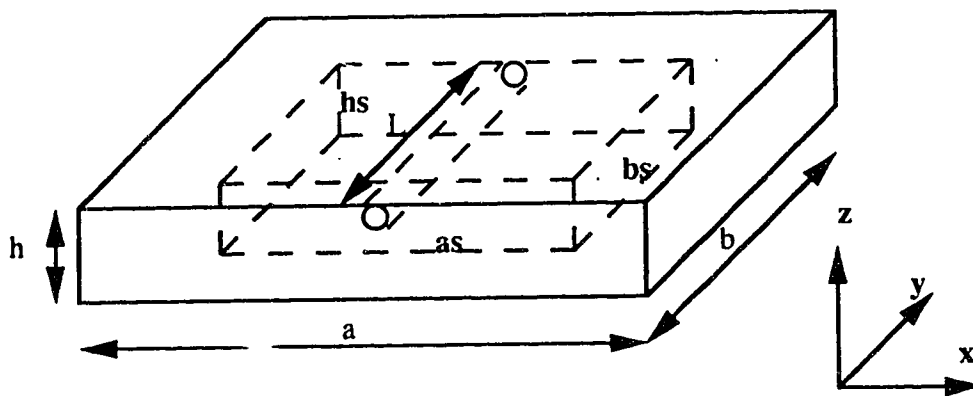
Fig. 4.1 Schematic of a horizontal well in a two-region composite reservoir

and

$$F = \frac{(\phi c_t h)_1}{(\phi c_t h)_2}$$

(4.2)

where

h_1 = swept region thickness

and

h_2 = unswept region thickness = (h-h_1)

For fully-penetrating vertical wells, since h_1 and h_2 are equal, Equations 4.1 and 4.2 simplify to

$$M = \frac{\left(\frac{k}{\mu}\right)_1}{\left(\frac{k}{\mu}\right)_2}$$

(4.3)

and

$$F = \frac{(\phi c_t)_1}{(\phi c_t)_2}$$

(4.4)

In the study of horizontal wells, h_1 and h_2 are different. Therefore, the definitions of mobility and storativity ratios are as per Equations 4.1 and 4.2, respectively. However,

throughout the current research, for the sake of simplicity, Equations 4.3 and 4.4 are used, respectively, as the mobility and the storativity ratios for a horizontal well.

4.2 Mathematical Development

Considering single-phase flow in an element of dimensions Δx, Δy and Δz, porosity, ϕ, directional permeabilities, k_x, k_y and k_z and combining the continuity equation and Darcy's law and neglecting gravity effects, the three-dimensional diffusivity equation governing fluid flow in a rectangular reservoir is given by:

$$\frac{\partial}{\partial x}\left(\frac{A_x k_x}{\mu}\frac{\partial p}{\partial x}\right)\Delta x + \frac{\partial}{\partial y}\left(\frac{A_y k_y}{\mu}\frac{\partial p}{\partial y}\right)\Delta y + \frac{\partial}{\partial z}\left(\frac{A_z k_z}{\mu}\frac{\partial p}{\partial z}\right)\Delta z + c\left(\frac{A_x k_x}{\mu}\frac{\partial p}{\partial x}\right)\frac{\partial p}{\partial x}$$

$$+ c\left(\frac{A_y k_y}{\mu}\frac{\partial p}{\partial y}\right)\frac{\partial p}{\partial y} + c\left(\frac{A_z k_z}{\mu}\frac{\partial p}{\partial z}\right)\frac{\partial p}{\partial z} + q^* = V_b \phi c_t \frac{\partial p}{\partial t} \tag{4.5}$$

The non-linear terms corresponding to the square of the pressure gradient are neglected and the final form of the preceding differential equation becomes:

$$\frac{\partial\left(\frac{A_x k_x}{\mu}\frac{\partial p}{\partial x}\right)}{\partial x}\Delta x + \frac{\partial\left(\frac{A_y k_y}{\mu}\frac{\partial p}{\partial y}\right)}{\partial y}\Delta y + \frac{\partial\left(\frac{A_z k_z}{\mu}\frac{\partial p}{\partial z}\right)}{\partial y}\Delta z + q^* = V_b \phi c_t \frac{\partial p}{\partial t} \tag{4.6}$$

The initial condition of uniform pressure at all locations is represented by:

$$p(x,y,z,0) = p_i \tag{4.7}$$

At the outer boundaries of the reservoir, the assumption of no fluid flow across the boundary results in the pressure derivatives in the direction normal to the boundary being zero. The no-flow outer boundary condition is written as

$$\frac{\partial p}{\partial x} = \frac{\partial p}{\partial y} = \frac{\partial p}{\partial z} = 0 \tag{4.8}$$

4.2.1 Numerical Solution

The finite-difference form of Equation 4.6, for the x-direction, becomes:

$$\frac{\partial\left(\frac{A_x k_x}{\mu}\frac{\partial p}{\partial x}\right)}{\partial x}\Delta x = T_{x_{i+\frac{1}{2},j,k}}\left(p^{n+1}_{i+1,j,k}-p^{n+1}_{i,j,k}\right) - T_{x_{i-\frac{1}{2},j,k}}\left(p^{n+1}_{i,j,k}-p^{n+1}_{i-1,j,k}\right) \tag{4.9}$$

where

$$T_{x_{i+\frac{1}{2},j,k}} = \frac{2A_{x_{i,j,k}}A_{x_{i+1,j,k}}k_{x_{i,j,k}}k_{x_{i+1,j,k}}}{A_{x_{i,j,k}}k_{x_{i,j,k}}\Delta x_{i+1,j,k}+A_{x_{i+1,j,k}}k_{x_{i+1,j,k}}\Delta x_{i,j,k}}\left(\frac{1}{\mu}\right) \tag{4.10}$$

In a reservoir simulator, flow is computed between elements or blocks of a rectangular grid. Flow between these elements is a function of mobility and pressure drop, as can be seen from Equation 4.9. In this study, a harmonic average value of kA's is used where the kA's are averaged as series resistances, while an upstream value is used for viscosity. Assuming 1-D flow between block i and block i+1 and using the definition for harmonic average, the transmissibilities for block i and block i+1 are computed as follows:

$$\frac{2\mu\Delta x}{kA} = \mu\left(\frac{\Delta x_i}{k_i A_i} + \frac{\Delta x_{i+1}}{k_{i+1}A_{i+1}}\right) = \mu\left(\frac{\Delta x_i k_{i+1}A_{i+1} + \Delta x_{i+1}k_i A_i}{k_i A_i k_{i+1}A_{i+1}}\right) \tag{4.11}$$

By rearranging Equation 4.11

$$\frac{kA}{\mu \Delta x} = \frac{2\, k_i A_i k_{i+1} A_{i+1}}{\Delta x_i k_{i+1} A_{i+1} + \Delta x_{i+1} k_i A_i}\left(\frac{1}{\mu}\right)_{upstream} = T_{i+\frac{1}{2}} \qquad (4.12)$$

Extending Equation 4.12 to a 3-D flow equation, Equation 4.10 is obtained. Equation 4.9 can be also written as

$$\frac{\partial\left(\frac{A_x k_x}{\mu}\frac{\partial p}{\partial x}\right)}{\partial x}\Delta x = T_{x_{i+\frac{1}{2},j,k}}\left(\delta p_{i+1,j,k}-\delta p_{i,j,k}\right) - T_{x_{i-\frac{1}{2},j,k}}\left(\delta p_{i,j,k}-\delta p_{i-1,j,k}\right)+c_{i_x} \qquad (4.13)$$

where

$$\delta p = p^{n+1}-p^n \qquad (4.14)$$

and

$$c_{i_x}=T_{x_{i+\frac{1}{2},j,k}}\left(p^n_{i+1,j,k}-p^n_{i,j,k}\right)-T_{x_{i-\frac{1}{2},j,k}}\left(p^n_{i,j,k}-p^n_{i-1,j,k}\right) \qquad (4.15)$$

The y- and z-direction finite-difference approximations follow the same argument. The right-hand side of the Equation 4.5 has the form:

$$V_b \phi c_t \frac{\partial p}{\partial t} = a_p \delta p_i \qquad (4.16)$$

where

$$a_p = \frac{V_b \phi c_t}{\Delta t} \qquad (4.17)$$

and

$$\delta p_i = p_i^{n+1} - p_i^n \tag{4.18}$$

The final finite-difference form of Equation 4.6 is

$$W\delta p_{i,j,k-1} + U\delta p_{i,j-1,k} + L\delta p_{i-1,j,k} + E\delta p_{i,j,k} + F\delta p_{i+1,j,k}$$
$$+ H\delta p_{i,j+1,k} + S\delta p_{i,j,k+1} = q_{i,j,k} \tag{4.19}$$

where

$$W = T_{z_{i,j,k-\frac{1}{2}}} \tag{4.20}$$

$$U = T_{y_{i,j-\frac{1}{2},k}} \tag{4.21}$$

$$L = T_{x_{i-\frac{1}{2},j,k}} \tag{4.22}$$

$$E = -\left(T_{x_{i+\frac{1}{2},j,k}} + T_{x_{i-\frac{1}{2},j,k}} + T_{y_{i,j+\frac{1}{2},k}} + T_{y_{i,j-\frac{1}{2},k}} + T_{z_{i,j,k+\frac{1}{2}}} + T_{z_{i,j,k-\frac{1}{2}}} + ap\right) \tag{4.23}$$

$$F = T_{x_{i+\frac{1}{2},j,k}} \tag{4.24}$$

$$H = T_{y_{i,j+\frac{1}{2},k}} \tag{4.25}$$

$$S = T_{z_{i,j,k+\frac{1}{2}}} \tag{4.26}$$

and

$$q_{i,j,k} = -\left(q^* + c_{i,j,k}\right)$$

(4.27)

The terms W,U,L,F,H and S are time independent, and are calculated once. The term E is time dependent and is updated at each time iteration. Then the problem is arranged as an N by N matrix. To solve the problem, the matrix was arranged in the form of a tri-diagonal matrix by multiplying the W, U, H and S coefficients by the guessed value for pressure drop and then moving the results to the right-hand side vector. The Thomas algorithm was used to solve the resulting problem. The pressure drop at each block at each time level was determined. The updated pressure drops were used to recalculate the right hand side. Then the iterations continued until the pressure drops converged for all grid blocks. By subtracting the pressure drop from the previous time step pressure, the pressure at each block was updated at each time iteration.

4.2.2 Dimensionless Variables

To consider the solution in dimensionless form. the following dimensionless variables are introduced (Issaka and Ambastha, 1992a):

$$t_D = \frac{k_x t}{\alpha L^2}$$

(4.28)

where, for field units,

$$\alpha = 3790.85\phi\mu c_t$$

(4.29)

The dimensionless pressure in field units is:

$$p_D = \frac{0.00708hk_x\Delta p}{\beta\mu q} \tag{4.30}$$

where

$$x_D = \frac{x}{L}, \tag{4.31}$$

$$y_D = \frac{y}{L}\sqrt{\frac{k_x}{k_y}} \tag{4.32}$$

and

$$z_D = \frac{z}{L}\sqrt{\frac{k_x}{k_z}} \tag{4.33}$$

By definition, the well length in dimensionless form is

$$L_D = y_{2D} - y_{1D} \tag{4.34}$$

Appendix A contains the computer program used in this research. Appendix B contains the results of a particular run of the computer program. Appendix C contains the development of the expression for the Cartesian derivative value to be expected during the pseudosteady-state period.

4.2.3 Horizontal Well Representation

The program calculates the pressure at each grid block at different time levels. In numerical reservoir simulation by finite differences, well models are used to relate the flowing bottomhole pressure of a well, p_{wf}, to the pressure calculated for the block (blocks)

containing the well, p_o. These two pressures are related to one another by means of the effective radius of the well block. The relation is expressed by the following equations (Peaceman, 1991):

$$P_{wf} = P_o - \frac{q}{I_w} \qquad (4.35)$$

where

$$I_w = \frac{2\pi \Delta y (k_x k_z)^{0.5}}{\mu \beta \ln\left(\frac{r_o}{r_w}\right)} \qquad (4.36)$$

and

$$r_o = \frac{0.28\left[\left(\frac{k_z}{k_x}\right)^{0.5} \Delta X^2 + \left(\frac{k_x}{k_z}\right)^{0.5} \Delta Z^2\right]^{0.5}}{\left(\frac{k_z}{k_x}\right)^{0.25} + \left(\frac{k_x}{k_z}\right)^{0.25}} \qquad (4.37)$$

The widely-used Equation 4.37 derived by Peaceman (1991) for the equivalent well block radius of a well in an anisotropic medium is based on the assumptions that the grid is uniform and that the well is isolated: that is, it is located sufficiently far from the grid boundaries. Although Peaceman's well model equation was written for a uniform grid system, it has been used routinely in the literature for non-uniform grids.

The reliability of Peaceman's (1991) equation for uniform and non-uniform grids has been studied. For this purpose, the simulator was run separately with uniform and non-uniform grid patterns. For both cases, a horizontal well with a penetration ratio of 0.5 (i.e, L/b =

0.5) was considered. The well was centrally located along the y-axis. The swept volume was also kept the same.

For a uniform grid pattern, the reservoir was divided into 21 gridblocks in the x-, 5 gridblocks in the y- and 21 gridblocks in the z-direction. The centrally-located inner region was represented by 11 gridblocks in the x-, 5 gridblocks in the y- and 7 gridblocks in the z-direction. The well was located in gridblocks 2, 3 and 4 in the y-direction. The wellbore gridblock size was 19x2.4 ft.

For a non-uniform grid pattern, the reservoir was divided into 11 gridblocks in the x-, 5 gridblocks in the y- and 11 gridblocks in the z-direction. The centrally-located inner region was represented by 7 gridblocks in the x-, 5 gridblocks in the y- and 10 gridblocks in the z-direction. Block sizes were made to increase gradually away from the center of the reservoir. The wellbore gridblock size was reduced to 3.2x0.4 ft.

In each case, the simulator was run for certain values of mobility ratio with different permeability and viscosity combinations. The results are plotted on Figures 4.2 and 4.3 for a uniform grid pattern and on Figures 4.4 and 4.5 for a non-uniform grid pattern. As can be seen from Figures 4.2 through 4.5, in each case, all results from different permeability and viscosity combinations fall on the same curve for a given value of mobility ratio. However, the results from a non-uniform grid pattern seem to be more accurate than those from a uniform grid pattern for the early time period. Figures 4.2 through 4.5 show that for a uniform grid pattern the early time is affected by wellbore storage and, as a result, the early radial flow period is masked, while the early radial flow period develops for a non-uniform grid pattern.

Based on the preceding discussion, Peaceman's (1991) equation can be be used for both a uniform and a non-uniform grid pattern with a reasonable degree of confidence. Throughout this study, the majority of the cases are based on the uniform grid pattern and a few are based on the non-uniform grid pattern.

Uniform grid
M = 100
k in md
μ in cp

$dp_{wD}/dlnt_D$

$\bullet$ k_1=2000, k_2=20, μ_1=0.1, μ_2=0.1

$\blacktriangle$ k_1=2000, k_2=2000, μ_1=0.1, μ_2=10

— k_1=2000, k_2=200, μ_1=0.1, μ_2=1

t_{DA}
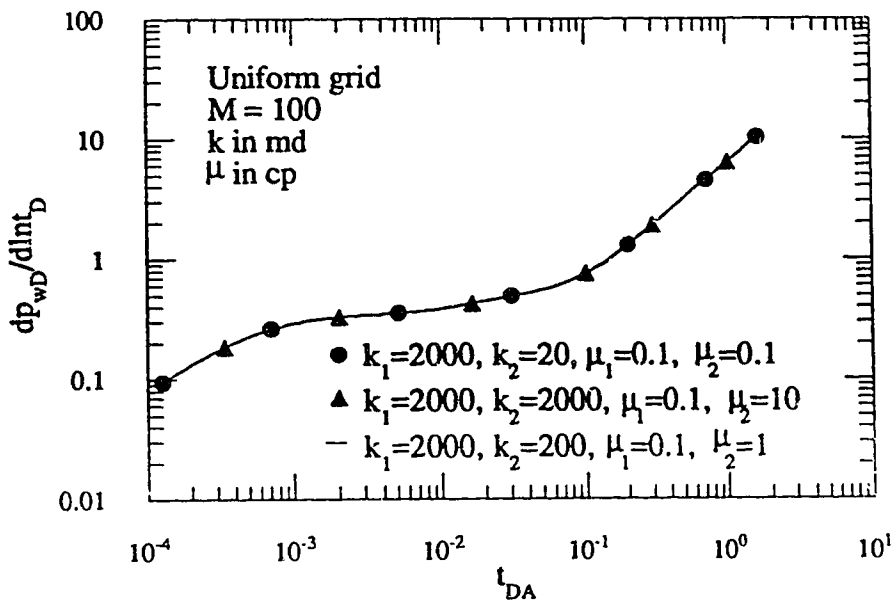
Fig. 4.2 Effect of different combinations of permeability and viscosity on the pressure derivative responses for a two-region composite reservoir with a horizontal well (M=100, uniform grid)

Uniform grid
M = 1000
k in md
μ in cp

$dp_{wD}/dlnt_D$

$\bullet$ k_1=2000, k_2=2, μ_1=0.1, μ_2=0.1

$\blacktriangle$ k_1=2000, k_2=2000, μ_1=0.1, μ_2=100

— k_1=2000, k_2=20, μ_1=0.1, μ_2=1

t_{DA}
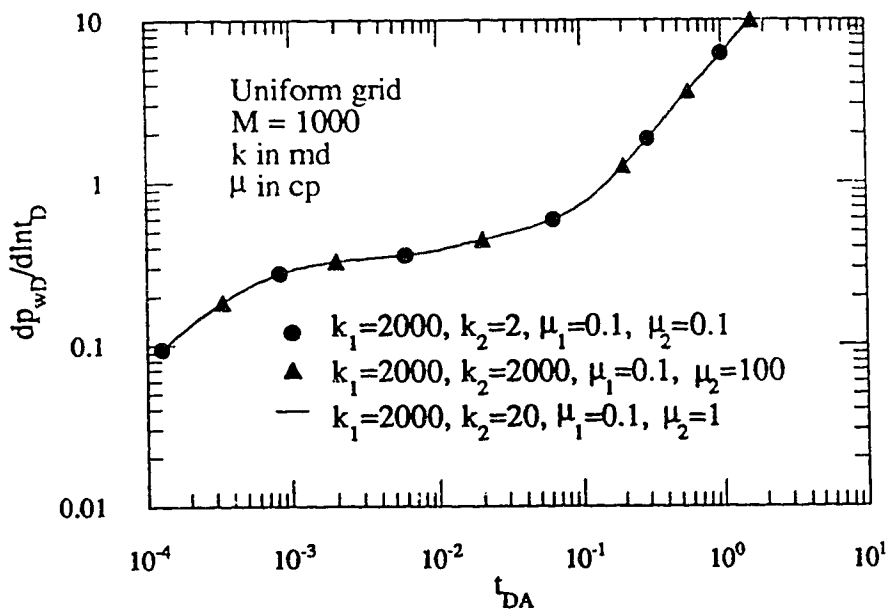
Fig. 4.3 Effect of different combinations of permeability and viscosity on the pressure derivative responses for a two-region composite reservoir with a horizontal well (M=1000, uniform grid)
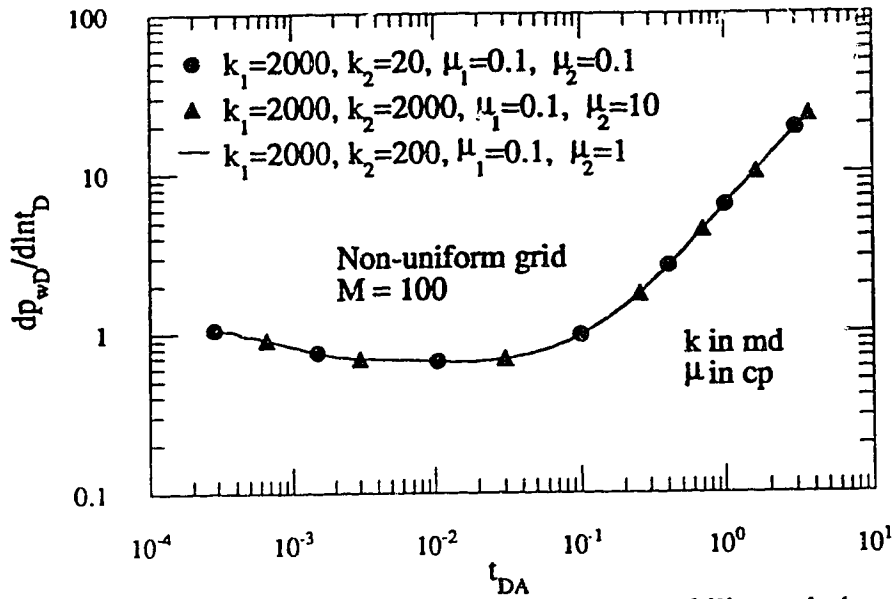
Fig. 4.4 Effect of different combinations of permeability and viscosity on the pressure derivative responses for a two-region composite reservoir with a horizontal well (M=100, non-uniform grid)
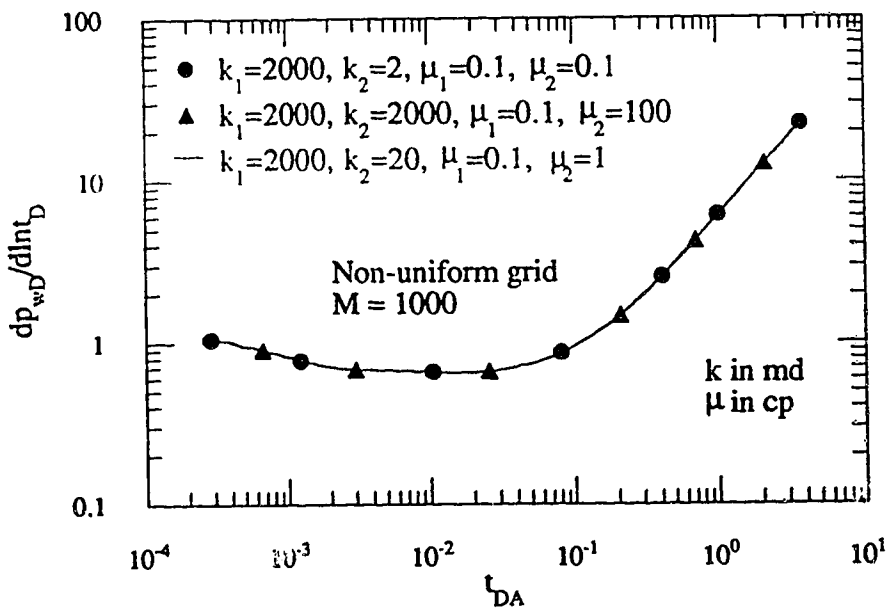
Fig. 4.5 Effect of different combinations of permeability and viscosity on the pressure derivative responses for a two-region composite reservoir with a horizontal well (M=1000, non-uniform grid)

4.2.4 Equivalent Wellbore Radius Discussion

The proper equivalent wellbore radius to use for a well in an anisotropic reservoir has been a subject of discussion in the literature for the last several years. Babu and Odeh (1989) use the actual wellbore radius in their deliverability equation. They argue that the concept of equivalent radius applies to wellbores subject to uniform pres. c conditions. They suggest that, in the immediate vicinity of the wellbore, the flow is ci. ⸳ ⸳erized by three main features: (1) the flux into the wellbore is uniform; (2) the pressure, p_{wf}, at the wellbore varies around the perimeter of the well; and (3) a representative average wellbore pressure, $\bar{p}_{wf}$, is the arithmetic average of the maximum and minimum value of p_{wf}. By this argument, they believe that the wellbore radius does not need to be corrected.

Brigham (1990) and Peaceman (1990) argue that, because of the considerable difference between directional permeabilities, during the time of interest, the wellbore behaves as though its radius is the arithmetic average of the major and minor axes of an ellipse with a major axis of $r_w\left(\dfrac{k_x}{k_z}\right)^{0.25}$ and a minor axis of $r_w\left(\dfrac{k_z}{k_x}\right)^{0.25}$. Both Brigham (1990) and Peaceman (1990) agree that the actual radius must be corrected to the equivalent radius as follows:

$$(r_w)_{eq} = \frac{1}{2}\left[r_w\left(\frac{k_x}{k_z}\right)^{0.25} + r_w\left(\frac{k_z}{k_x}\right)^{0.25}\right]$$

(4.38)

To observe the effect of equivalent wellbore radius, the program was run for three different cases of an anisotropic two-region composite reservoir with different ratios of k_x and k_z ($k_x=10k_z$, $k_x=100k_z$, and $k_x=1000k_z$) with a mobility ratio of 1000 and a storativity ratio of 10. The reservoir was divided into 25 gridblocks in the x-, 5 gridblocks in the y-, and 11 gridblocks in the z-direction. A uniform grid pattern was used. The wellbore gridblock size was 16x4.5 ft. The centrally-located inner-region was represented by 11 gridblocks in the x-, 5 gridblocks in the y-, and 7 gridblocks in the z-direction. The half-penetrated well

was centrally located along the y-axis. Figures 4.6 through 4.8 show the dimensionless

semi-log pressure derivative versus dimensionless time on a log-log scale based on actual

and equivalent wellbore radii for different permeability ratios. These figures show that the

dimensionless semi-log pressure derivative responses are the same for actual and equivalent

wellbore radii, for different permeability ratios. Throughout this study, the actual wellbore

radius is used.
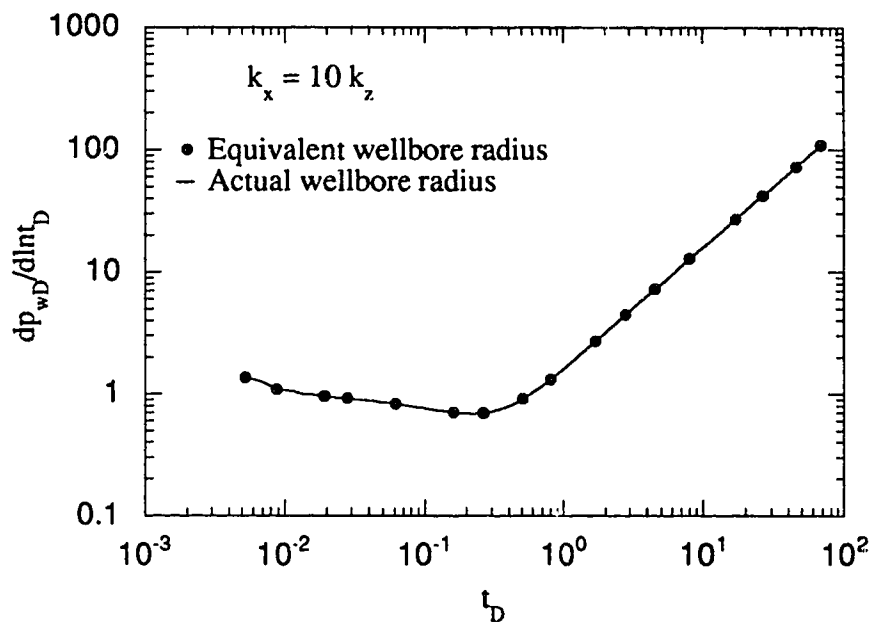
Fig. 4.6 Effect of the equivalent wellbore radius on the semi-log pressure derivative response for a horizontal well for $k_x/k_z=10$.
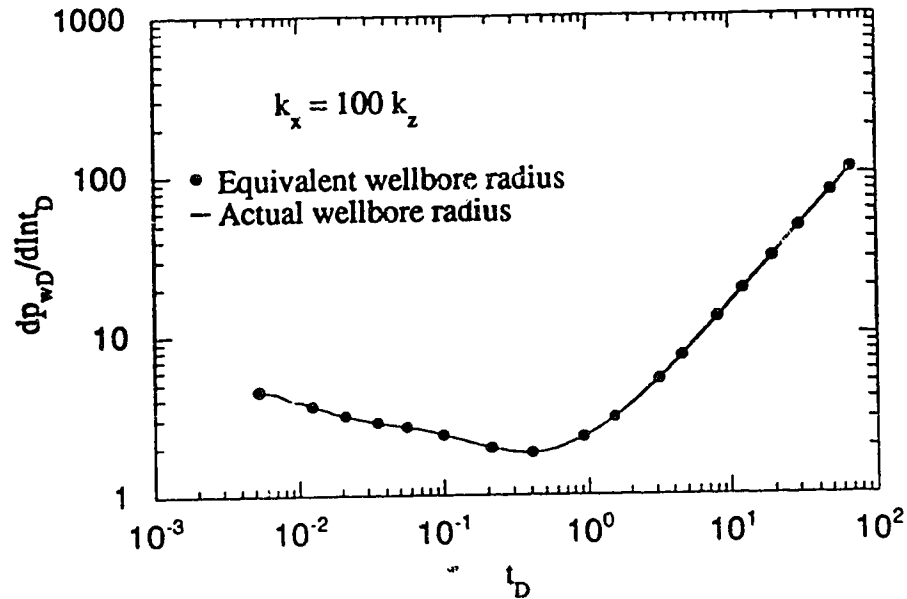
Fig. 4.7 Effect of the equivalent wellbore radius on the semi-log pressure derivative response for a horizontal well for $k_x/k_z=100$.
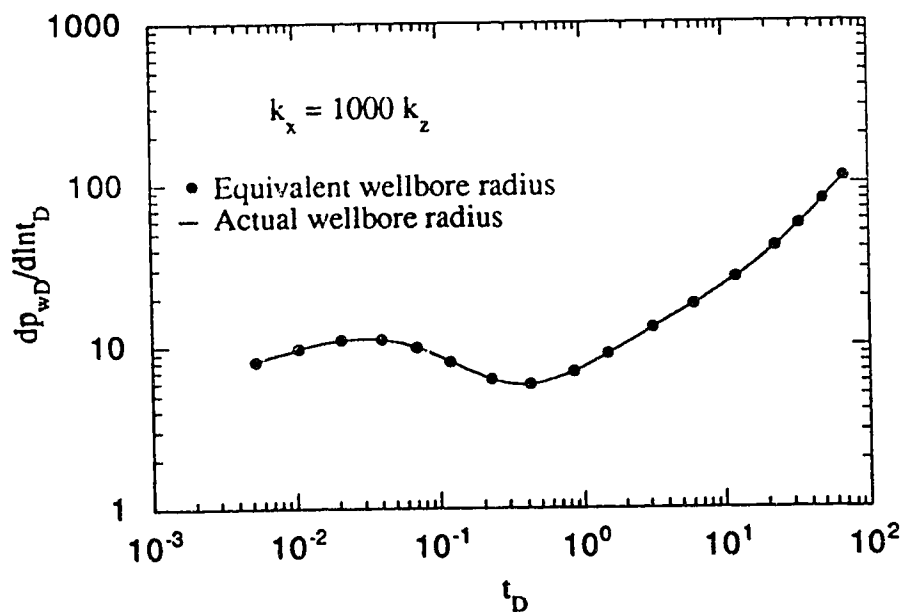
Fig. 4.8 Effect of the equivalent wellbore radius on the semi-log pressure derivative response for a horizontal well for $k_x/k_z=1000$.

4.3 Validation of the Numerical Results

The solution presented by Odeh and Babu (1990) for the transient pressure behaviour of a horizontal well in a closed, box-shaped and anisotropic reservoir is evaluated numerically. The solution presented by Issaka and Ambastha (1992a) for the drawdown pressure derivative for a horizontal well is also evaluated numerically. The analytical solution of dimensionless pressure derivative behaviour for a vertical well in a two-region composite reservoir with a closed outer boundary by Ambastha (1988) is evaluated numerically. This study has also been verified against the analytical solution for a multi-region composite reservoir presented by Acosta (1994).

4.3.1 Validation against Odeh and Babu's (1990) Solution

The numerical solution presented in this study was validated against the analytical solution presented by Odeh and Babu (1990). To reproduce Odeh and Babu's (1990) results by using this solution, the current model was run as a single-region, and as an anisotropic model. The reservoir was divided into 19 gridblocks in the x-, 5 gridblocks in the y- and 13 gridblocks in the z-direction. A non-uniform grid pattern was used. Wellbore gridblock sizes were 2x0.8 ft, 2x0.4 ft, 2x0.6 ft and 2x0.6 ft for Examples 1 through 4, respectively. The half-penetrated well was centrally located along the y-axis. In Figures 4.9 through 4.12, the results of this study are compared with those of Examples 1, 2, 3, and 4 of Odeh and Babu (1990), respectively. These figures demonstrate reasonable matches between the two studies for the early radial , early linear, late pseudo-radial and late linear flow periods, respectively. As can be seen from Figure 4.12, the simulated answer deviates significantly from the analytical solution as time increases. The reason for this phenomenon could be that in Examples 3 and 4 of Odeh and Babu (1990), the length and width of the reservoir are not specified. Therefore, some random values have been

used for the length and width of the reservoir for both cases. Another source of deviation could be that the numerical solution could be affected by discretization problems and computational errors such as truncation and round-off errors. The maximum percentage error occurs for the late linear flow period (Figure 4.12) at about $t^{1/2}=13.8$ $hr^{1/2}$. The difference between the pressure drops of the two studies is about 0.87 psia which yields a 1.7 percent error.
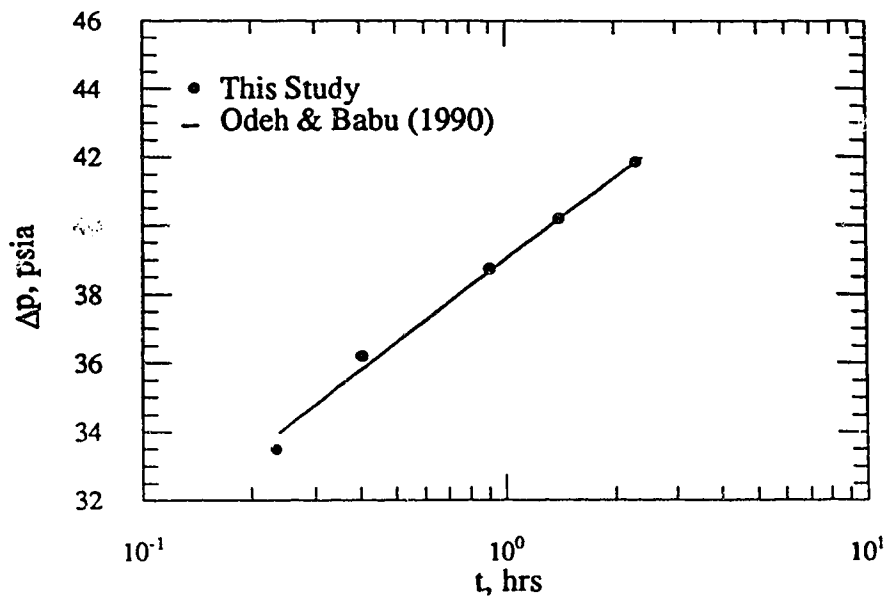
Fig. 4.9 Comprison of the pressure response from this
study with the Odeh and Babu study for the early
radial flow period.
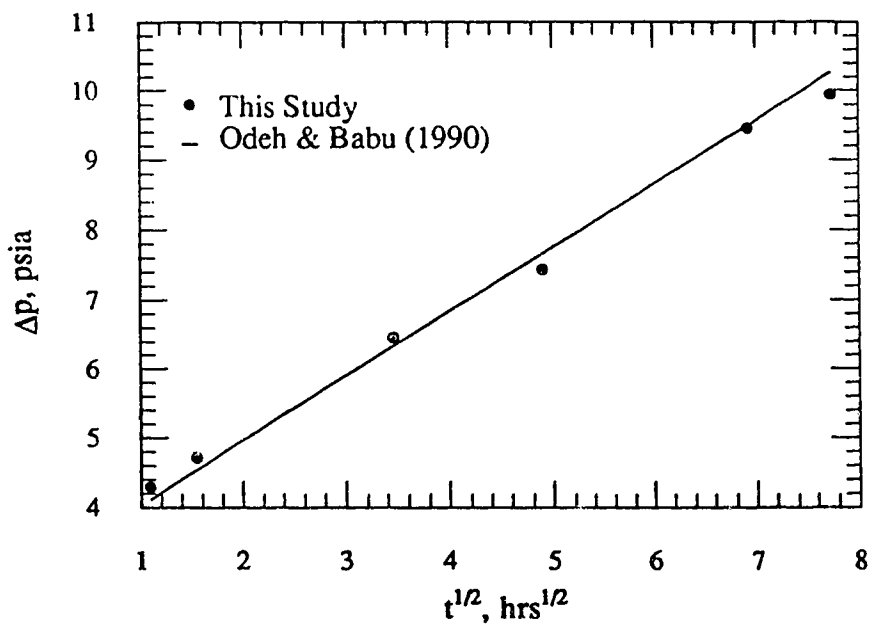
Fig. 4.10 Comprison of the pressure response from this
study with the Odeh and Babu study for the early
linear flow period.
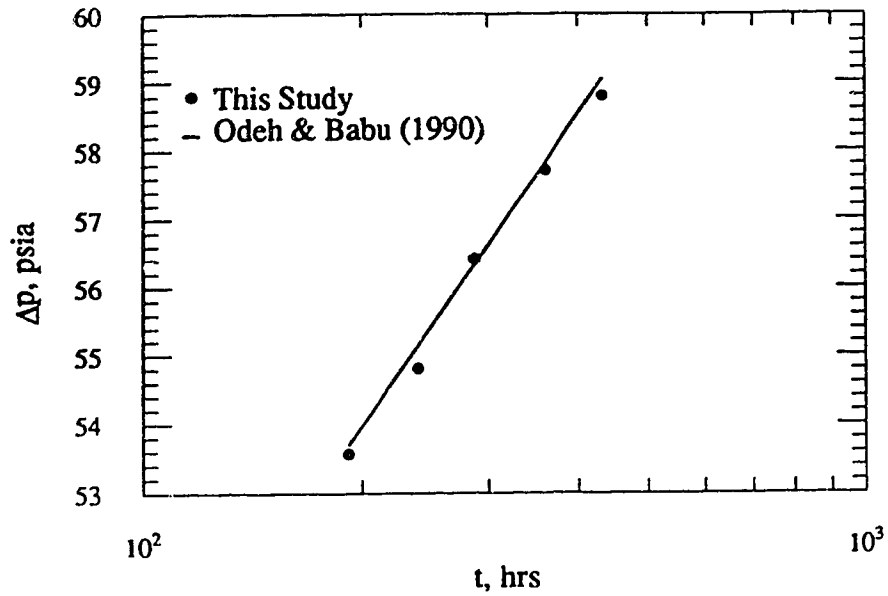
Fig. 4.11 Comprison of the pressure response from this
study with the Odeh and Babu study for the late
pseudo-radial flow period.
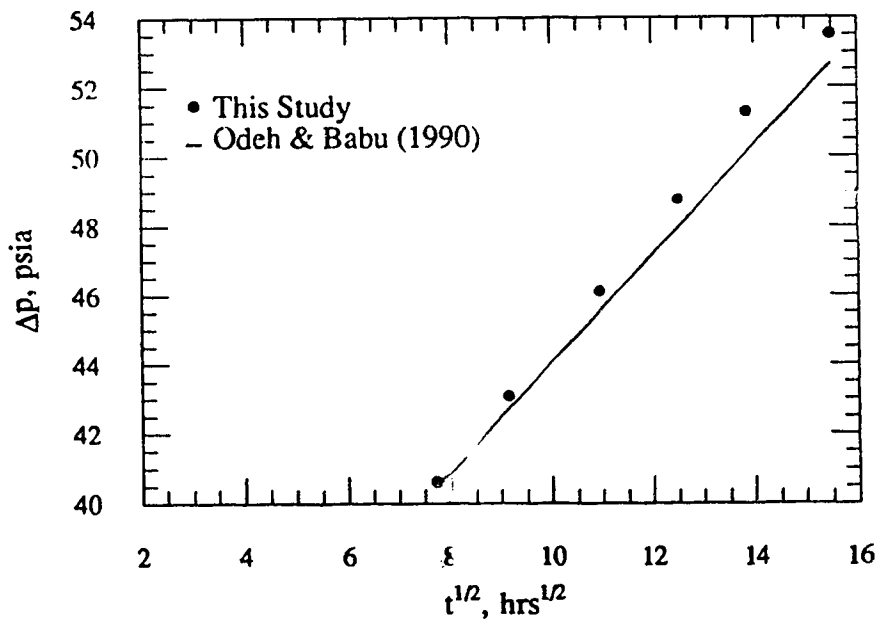
Fig. 4.12 Comprison of the pressure response from this
study with the Odeh and Babu study for the late
linear flow period.

4.3.2 Validation against Issaka and Ambastha's (1992a) Solution

The current model was also validated against the Issaka and Ambastha (1992a) solution for a horizontal well. The current model was run as a single-region reservoir. The reservoir was divided into 15 gridblocks in the x-, 5 gridblocks in the y- and 11 gridblocks in the z-direction. A non-uniform grid pattern was used. The wellbore block size was 7.8x0.8 ft. The well was centrally located along the y-axis with a penetration ratio of 0.25. To validate the model, the semi-log pressure derivative in dimensionless form was plotted versus time. In Figure 4.13, the results of this study are compared with those of Figure 4 of Issaka and Ambastha (1992a) on a log-log graph of $dp_{wD}/dlnt_D$ versus t_D. Early radial, early-linear, late pseudo-radial and pseudosteady-state flow regimes are covered in this figure. Both studies have employed the Bourdet et al. (1989) algorithm to calculate the pressure derivatives. Figure 4.13 shows a fairly reasonable match between the two studies.

4.3.3 Validation against Ambastha's (1988) Solution

This study was also verified against Ambastha's (1988) two-region radial composite reservoir model pressure derivative response. The current model was run as a two-region composite reservoir with a vertical well for $r_{eD}/R_D = 10$ and $r_{eD}/R_D = 100$. Using the current model to simulate a vertical well, since gravity effects are neglected, it appeared to be sufficient to interchange the y and z axes, as well as k_y and k_z. Since the current model is a rectangular reservoir and a cylindrical reservoir is considered for the vertical well, a square base is assumed to yield an equivalent radius for a cylindrical reservoir ($r=a^2/\pi$). The reservoir was divided into 15 gridblocks in the x-, 15 gridblocks in the y- and 5 gridblocks in the z-direction. A non-uniform grid pattern was used. The wellbore gridblock sizes were 0.9x0.9 ft and 9x9 ft for $r_{eD}/R_D = 10$ and $r_{eD}/R_D = 100$,
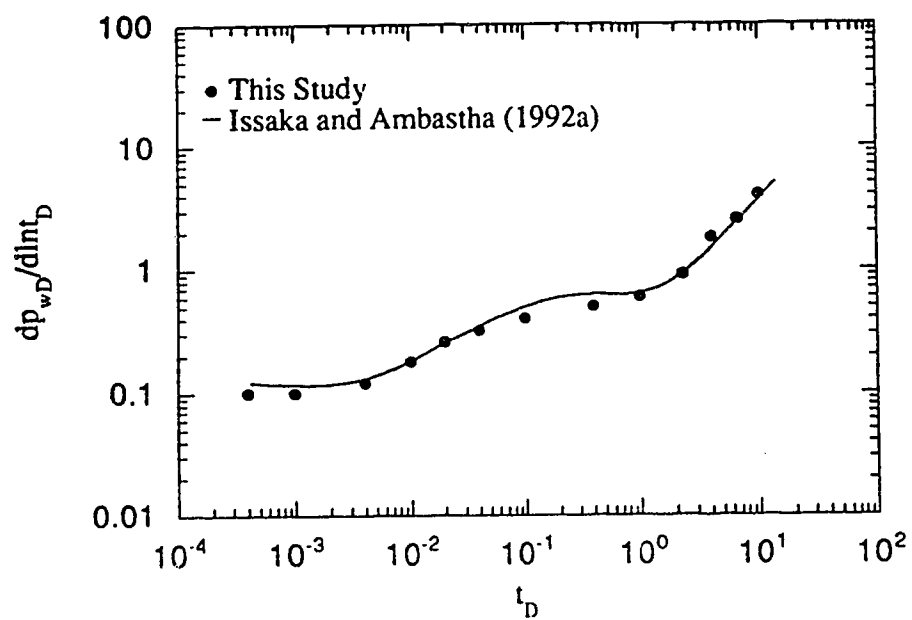
Fig. 4.13 Comparison of the semi-log presure derivative response
from this study and Issaka's study

respectively.The fully-penetrated well was centrally located along the z-axis. The model successfully reproduced Ambastha's (1988) results. Figures 4.14 and 4.15 show good agreement between the two solutions. However, for the early radial period and also for the pseudosteady-state period corresponding to an outer boundary, the two sets of data do not match perfectly. The reason for this phenomenon for the early radial period could be error in the numerical solution such as wellbore storage effects which dominate the early time portion of the test.

4.3.4 Validation against Acosta's (1994) Solution

This solution was also verified by generating Acosta's (1994) multi-region radial composite reservoir model pressure derivative response. To reproduce the results, the model was treated as a multi-region composite reservoir, with a vertical well as described in Section 4.3.3. The modified model was run for three- and ten-region composite reservoirs for R_{D1} = 100, R_{Dn-1} = 1000, m_{tr} = 0.02, and F_{sli} = 1. The mobility ratio increases gradually towards the outer boundary, while the storativity ratio remains constant at unity for each case. The mobility ratio of the swept region is defined as unity, while that of the unswept region is defined as 1000. The transition region's slope (m_{tr}) is the slope of the line that represents the transition region's relationship between the mobility and/or storativity ratios, and the dimensionless radius. A widely used algorithm (Bourdet et al. , 1989) has been employed to calculate the pressure derivative. Figures 4.16 and 4.17 show reasonable agreement between the two solutions.
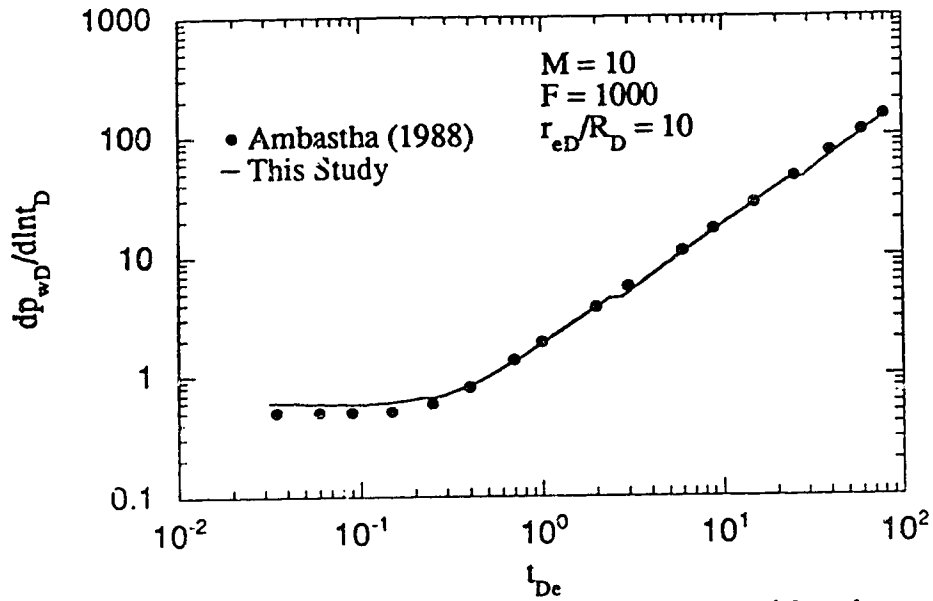
Fig. 4.14 Comparison of the effect of r_{eD}/R_D on the semi-log slope response
for a two-region composite reservoir from this study and Ambastha's
study
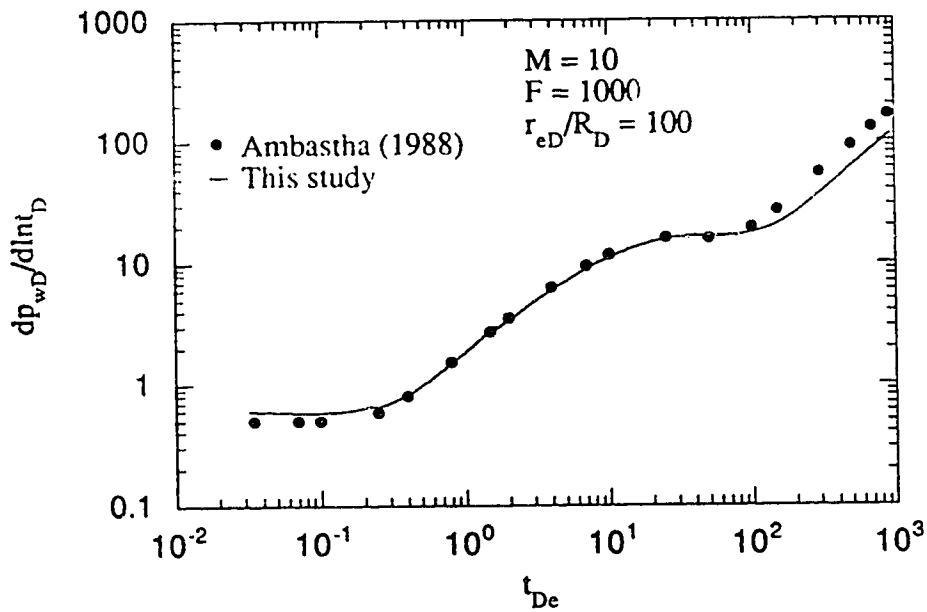
Fig. 4.15 Comparison of the effect of r_{eD}/R_D on semi-log slope response
for a two-region composite reservoir from this study and Ambastha's
study
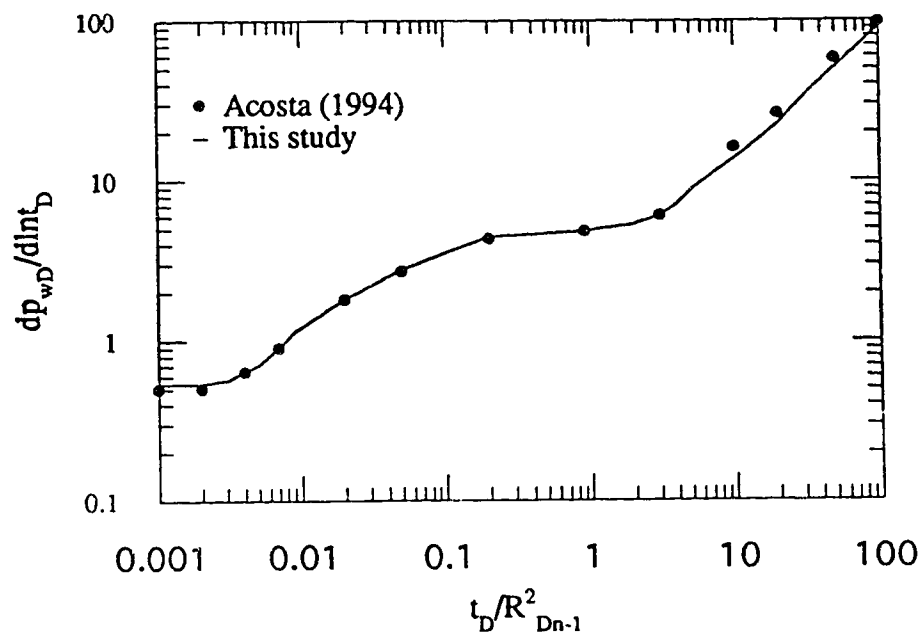
Fig. 4.16 Comparison between this study and Acosta's (1994) study
for a three-region composite reservoir
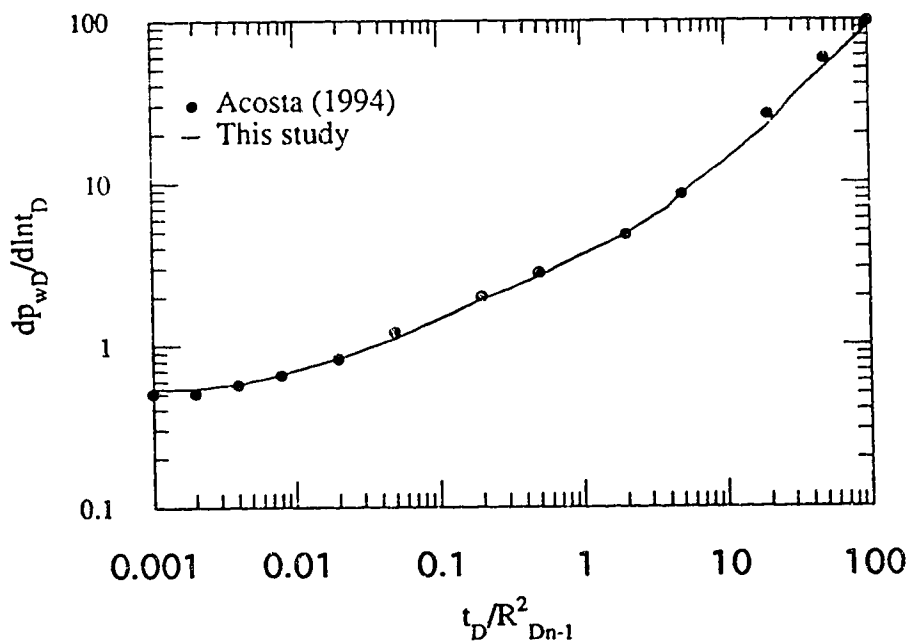
Fig. 4.17 Comparison between this study and Acosta's (1994) study
for a ten-region composite reservoir

5. HORIZONTAL WELL TESTING IN COMPOSITE RESERVOIRS

It is important to have a knowledge of the growth of the steam chamber volume with time. For this purpose, a single-phase, 3-D reservoir simulator is developed on the basis of the assumptions and mathematical formulation outlined in Chapter 4. The numerical model simulates the pressure response during the test by recording the wellbore gridblock pressure with time, for a specified reservoir swept volume. This chapter presents a detailed study of a two-region composite model and a brief look at multi-region (more than two regions) composite models.

5.1 Reservoir Model

Figure 5.1 shows a schematic of the 3-D rectangular reservoir model used in the present study. The reservoir and fluid data used for the base case in this study are shown in Table 5.1. A steam chamber with high mobility fluid is represented by blocks of large permeability and/or small viscosity in the simulator. Similarly, a low mobility fluid surrounding the steam chamber is represented by blocks of small permeability and/or large viscosity in the simulator. Although the developed model is not a thermal simulator, attempts have been made to use such a set of input data as if it were a thermal one. By surveying the literature on the steam injection subject, efforts have been made to use a combination of data which is as realistic as possible.
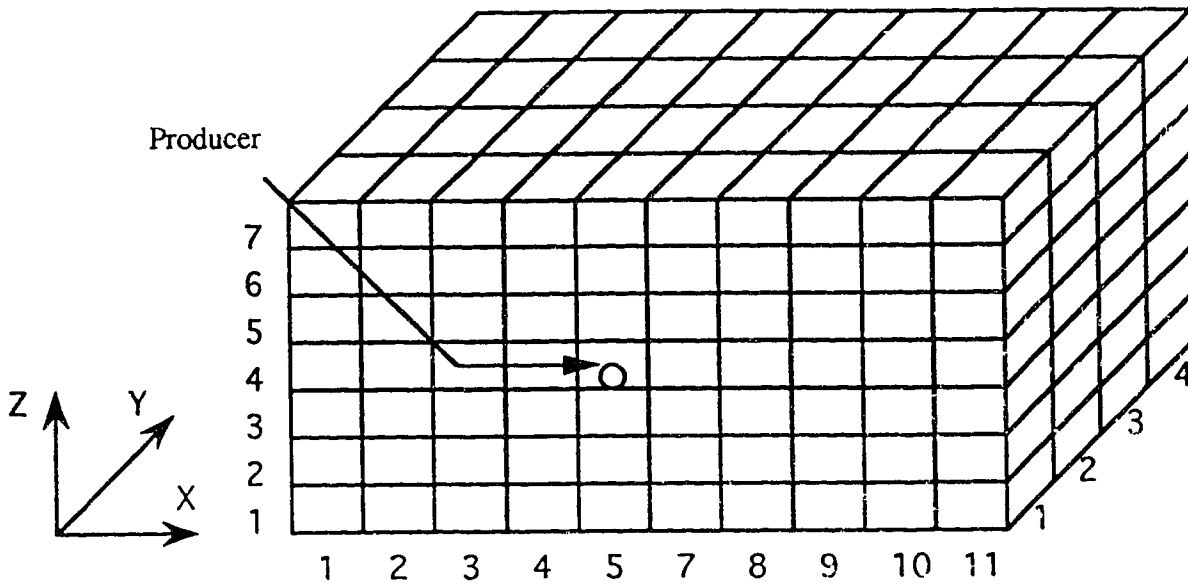
Fig.5.1- Schematic of 3-D reservoir model used for simulation

Table 5.1   Typical reservoir and fluid properties used in base case simulation

Reservoir initial pressure, psia	1000
Swept region compressibility, psi^{-1}	15×10^{-3}
Unswept region compressibility, psi^{-1}	15×10^{-6}
Swept region viscosity, cp	0.1
Unswept region viscosity, cp	100
Production rate, BPD	800
Wellbore radius, ft	0.25
Porosity, %	20
Swept region horizontal permeability, md	2000
Swept region vertical permeability, md	200
Unswept region horizontal permeability, md	2000
Unswept region vertical permeability, md	200
Formation volume factor, RB/STB	1.25

A value of 15×10^{-3} psi^{-1} is used as the swept region compressibility. Walsh et al. (1981) used 10.8×10^{-3} psi^{-1}, Brown (1985) used 9×10^{-6} psi^{-1} and Satman et al. (1980) used 3.3×10^{-3} psi^{-1}. A value of 15×10^{-6} psi^{-1} is used as the unswept region compressibility. This value is a very typical value for total compressibility for the unswept region widely used by different authors such as Onyekonwu et al. (1984), Brown (1985), Fassihi (1988) and Farouq Ali and Ferrer (1977). A value of 0.1 cp is used as the swept region viscosity. Brown (1985) used 0.9 cp, Satman et al. (1980) used 0.0275 cp and Da Prat et al. (1985) used 0.0245 cp. A value of 100 cp is used as the unswept region viscosity. Depending on the reservoir depth and temperature, a wide range of values including 100 cp has been used

as the oil viscosity. Fassihi (1988) used 13.5 cp for light oil at 88 °F and 2700 cp for heavy oil at 75 °F. A value of 2000 md is used as the horizontal permeability, and 200 md as the vertical permeability of the reservoir. Farouq Ali and Ferrer (1977) used 2000 md, Satman et al. (1980) used 8000 md for the swept region and 25 md for the unswept region, Da Prat et al. (1985) used 1000 to 10,000 md and Onyekonwu et al. (1984) used 800 to 1000 md. The choice of the combination of data shown in Table 5.1 is also based on computation time considerations to obtain sufficient information to analyze pressure transient tests.

To observe as many flow regimes as possible, the program has also been run with a different set of data than that of Table 5.1 with M=1000, F=10 and a penetration ratio of 0.5. The results are plotted on Figures 5.2 and 5.3. These figures show the typical semi-log pressure and pressure derivative and Cartesian pressure derivative responses for a two-region composite reservoir with a horizontal well based on the data shown on Figures 5.2 and 5.3. Different flow regimes are labeled on the Figure 5.2 pressure derivative curve. The first flow regime marked by a zero slope line is the early radial flow period corresponding to the swept region immediately after the well is put on production. The first flow regime marked by a unit slope line is the pseudosteady-state period corresponding to the swept region due to the mobility and storativity contrast between the swept and unswept regions. As can be seen from the same curve, none of the early linear, late pseudo radial and late linear flow regimes has developed. To observe an early linear flow regime, the well length should be significantly longer than the formation thickness and the contribution to the well flow from beyond its ends should be negligible (Odeh and Babu, 1989). Since in this case the penetration ratio is 0.5, the contribution to the well flow beyond its ends can not be negligible. Thus, an early linear flow period can not develop. To observe a pseudo radial flow period, the penetration ratio should be less than 0.45 (Odeh and Babu, 1989). This requirement has not been met either. To observe the
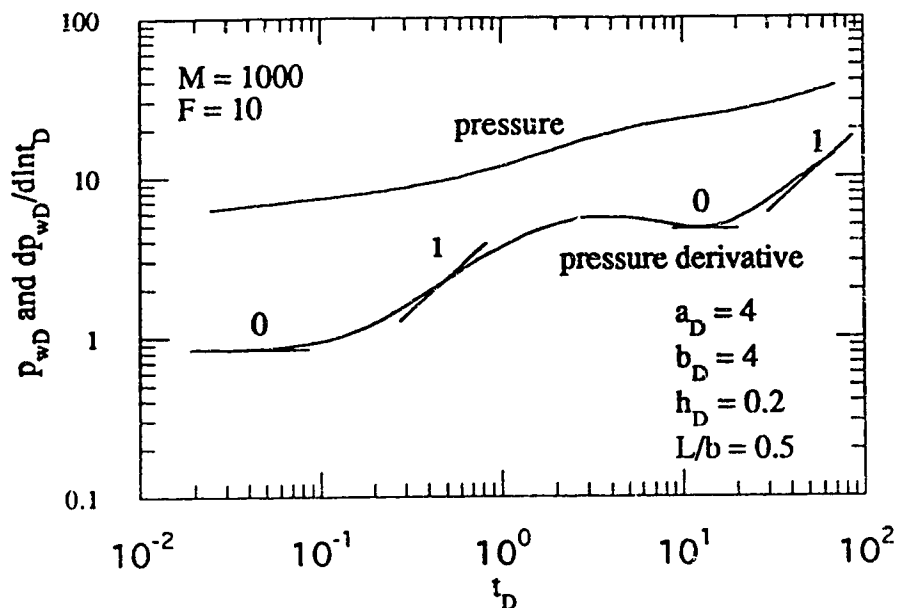
Fig. 5.2 Dimensionless pressure and semi-log pressure derivative responses
for a horizontal well in a box-shaped two-region composite reservoir.
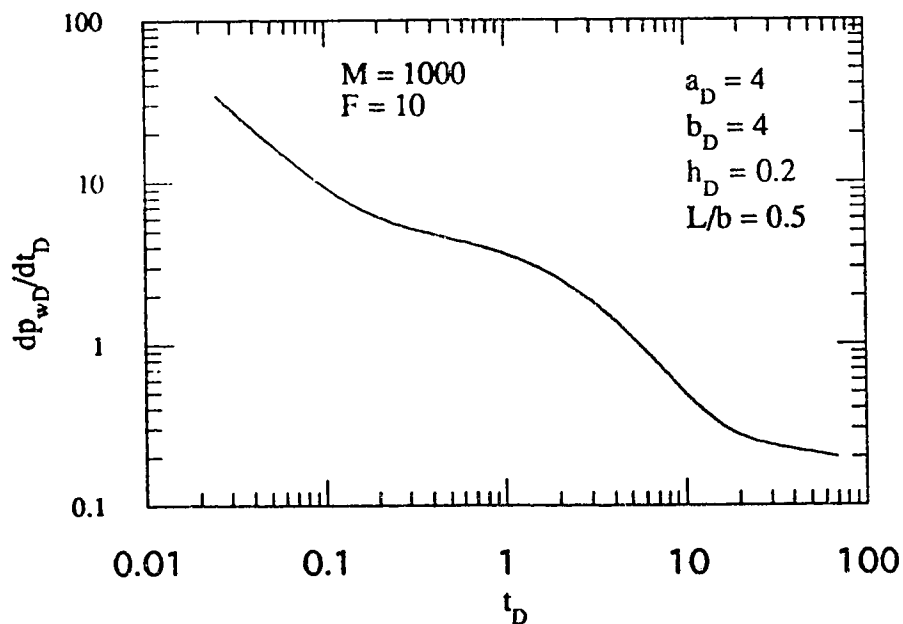
Fig. 5.3 Dimensionless cartesian pressure derivative response of a
horizontal well in a two-region composite reservoir.

late linear flow period, the length of the swept region should be significantly longer than the width of the swept region. This condition is not valid either. Thus, only the early radial flow regime corresponding to the swept region has developed before the onset of the pseudosteady-state flow period. The second zero slope line and the second unit slope line are indicative of the early radial flow regime and the pseudosteady-state regimes corresponding to the unswept region, respectively.

5.1.1 Reservoir Size

The reservoir is 400 ft long, 200 ft wide and 50 ft thick with a 100 ft long well in the y-direction. These values in dimensionless form are 4, 2, 1.6 and 1, respectively. The reason behind using small values for reservoir dimensions and well length is to avoid the use of a large number of grids in different directions and, consequently, to reduce the computation time. However, the simulator is able to simulate large reservoirs with a large numbers of grids. The pressure responses for a reservoir with 200 ft thickness, 4000 ft length and 4000 ft width are shown in Figures 5.2 and 5.3 (the dimensionless values are shown on the graphs). The reservoir was divided into 19 gridblocks in the x-, 5 gridblocks in the y- and 13 gridblocks in the z-directions. A horizontal well with a length of 2000 ft was located along the y-axis in gridblocks 2, 3 and 4. The wellbore gridblock size was 1.95x0.79ft. A non-uniform grid pattern was used. To consider the swept region, a number of gridblocks are specified with different reservoir and fluid properties than those used in the outer region. The swept region volume is kept fixed for each case studied to observe the effects of different parameters on the same swept volume estimation. The producer is located in the center of the reservoir in the y-direction.

5.2 Cases Studied

Various simulation runs were conducted to investigate the effects of different parameters on the swept volume estimation and the constant Cartesian derivative value expected during the pseudosteady-state period. Table 5.2 shows a summary of the cases studied in this research. The base case was Run 1 with the reservoir size the same as in Section 5.1.1. For Run 1, the half-penetrated well is centrally located in all directions. Runs 1 and 2 were used to investigate the effects of grid refinement. Various other runs were designed to study the effects of the other parameters as shown in Table 5.2.

Table 5.2   List of cases studied for the effects of various parameters on the   swept volume estimation

Run number	Description
1 and 2	Effect of grid refinement
1, 3, and 4	Effect of grid size
1, 5, and 6	Effect of well location in the x-direction
1, 7, and 8	Effect of well location in the y-direction
1, 9, and 10	Effect of well location in the z-direction
1, 11, 12, 13, and 14	Effect of swept region shape
1, 15, 16, 17,18, and 19	Effect of mobility ratio
1, 20, 21, 22, 23, and 24	Effect of storativity ratio
25, 26, 27,28, and 29	Effect of the number of regions

5.3 Simulation Results and Discussion

The results of Run 1 are presented to explain in detail the calculation procedure for the mobility and swept volume estimation. In the latter parts of this chapter, the discussion on the effects of grid size, well location, swept region shape, mobility ratio, storativity ratio and the number of regions on the estimation of swept volume are presented. For this purpose, the dimensionless semi-log pressure derivative ($dp_{wD}/dlnt_D$) responses are plotted versus area-based dimensionless time (t_{DA}). To investigate the effects of the different parameters on the estimation of the swept volume, the portion of the pressure response data, corresponding to pseudosteady-state due to the mobility and storativity contrasts of the swept and unswept regions, is considered. If the unit-slope lines corresponding to pseudosteady-state for different values of each parameter contain the same set of data, there will not be a considerable effect on the swept volume estimation due to the change in the corresponding parameter values.

To observe the effect of different values of each parameter on the constant value of the Cartesian derivative, the dimensionless Cartesian pressure derivative (dp_{wD}/dt_D) responses are plotted versus area-based dimensionless time (t_{DA}). If pseudosteady-state flow corresponding to the inner region develops, the graph will show a zero-slope (flat) line. Any differences in the constant value of the Cartesian derivative with respect to the theoretical constant for the Cartesian derivative will be indicative of errors due to the variation of a particular variable.

5.3.1 Results of Run 1

For Run 1, the reservoir was divided into 41 equal grids in the x-direction, 5 non-equal grids in the y-direction and 11 equal grids in the z-direction. The centrally-located inner

region was represented by 21 gridblocks in the x-direction, 5 gridblocks in the y-direction and 7 gridblocks in the z-direction. The half-penetrated horizontal well extends along the y axis from gridblock 2 to gridblock 4. The well is centrally located with respect to the x- and z-axes. A value of 1000 was used as the mobility and storativity contrasts between the inner and the outer regions. Oil was produced from the reservoir through a single horizontal well at the rate of 800 STB/D for 100 h. rs. Figure 5.4 shows the wellbore gridblock pressure and wellbore flowing pressure responses, during the test, graphed against time. This figure shows that the wellbore gridblock pressure is equal to the actual wellbore flowing pressure plus a constant value. The relationship between the wellbore gridblock and the wellbore flowing pressures is defined in Equation 4.35. Generally speaking, the wellbore gridblock pressure is essentially equal to the wellbore flowing pressure at a radius of r_o.

5.3.1.1 Identification of Flow Regimes

To identify the various flow regimes, semi-log pressure derivatives were calculated from the wellbore flowing pressure response data using a suitable algorithm (Bourdet et al., 1989). A log-log graph of the semi-log pressure derivatives $(dp_{wf}/dlnt)$ versus t are shown in Figure 5.5 for both uniform and non-uniform grid patterns. This figure shows an early-time response dominated by wellbore storage for a uniform grid pattern up to about 0.03 hours. For a non-uniform pattern, an early radial flow regime starts at about 0.03 hours and lasts up to 0.2 hours. Applying the Odeh and Babu (1989) time criteria equations, the early radial flow regime should end at a time of about 0.17 hours, which is consistent with what is observed in Figure 5.5. After a transition period of about one and half log cycles, a unit-slope line corresponding to pseudosteady-state flow in the swept region develops at about 2.5 hours. Converting this value to t_{DA}, a value of 0.12 is obtained which is
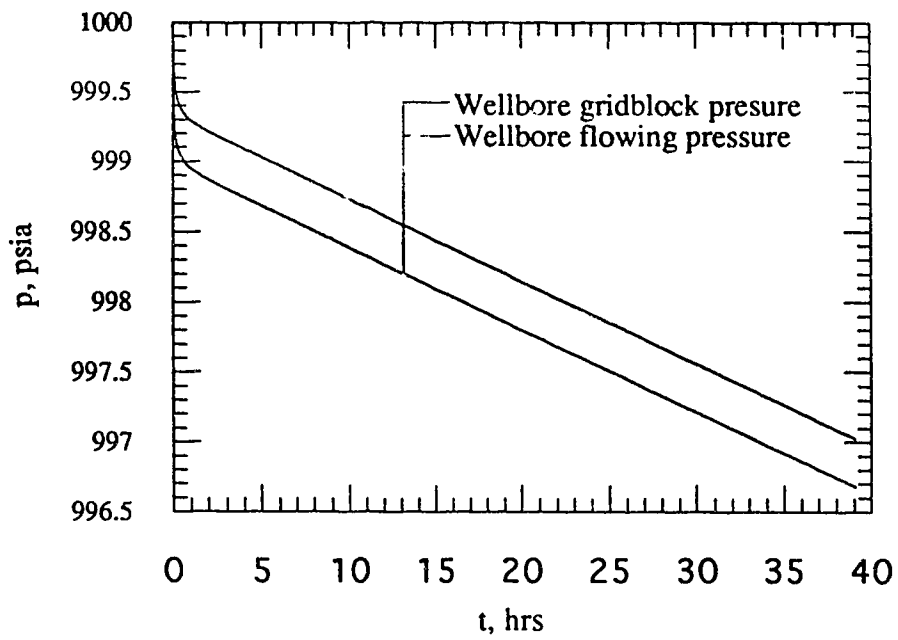
Fig. 5.4 Cartesian graph of pressure response for Run 1
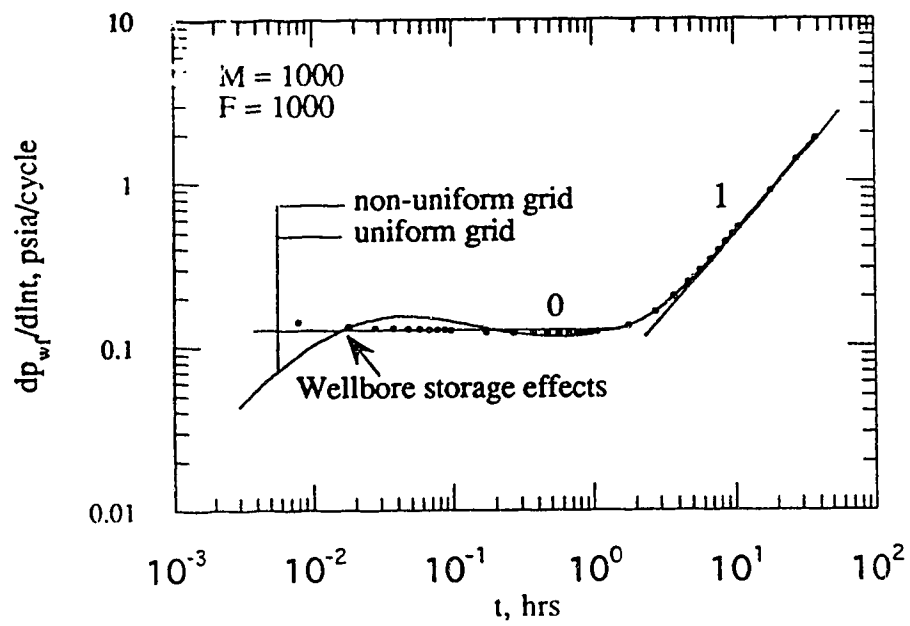
Fig. 5.5 Semi-log pressure derivative response for a two-region
composite reservoir with a horizontal well for Run 1

basically the same as the expected theoretical value (0.1). Therefore, prior to pseudosteady-state, only the early-radial flow period has occurred. This observation is consistent with what Issaka (1991) reported.

5.3.1.2   Estimation of Steam Chamber Mobility

Based on the reservoir and fluid properties in the swept region and using the equation presented by Odeh and Babu (1990), the expected slope of the semi-log straight line corresponding to early-radial flow is:

$$m_{sl} = \frac{162.6q\mu\beta}{L\sqrt{k_xk_z}}$$ (5.1)

Equation 5.1 uses field units.

The early-time portion of the data from Figure 5.5, representing the early-radial flow period, is plotted on a semi-log scale (Figure 5.6). The slope of this straight line is 0.274 psi/cycle. Based on the fluid and reservoir properties of the inner region and using Equation 5.1, the calculated slope is:

$$m_{sl} = \frac{162.6(800)(0.1)(1.25)}{(100)\sqrt{(2000)(200)}} = 0.257 \text{ psi/cycle}$$

The slope calculated from the pressure response data is 106 percent of the theoretically expected slope. Therefore, the steam chamber mobility is underestimated by about 6 percent. Such a slightly underestimated value of the steam chamber mobility is not unreasonable, given that simulated data are affected by discretization problems and computational errors such as truncation and round-off errors.
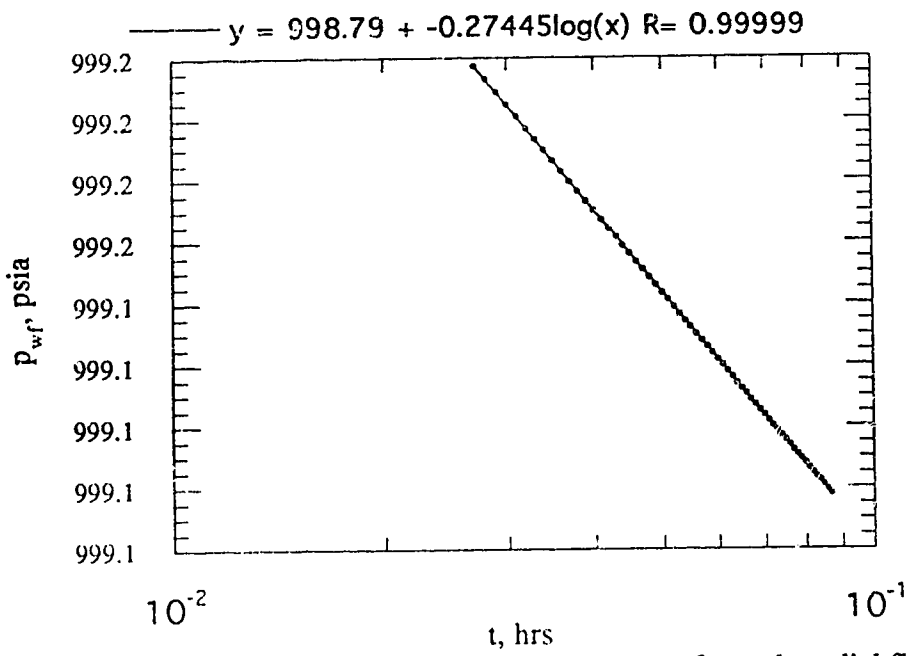
Fig. 5.6 Semi-log graph of pressure response for early radial flow period for Run 1

5.3.1.3   Estimation of Swept Volume

The simulated swept volume was calculated by adding the gridblock volumes within the swept region (region of high mobility fluid). This volume was about 1.30×10^6 ft^3. The swept volume was also calculated from the simulated pressure response data using the pseudosteady-state method. From the semi-log pressure derivative response shown in Figure 5.5, pseudosteady-state for the swept region occurs for the data after 5 hours. This set of data was plotted on a Cartesian graph of p_{wf} versus t on Figure 5.7. The slope of this straight line was 5.97 psi/hour. By using the simulated input data corresponding to the inner region and Equation 2.1, the swept volume was calculated as:

$$V_s = \frac{5.614(800)(1.25)}{24(0.2)(15E\text{-}3)(0.059)} = 1.32 \times 10^6 \text{ ft}^3$$

A comparison between the calculated and the simulated swept volumes shows that the swept volume is overestimated by 1.5 per cent, an amount which is quite reasonable for all practical purposes. Effects of various other parameters on the swept volume estimation are discussed in the following sections.
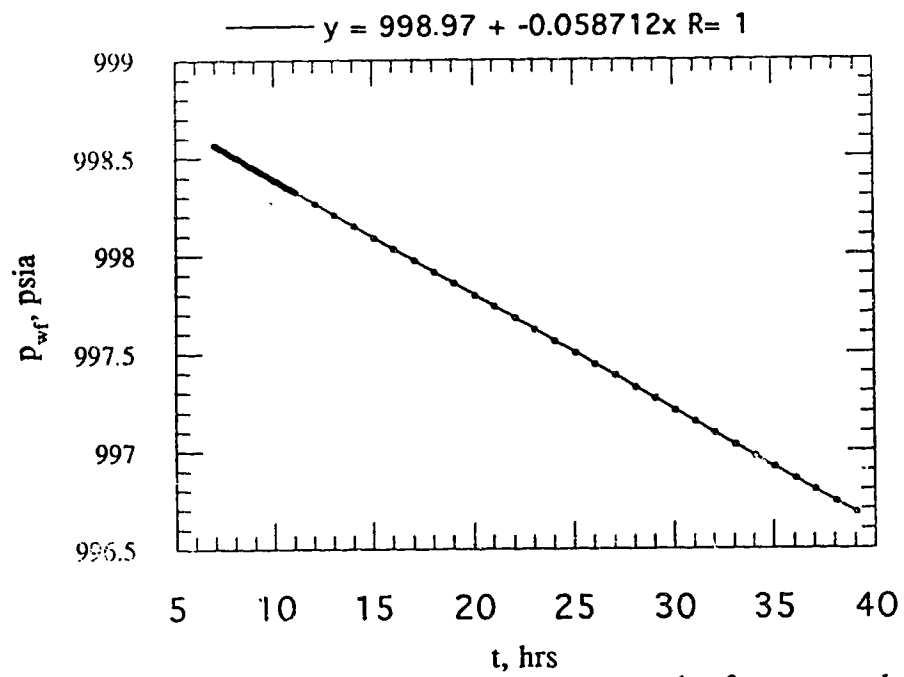
Fig. 5.7 Cartesian graph of pressure response the for the pseudosteady-
state flow period for Run 1

5.4   Possible Causes of Errors in   Swept Volume Estimation

Issaka (1991) studied the effects of wellbore gridblock size, injection time, injection rate and anisotropy of the reservoir on the swept volume estimation. He concluded that the smaller the gridblock sizes, the shorter the injection times, and the higher the injection rates, the more accurate was the swept volume estimation. Since current research is based on a specified swept volume, the effects of injection time and injection rate need not be studied. For the purposes of investigating the possible causes of errors in swept volume estimation, attempts have been made to observe the effects of grid refinement, wellbore gridblock size, swept region shape, well location, mobility ratio, storativity ratio and the number of regions of the multi-region system on the swept volume estimation.

5.4.1 Effect of Grid Refinement on the Swept Volume Estimation

The effect of grid refinement was studied through two different runs. Both runs had the same specified swept volume. In the first run, grids were distributed uniformly for the whole reservoir including the wellbore gridblocks, with a gridblock size of 9.75x4.5 ft in the x- and the z-directions. For the second run, the grid refinement pattern was applied, where the block sizes were made to increase gradually away from the center of the reservoir in the x- and the z-directions with a wellbore gridblock size of 0.78x0.4 ft. Figures 5.8 and 5.9 show the dimensionless semi-log and Cartesian pressure derivatives plotted versus t_{DA} for both runs. Figure 5.8 indicates that pseudosteady-state periods for both cases start and end at the same time. Thus, the calculated swept volume will have the same value for both grid patterns. Figure 5.9 also demonstrates the same constant value of the Cartesian derivative equal to 2π for the two different grid pattens. Comparing this value with the theoretical value, negligible error is expected in the swept volume estimation.

Fig. 5.8 Effect of grid refinement on the dimensionless semi-log pressure derivative response for a two-region composite reservoir with a horizontal well

Fig. 5.9 Effect of grid refinement on the dimensionless Cartesian pressure derivative response for a two-region composite reservoir with a horizontal well

5.4.2 Effect of Wellbore Gridblock Size on the Swept Volume Estimation

To observe the effect of wellbore gridblock size, three different runs were made. In the first run, the gridblock size was 36x4.5 ft (10.97x1.37 m) in the x- and z-directions, respectively. This gridblock size was based on uniform grids for the whole reservoir including the wellbore gridblock. For the second run, the gridblock size was reduced to 19x4.5 ft (5.79x1.37 m). For the third run, the gridblock size was reduced to 9.5x4.5 ft (2.89x1.37 m). The reservoir dimensions, the well length and the swept region volume . . . the same for all three cases. The well was producing at 800 STB/D (0.0015 m^3/s). The dimensionless semi-log and Cartesian pressure derivatives for all runs were plotted versus t_{DA} in Figures 5.10 and 5.11, respectively. Figure 5.10 shows that the pseudosteady-state period for all cases starts and ends at the same time. Therefore, the swept volume calculated for all three cases has the same value. Figure 5.11 also demonstrates the same constant value of the Cartesian derivative equal to 6.28 (2π) for different wellbore gridblock sizes. A comparison of this value with the theoretical value of 2π, obtained in Appendix C, shows that the swept volume is estimated quite accurately with essentially no error.

Fig. 5.10 Effect of gridblock size on the dimensionless semi-log
pressure derivative response for a two-region composite
reservoir with a horizontal well

Fig. 5.11 Effect of gridblock size on the dimensionless Cartesian
pressure derivative response for a two-region composite
reservoir with a horizontal well

5.4.3 Effect of Well Location on the Swept Volume Estimation

Effect of well location on the pseudosteady-state period corresponding to the swept region was investigated by changing the location of the well along the x-, y- and z-directions inside the swept region. The base case was that consisting of a centrally-located well in all three directions and a penetration ratio of 0.5.

Figure 5.12 shows the dimensionless semi-log pressure derivative responses for different xs_{oD}/as_D (0.5, 0.7, 0.9). The well was centrally-located with respect to the y- and z-axes. The pseudosteady-state flow period corresponding to the swept region starts at an earlier time for $xs_{oD}/as_D = 0.5$, and at a later time for the other cases. However, as xs_{oD}/as_D increases, the pseudosteady-state flow period starts later. Since the late portion of the data for all three cases falls on the same straight line, all three cases estimate more or less the same volume for the swept region. However, the calculated swept volumes for longer pseudosteady-state periods are more accurate. Figure 5.13 shows the dimensionless Cartesian pressure derivative responses for different xs_{oD}/as_D. Figure 5.13 shows that the constant value for the Cartesian derivative for all three cases is about 6.28. Comparing this value with the theoretical value, negligible error is expected in swept volume estimation.

For the effect of well location along the width of the swept region, three cases of ys_{1D} (0, 0.5, 1) were considered. The parameter ys_{1D} is the dimensionless starting point of the well along the swept region width. Figure 5.14 shows the dimensionless semi-log pressure derivative graph for three cases. Figure 5.14 shows that when the well is centrally-located with respect to the y-axis, the pseudosteady-state period starts at an earlier time. As the well location moves away from the center of the swept region, the pseudosteady-state period starts at later times. Since all three cases have the same late time set of data, the
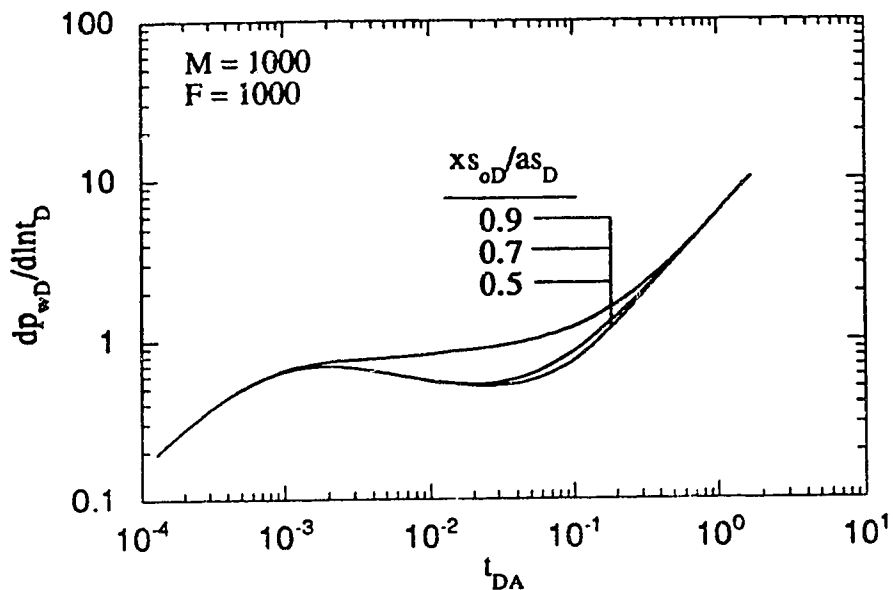
Fig. 5.12 Effect of well location in the X-direction on the dimensionless semi-log pressure derivative for a horizontal well in a two-region composite reservoir
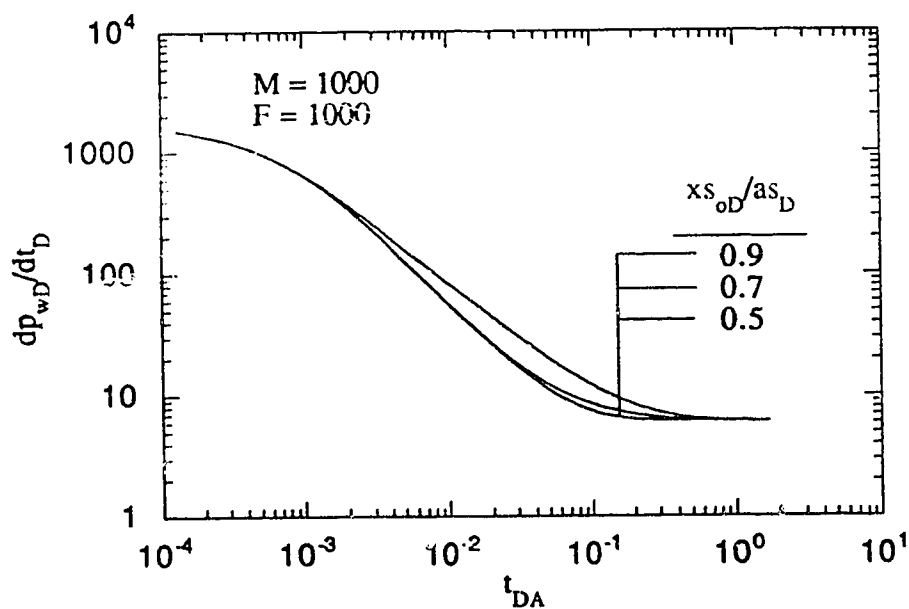
Fig. 5.13 Effect of well location in the X-direction on the dimensionless Cartesian pressure derivative for a horizontal well in a two-region composite reservoir

Cartesian straight lines corresponding to pseudosteady-state for all three cases have the same slope.

Therefore, there is not a significant difference between the volume estimations of the three cases. However, the longer the pseudosteady period, the more accurate the swept volume estimation. Figure 5.15 shows the dimensionless Cartesian pressure derivative responses for different ys_{1D}. This figure shows that the constant value for the Cartesian derivative for the three cases is about 6.28. By comparing this value with the theoretical value, negligible error is expected in swept volume estimation.

The effect of well location along the z-direction is studied through various zs_{oD}/hs_D (0.5, 0.6, 0.9). Figure 5.16 shows the dimensionless semi-log pressure derivative responses for three different cases. Since the thickness of the swept region is small compared to the length and the width of the swept region, change in the well location in the z-direction does not have a significant effect on the start of the pseudosteady-state period. From Figure 5.16, the Cartesian straight lines corresponding to the pseudosteady-state periods have the same slopes for all three cases. Therefore, the calculated volumes based on the slopes of these straight lines will be approximately the same. Figure 5.17 shows the dimensionless Cartesian pressure derivative responses for various cases. From Figure 5.17, the constant value of the Cartesian derivative is about 6.28 implying negligible error in swept volume estimation.
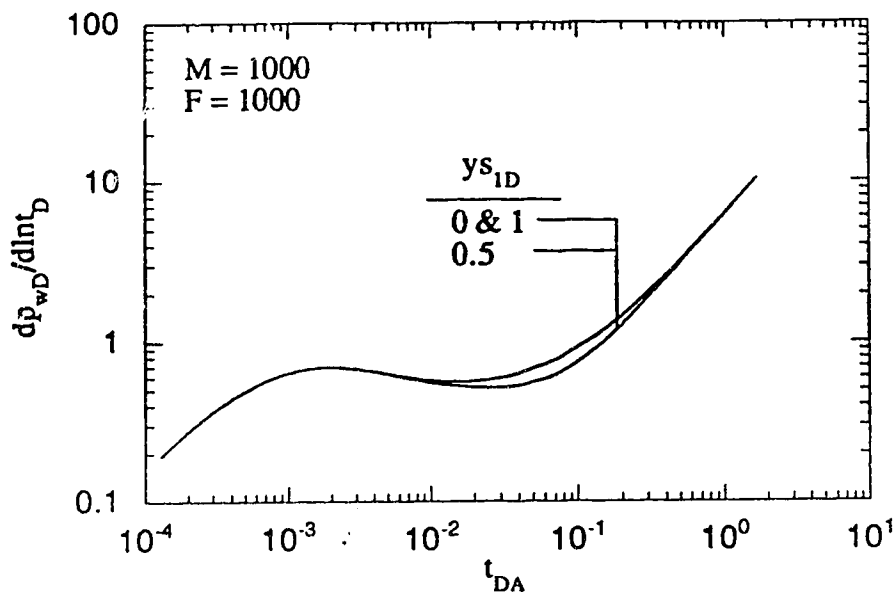
Fig. 5.14 Effect of well location in the Y-direction on the dimensionless semi-log pressure derivative for a horizontal well in a two-region composite reservoir
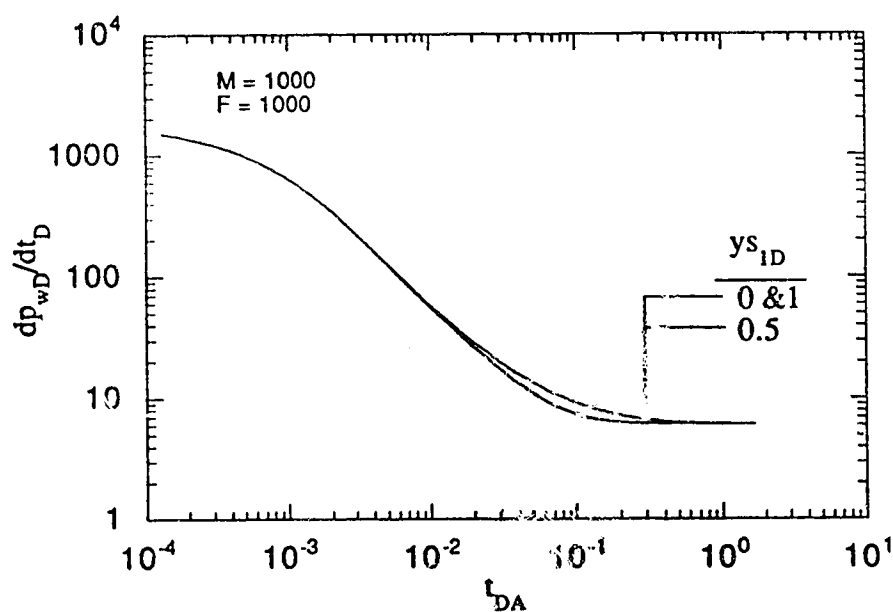
Fig. 5.15 Effect of well location in the Y-direction on the dimensionless Cartesian pressure derivative for a horizontal well in a two-region composite reservoir
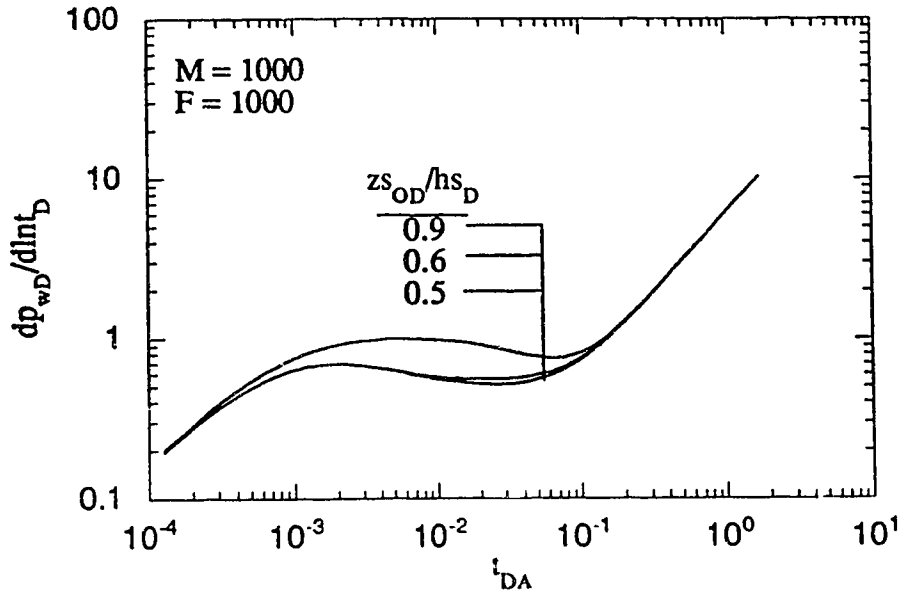
Fig. 5.16 Effect of well location in the Z-direction on the dimensionless
semi-log pressure derivative for a horizontal well in a two-region
composite reservoir
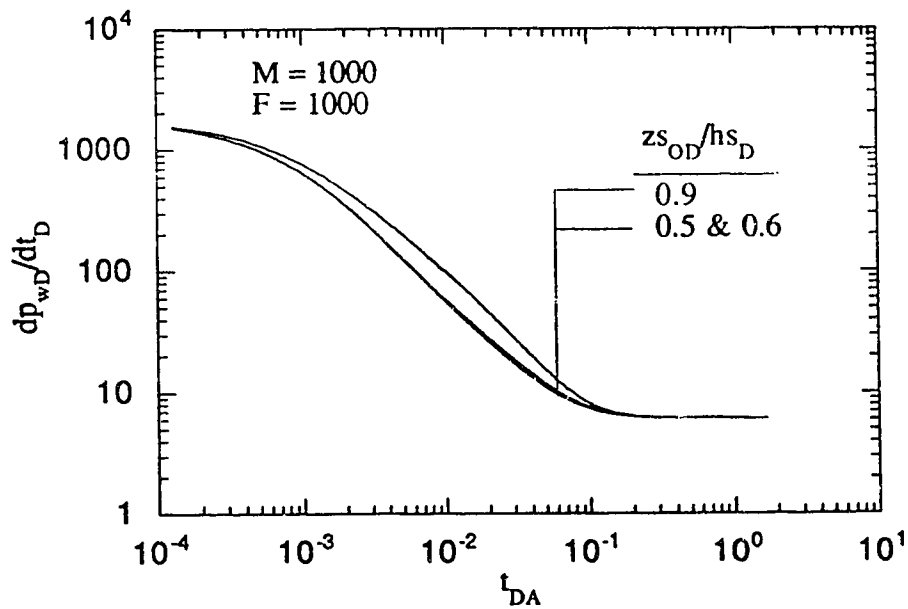
Fig. 5.17 Effect of well location in the Z-direction on the dimensionless
Cartesian pressure derivative for a horizontal well in a two-region
composite reservoir

5.4.4 Effect of Swept-Region Shape on the Swept Volume Estimation

For the purpose of investigating the effect of swept region shape on the swept-volume estimation, five different runs with different shapes of the swept region have been conducted. Figure 5.18 shows the vertical cross-sections, normal to the producer, of the swept volume shapes. For all runs, the reservoir and fluid properties are the same. The volume of the swept region has been kept constant for all runs. Figure 5.19 shows the dimensionless semi-log pressure derivative responses for the various cases. This figure shows that, for any swept region shape, the pressure transient effects are felt at the inner region boundary at the same time. Thus, for all different shapes, the pseudosteady-state period starts at the same time, and the slopes of the Cartesian straight lines, corresponding to the pseudosteady-state period, are the same. Figure 5.20 shows the Cartesian pressure derivative responses for different swept region shapes. This figure shows a zero-slope (flat) line. Since all different shapes have the same constant value of 2π for the Cartesian derivative, swept region shape does not affect swept volume estimation for the cases considered in this study.
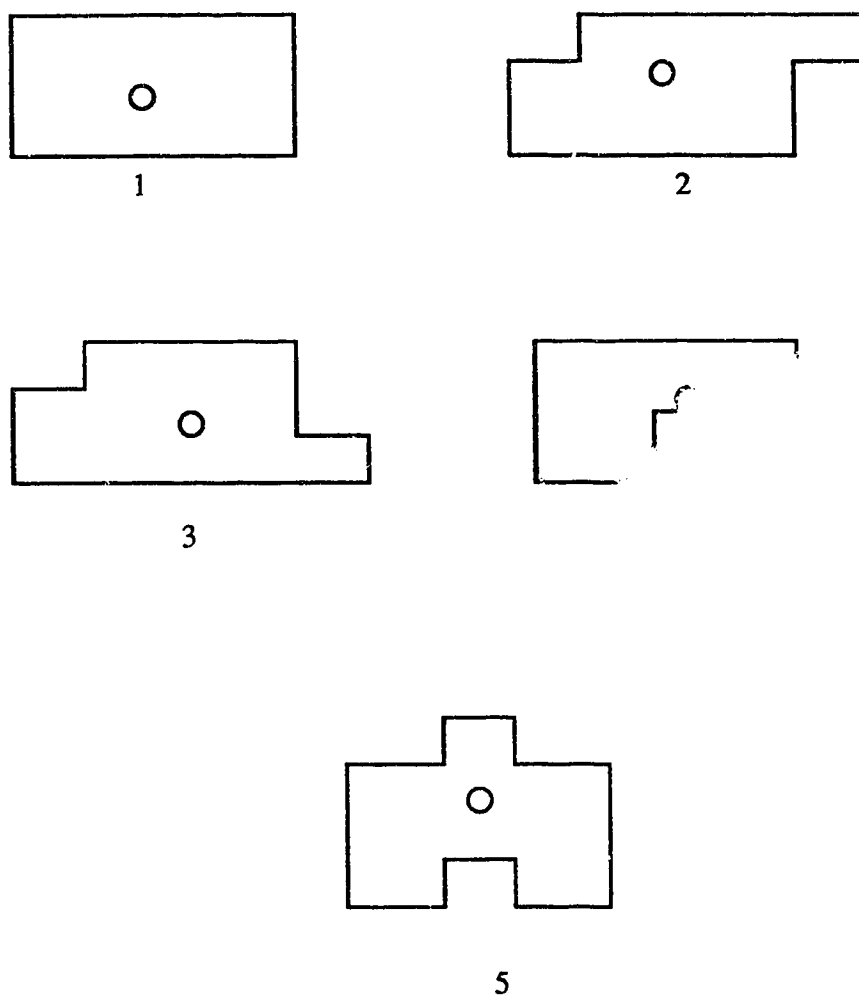
Fig. 5.18 Swept region shapes for the data sets of Figures 5.19 and 5.20
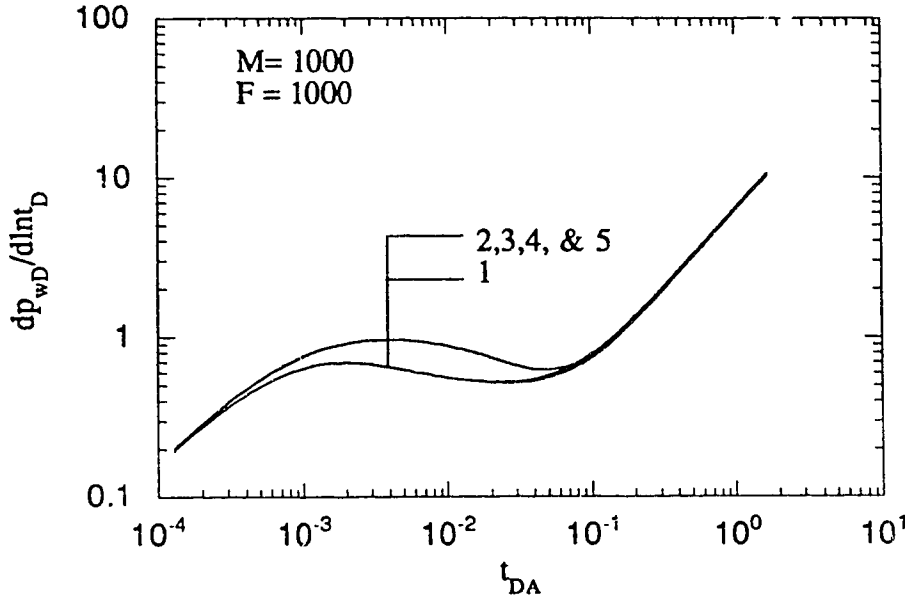
Fig. 5.19 Effect of swept-region shape on the semi-log presure
derivative response for a two-region compcsite reservoir
with a horizontal well.
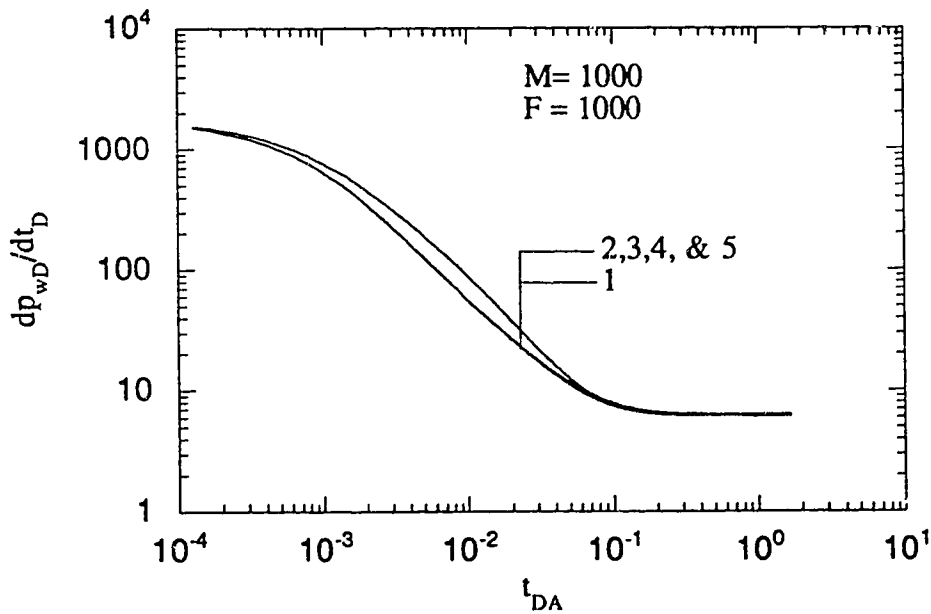
Fig. 5.20 Effect of swept-region shape on the Cartesian presure
derivative response for a two-region composite reservoir
with a horizontal well.

5.4.5 Effect of Mobility Ratio on the Swept-Volume Estimation

To observe the effect of mobility ratio on the swept-volume estimation, six runs with different mobility ratios were conducted. For all cases, the other reservoir and fluid properties and the swept volume were considered constant. The dimensionless semi-log pressure derivative responses are plotted versus t_{DA} on Figure 5.21. Figure 5.21 shows the same response for all mobility ratios. Therefore, a change in mobility ratio does not affect the swept volume estimation for F=1000. Figure 5.22 shows the dimensionless Cartesian pressure derivative responses versus t_{DA} for different mobility ratios. This figure shows that for all mobility ratios the constant value of the derivative is 6.28 implying no error in swept-volume estimation. Figure 5.23 shows the semi-log pressure derivative responses for different values of M for F=10. This figure shows that the pseudosteady-state period starts at the same time, but the pseudosteady-state period for M=10 and 100 deviates more from the unit slope line. Figure 5.24 shows the dimensionless Cartesian pressure derivative responses for various mobility ratios for F=10. From this figure, the constant value for the Cartesian derivative for M=1000 is 6, while M=100 and 10 have the same constant value of the Cartesian derivative of 5.28. Thus, for M=1000, the swept volume is overestimated by 4.5 percent, while a 16 percent error is expected for swept volumes estimated at M=100 and 10.
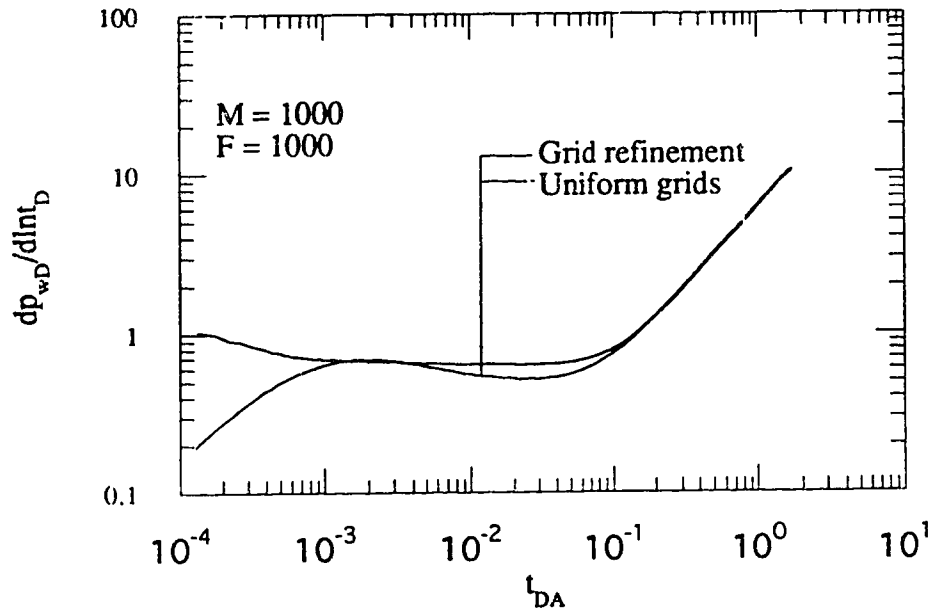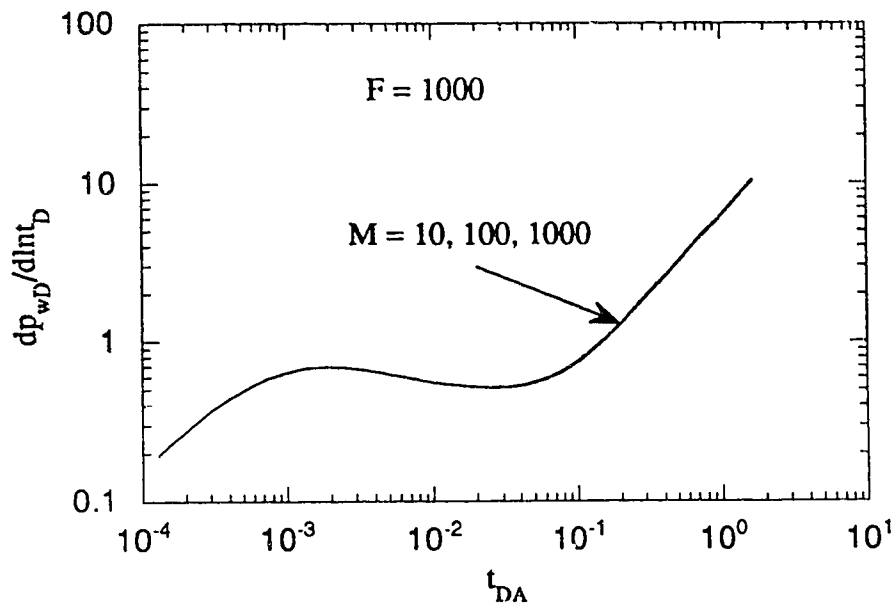
Fig. 5.21 Effect of mobility ratio on the dimensionless semi-log pressure
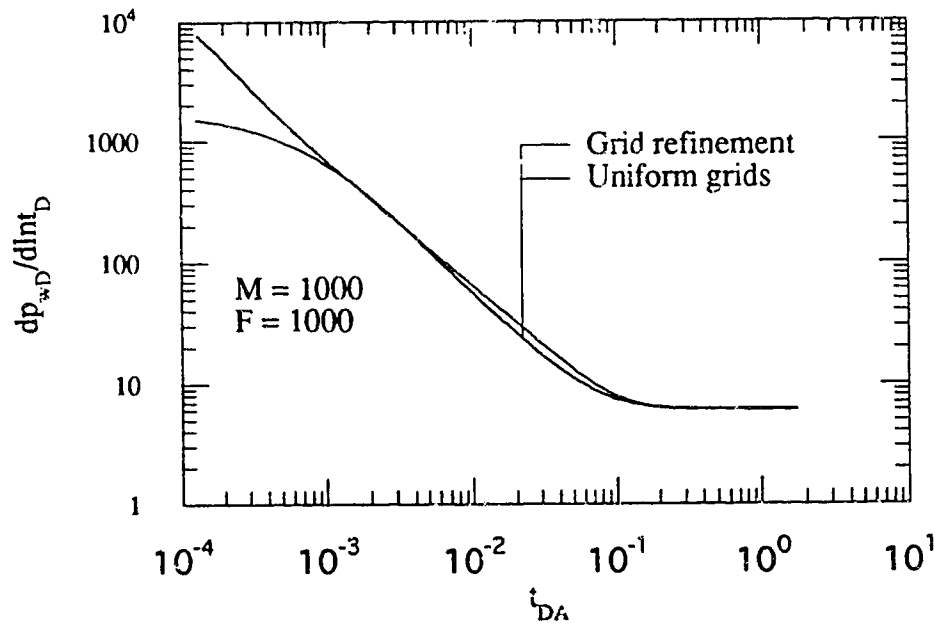derivative response for a two-region composite reservoir with
a horizontal well
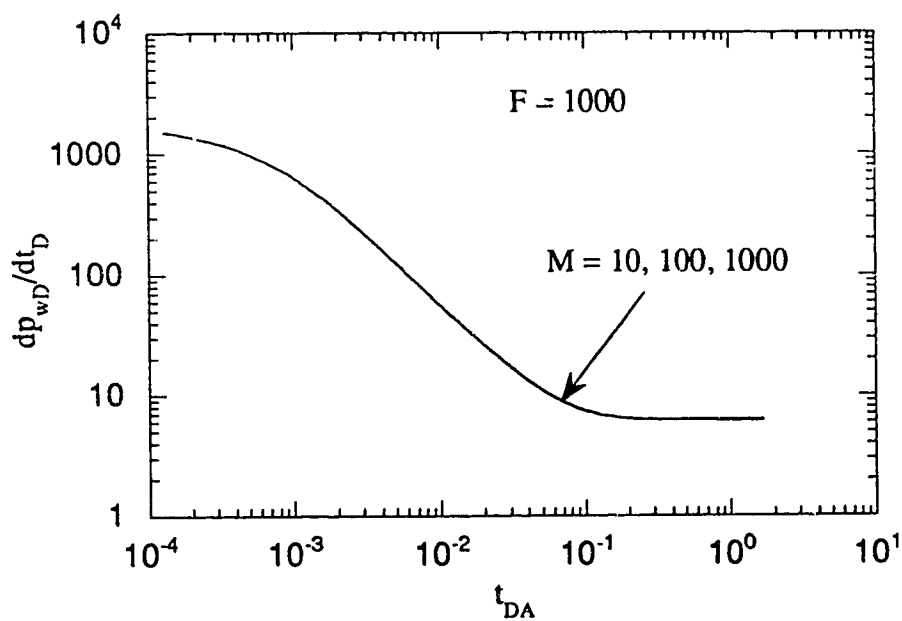
Fig. 5.22 Effect of mobility ratio on the dimensionless Cartesian pressure
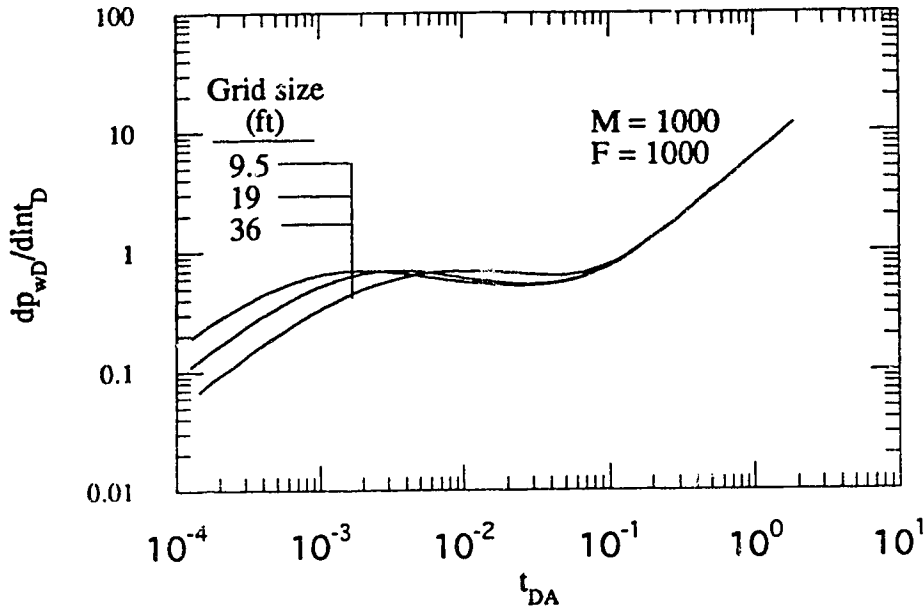derivative response for a two-region composite reservoir with a
horizontal well
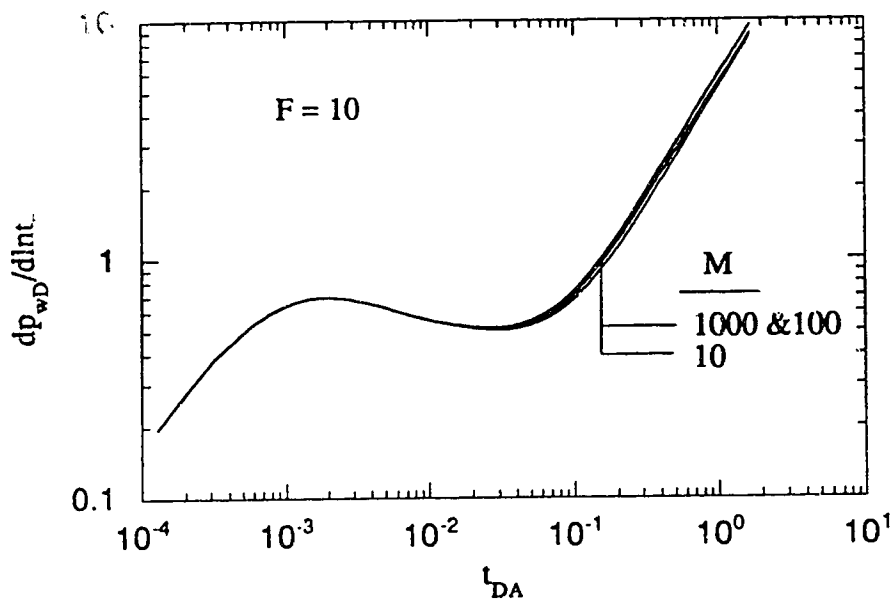
Fig. 5.23 Effect of mobility ratio on the dimensionless semi-log pressure
derivative response for a two-region composite reservoir with
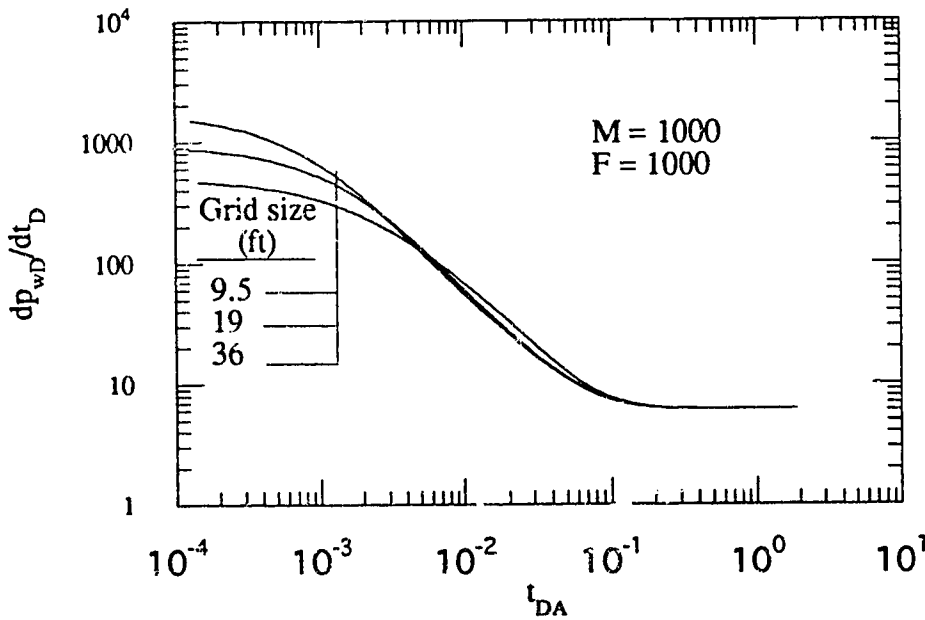a horizontal well
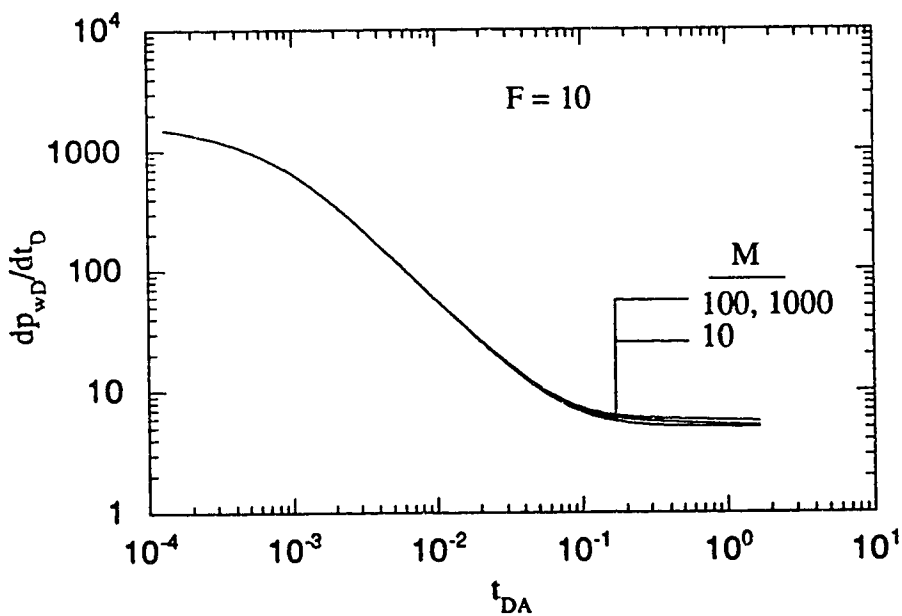
Fig. 5.24 Effect of mobility ratio on the dimensionless Cartesian pressure
derivative response for a two-region composite reservoir with a
horizontal well

5.4.6 Effect of Storativity Ratio on the Swept-Volume Estimation

The effect of storativity ratio on the swept-volume estimation is also studied through three runs with different storativity ratios. In all these runs, the other reservoir and fluid properties and the swept volume were kept constant. The dimensionless semi-log pressure derivative responses of the three cases are plotted versus t_{DA} in Figure 5.25. For all three runs, the pseudosteady-state period starts at the same time, but the pseudosteady-state period for F=10 deviates from the unit slope line earlier. However, for all three runs, practically speaking, the data set for the pseudosteady-state period lies on the same Cartesian straight line. Therefore, a change in storativity ratio does not have a noticeable effect on the swept region volume estimation for the cases considered in this study with M=1000. Figure 5.26 shows the dimensionless Cartesian pressure derivative responses for various storativity ratios. From this figure, the constant value for the Cartesian derivative for F=10 falls below 6.28, while F=100 and 1000 show the same constant value of the Cartesian derivative to be 6.28. Thus, for F=10, the swept volume is overestimated by 4.5 percent, while no error is expected for swept volumes estimated at F=100 and 1000. Figures 5.27 and 5.28 show the effect of the storativity ratio for M=10 on swept-volume estimation. These figures show that as the storativity ratio increases, the constant value of the Cartesian derivative approaches 2π. Thus, an increase in storativity ratio improves the swept volume estimation.

Generally speaking, as the mobility ratio and/or storativity ratio increase, the estimation of the swept volume improves. Also, as the mobility ratio and/or storativity ratio increase, the constant value of the Cartesian derivative approaches the theoretical value of 2π.
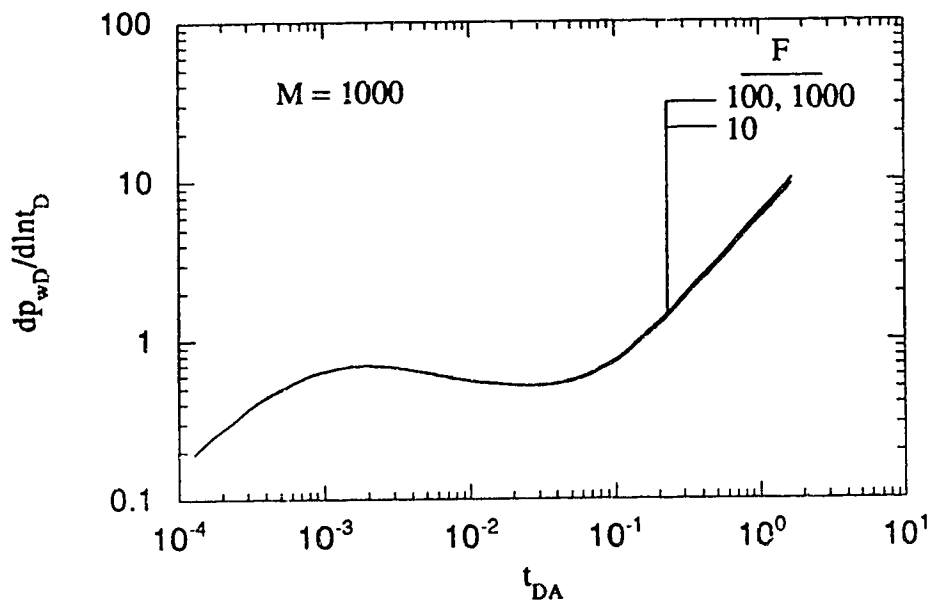
Fig. 5.25 Effect of storativity ratio on the dimensionless semi-log
pressure derivative response for a two-region composite
reservoir with a horizontal well
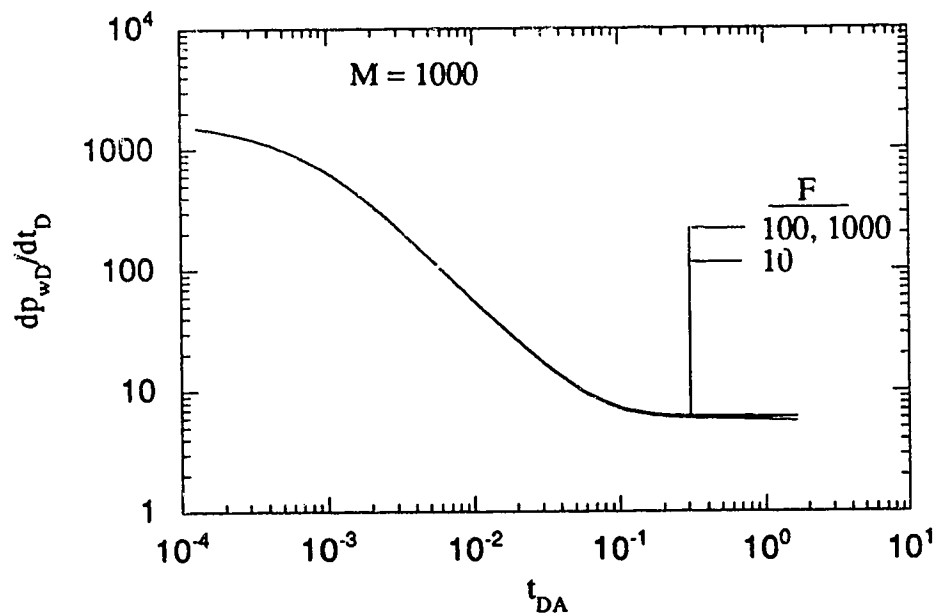
Fig. 5.26 Effect of storativity ratio on the dimensionless Cartesian
pressure derivative response for a two-region compo
reservoir with a horizontal well
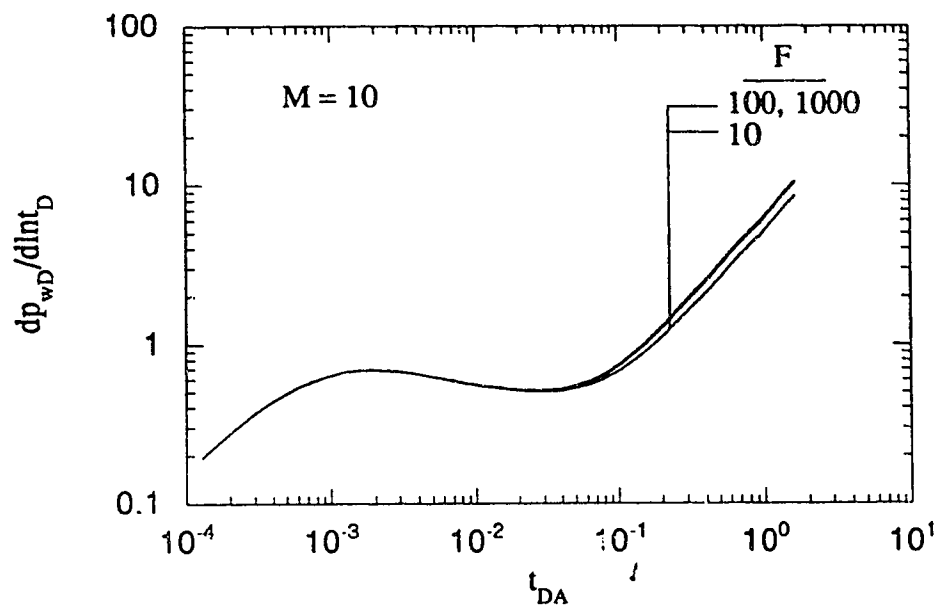
Fig. 5.27 Effect of storativity ratio on the dimensionless semi-log
pressure derivative response for a two-region composite
reservoir with a horizontal well
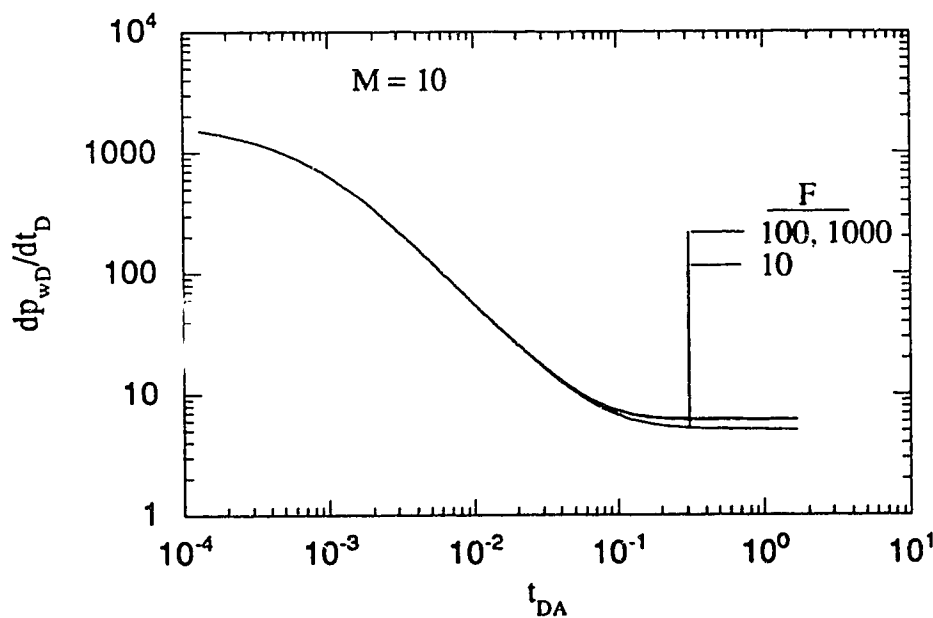
Fig. 5.28 Effect of storativity ratio on the dimensionless Cartesian
pressure derivative response for a two-region composite
reservoir with a horizontal well

5.5 Description of a Multi-Region Composite Reservoir Undergoing Steam Injection

A two-region composite reservoir consists of an inner region, called the "swept region", and an outer region, called the "unswept region". The inner region is characterized by high mobility and high storativity values. The outer region is characterized by low mobility and low storativity. However, in reality, there is not a sharp boundary between the swept and the unswept regions. In enhanced oil recovery processes, such as in-situ combustion and steam injection, a composite reservoir is created artificially. Depending on the type of process, injection rate, injection duration, etc., the mobility and storativity in the reservoir decrease gradually towards the outer boundary. In such cases, a two-region composite model is not adequate. Therefore, a multi-region composite reservoir, characterized by three or more zones, should be considered. The inner zone, called the "swept region", is full of steam and has the greatest values of mobility and storativity. After the inner zone, one or more zones exist in which the mobility and/or storativity continuously change. These zones represent the "transition zone". Steam, oil and also condensed water could be present in the transition zone. Beyond the transition zone, towards the reservoir outer boundary, there is a cold heavy oil region called the "unswept zone". The unswept zone has the lowest mobility and storativity values.

In the literature, very little work has been done on multi-region (more than two regions) composite reservoirs. A few authors have reported research on three- and multi-region composite reservoirs (Acosta, 1994, Acosta and Ambastha, 1994 and Ambastha and Ramey, 1992). All of these studies have concentrated on the application of multi-region composite models to vertical wells. To the best of my knowledge, there is no study available in the literature considering an application of a multi-region model for horizontal wells. The current research reports on a brief study of drawdown responses for multi-

region composite reservoirs with a horizontal well. The effect of the number of regions on the application of the pseudosteady-state method to estimate the swept volume has been studied. For this purpose, the two-region composite model is modified to simulate the pressure responses for composite models with more than two regions.

In a multi-region composite model, as the pressure transient effects are felt beyond the swept region, the mobility and/or storativity encountered decrease. Acosta (1994) defined the mobility and storativity ratios in such a way that these increase from the swept region to the unswept region. He also defined the mobility and storativity ratios of the swept region as unity, and those of the unswept region as the largest values of mobility and storativity ratios. In this study, the values used for mobility and storativity ratios are the same as those which were used by Acosta (1994) for a circular reservoir with a vertical well. In this study, three-, four-, six-, eight- and ten-region composite models are analyzed. In all models, the swept and the unswept regions are represented by one region each. In all models, the volumes of the swept, transition and unswept regions remain constant. The three-region model has a transition region represented by one region, while the transition region of a six-region model is represented by four regions, and that of a ten-region model by eight regions.

Depending on the reservoir and fluid properties, well conditions and the amount of steam injected, a reservoir undergoing steam injection may be represented by different flow regimes. By using pressure derivative graphs, the pressure transient analysis from a reservoir may be conducted. A plot of the dimensionless semi-log pressure derivative $(dp_{wD}/dlnt_D)$ versus area-based dimensionless time (t_{DA}) on a log-log scale can be used to identify the different flow regimes. Throughout this study, the area used in the definition of area-based dimensionless time is the area of the swept region. Since, in this study, the analysis is directed toward the application of the pseudosteady-state method to estimate the

swept volume, only the pseudosteady-state period is considered. The pseudo-steady state period, reflecting a large mobility and/or storativity contrast between the swept and the unswept zones, is expected to yield a unit slope line.

5.5.1 Drawdown Test Analysis for a Multi-region Composite Reservoir with a Horizontal Well

In this section, se i-log and Cartesian pressure de 've responses of a multi-region composite reservoir with a horizontal well are studied.

Figures 5.29 and 5.30 show the semi-log pressure derivative and the Cartesian pressure derivative of a reservoir in which the mobility in the transition region changes continuously. The overall mobility ratio is 1000, and a constant storativity throughout the whole reservoir has been used. Therefore, the storativity ratio is equal to unity everywhere in the reservoir. From Figure 29, for all models, an early radial flow period corresponding to the swept zone mobility develops between $t_{DA}=0.00065$ and $t_{DA}=0.003$. A pseudosteady-state period corresponding to the mobility contrast between the swept and unswept regions starts at about $t_{DA}=2$. The semi-log pressure derivative has a value of about 0.3 for the early radial flow period. However, this value should be equal to $(hs_D/2)$ for horizontal wells. By using Equation 4.33 for an appropriate definition of hs_D, the theoretical value is:

$$\frac{hs_D}{2} = \frac{40}{2(300)} \sqrt{\frac{2000}{200}} = 0.21$$

Thus, the semi-log pressure derivative for the early radial flow is overestimated by 43 percent. The difference between the theoretical value and the simulated value could be because of the wellbore storage effect which masks portions of the early radial flow period.
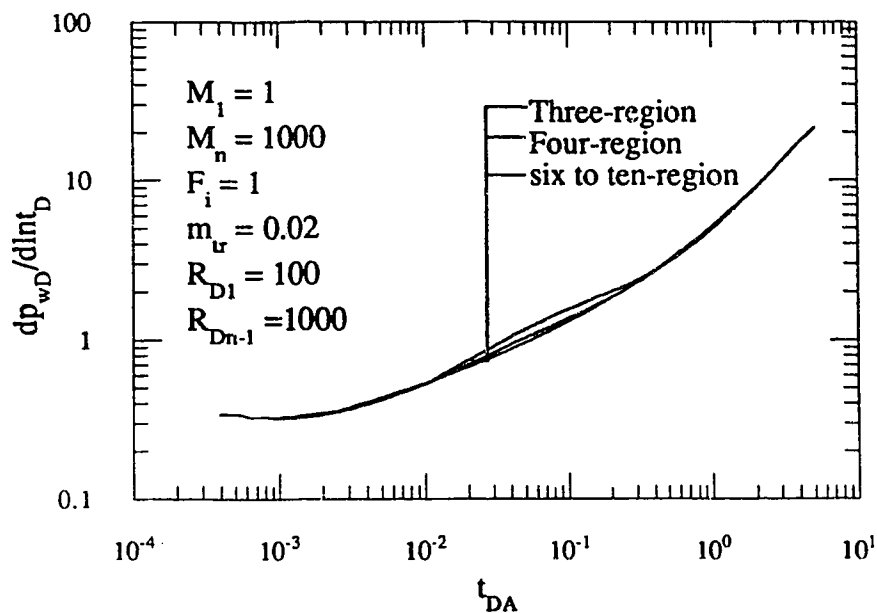
Figure 5.29 Dimensionless semi-log pressure derivative response
for a multi-region composite reservoir with mobility
variation
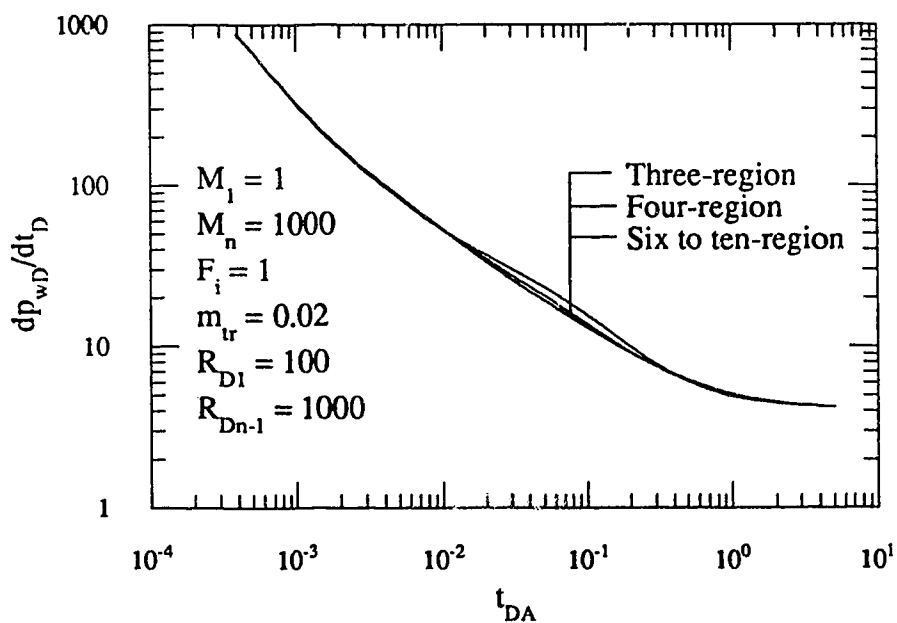
Figure 5.30 Dimensionless Cartesian pressure derivative response
for a multi-region composite reservoir with mobility
variation

Moreover,it could be due to inaccuracies in the numerical solution. In Figure 5.29, neither the departure time from the early radial flow period nor the pseudosteady-state response are significantly affected by the number of regions of the composite model. Thus, a change in the number of the regions does not affect the swept volume estimation. However, the transition region's transient pressure behaviour is affected by the number of regions of the model. From Figure 5.29, the transition region's values for the semi-log pressure derivative for the three-region composite model are higher than those for the other composite models. The preceding observations are the same as those reported by Acosta (1994) for a multi-region composite reservoir with a vertical well.

Figure 5.30 shows the dimensionless Cartesian pressure derivative plotted versus area-based dimensionless time. This figure confirms the existence of the early radial flow period by a negative unit slope line, and a pseudosteady-state flow period by a flattening of the Cartesian pressure derivative. This flattening occurs when the Cartesian pressure derivative has a value lower than 2π of about 4.2. This behaviour suggests that estimating the swept volume by the pseudosteady-state method yields an overestimation of the actual swept volume. However, this value should be 6.28 theoretically (see Appendix C). Thus, there is a 33 percent error in estimating the swept volume consisting of the volume to the end of the transition region.

From Figure 5.29, soon after the early radial flow period, the dimensionless semi-log pressure derivative falls on a straight line, for the three-region composite model. This line appears because of the mobility contrast of the inner region and the single transition region. The slope of this line is significantly less than unity because of the low mobility contrast between the inner region and the transition region. Correspondingly, as expected, Figure 5.30 does not show a complete flattening for the three-region composite model during intermediate time. From Figure 5.29, as the number of transition regions increases, the

slope of the aforementioned straight line decreases, because the mobility contrast between the inner region and the first region of the transition zone decreases.

Figure 5.29 shows that at a later time in the transition region response, all composite models join together and the semi-log pressure derivative falls on a straight line with a slope of unity. This unit slope line is an indication of a pseudosteady-state period due to the high mobility contrast between the transition region and the unswept region. Figure 5.30 confirms this high mobility contrast by a flattening of the Cartesian pressure derivative. This flattening occurs when the constant value for the Cartesian derivative is about 4.2 implying 33 percent error in the swept volume estimation.

A summary of the effect of different variables on the swept volume estimation is presented in Table 5.3. A summary of the constant value of the Cartesian derivative and the percent error in the swept volume estimation for various cases studied is presented in Table 5.4.

Table 5.3   Summary of the effect of different variables on the swept volume estimation

Description	Effect on the swept volume estimation
Grid size	0
well location (x-direction)	0
well location (y-direction)	0
well location (z-direction)	0
Swept region shape	0
Mobility ratio	The larger the M, the better the swept volume estimation
Storativity ratio	The larger the F, the better the swept volume estimation
Multi-region	0

Table 5.4   Constant value of the Cartesian derivative for various cases

Description	Constant value of Cartesian derivative	Percent Error in swept volume estimation
Grid size	6.28	0
well location (x-direction)	6.28	0
well location (y-direction)	6.28	0
well location (z-direction)	6.28	0
Swept region shape	6.28	0
Mobility ratio	5.28-6.28	0-16
Storativity ratio	5.28-6.28	0-16
Multi-region	4.2	33

6. CONCLUSIONS AND RECOMMENDATIONS

In the current research, the pressure transient behaviour of a horizontal well in a closed, and box-shaped composite reservoir was studied. The pressure responses were studied. The main focus was on the application of the pseudosteady-state method in the estimation of the steam chamber volume and the steam chamber mobility from the well test data. Also, the effect of different parameters on the steam chamber volume estimation was studied.

6.1 Conclusions

From the study of the pressure transient responses for a composite reservoir with a horizontal well, the following conclusions may be drawn:

1. The numerical solution for the pressure transient response of a horizontal well in a closed, box-shaped, composite reservoir can be generated with a reasonable degree of accuracy.

2. The pseudosteady-state method may be used to estimate the swept volume for steam injection through a horizontal well. Various parameters, such as grid pattern, grid size, well location in the x-, y-, and z-directions, swept region shape, mobility ratio and storativity ratio do not affect significantly swept volume estimation and the constant value of the Cartesian pressure derivative during the pseudosteady-state flow regime for the cases presented in this study.

3. For the cases studied, early radial flow followed by a pseudosteady-state flow regime appeared in all simulated tests. Early linear, late pseudo-radial and late

linear flow regimes did not appear for any simulated test. This must have occurred due to the specific swept volume dimensions, horizontal well lengths and horizontal well locations considered in this study.

4. For a multi-region representation of the swept volume, the pseudosteady-state method may yield a significantly overestimated swept volume for a horizontal well. This conclusion is consistent with the findings of Acosta (1994) based on an analytical study of a multi-region composite reservoir with production (or injection) occuring through a vertical well.

6.2 Recommendations

1. The effect of steam assisted gravity drainage on the swept volume estimation should be studied for horizontal wells in composite reservoirs.

2. An analytical study of the pressure behaviour of a horizontal well in a composite reservoir should be conducted for comparison with the results from the numerical studies.

REFERENCES

Acosta, L. G.: "Thermal Well Test Analysis and Evaluation of Reservoir Characterization Methods Using an Analytical Multi-Region Composite Reservoir Model," M.Sc. Thesis, University of Alberta, Edmonton, Alberta (March 1994) 193 pp.

Acosta, L. G. and Ambastha, A. K.: "Thermal Well Test Analysis Using an Analytical Multi-Region Composite Reservoir Model," paper SPE 28422 presented at the Annual Technical Conference of SPE of AIME in New Orleans, LA (Sept. 25-28, 1994).

Ambastha, A. K.: "Pressure Transient Analysis for Composite Systems," Ph.D. Thesis, Stanford University (October 1988) 193 pp.

Ambastha, A. K. and Ramey, H. J. Jr.: "Thermal Recovery Well Test Design and Interpretation," *SPE Form. Eval.* (June 1989) 173-180.

Ambastha, A. K. and Ramey, H. J. Jr.: "Injection-Time Effects on Falloff Responses from Composite Reservoirs," *SPE Form. Eval.* (December 1990) 385-388.

Ambastha, A. K. and Ramey, H. J. Jr.: "Pressure Transient Analysis for a Three-Region Composite Reservoir," paper SPE 24378 presented at the SPE Rocky Mountain Regional Meeting in Casper, Wyoming (May 18-21, 1992).

Babu, D. K. and Odeh, A. S.: "Productivity of a Horizontal Well," *SPE Res. Eng.* (Nov. 1989) 417-21.

Bourdet, D., Ayoub, J. A. and Pirard, Y. M.: "Use of Pressure Derivative in Well-Test Interpretation, " *SPE Form. Eval.* (June 1989) 293-302.

Brigham, W. E.: "Discussion of Productivity of a Horizontal Well," *SPE Res. Eng.* (May 1990) 254-55.

Brown, L. P.: "Pressure Transient Behaviour of the Composite Reservoir," paper SPE 14316 presented at 60th Annual Technical Conference & Exhibition Las Vegas, NV (Sept. 22-25, 1985).

Butler, R. M.: "Steam-Assisted Gravity Drainage: Concept, Development, Performance and Future," JCPT (Feb. 1994) 44-50.

Clonts, M. D. and Ramey, H. J., Jr.: "Pressure Transient Analysis for Wells with Horizontal Drainholes," paper SPE 15116 presented at the SPE California Regional Meeting, Oakland, CA (April 2-4, 1986).

Da Prat, G., Bockh, A. and Prado, L.: "Use of Pressure Falloff Testing to Locate the Burning Front in the Miga Field, Eastern Venezuela," paper SPE 13667 presented at the California Regional Meeting, Bakersfield, CA (March 27-29, 1985).

Economides, M. J., Deimbacher, F. X., Brand, C. W. and Heinemann, Z. E.: "Comprehensive Simulation of Horizontal-Well Performance," SPE Form. Eval. (Dec. 1991) 418-26.

Eggenschwiler, M., Satman, A. and Ramey, H. J., Jr.: "Interpretation of Injection Well Pressure Transient Data in Thermal Oil Recovery," paper SPE 8908 presented at the California Regional Meeting of SPE of AIME, Pasadena, CA (April 9-11, 1980).

Farouq Ali, S. M. and Ferrer, J.: "A Three-Phase, Two-Dimensional Compositional Thermal Simulator for Steam Injection Processes," JCPT (Jan.-Mar 1977) 78-90.

Farouq Ali, S. M., Thomas, S. and Kristoff, B. J.: "How Horizontal Wells are Revolutionizing Heavy Oil Production," paper 7 presented at the Fifth Petroleum Conference of South Saskatchewan Section, The Petroleum Society of CIM, held with CANMET in Regina, SK (Oct. 18-20, 1993).

Fassihi, M. R.: "Evaluation of an Analytic Technique for Estimating Swept Volume from Thermal Pressure Falloff Tests in Heterogeneous Systems," SPE Form. Eval. (June 1988) 449-58.

Goode, P. A. and Kuchuk, F. J.: "Inflow Performance of Horizontal Wells," SPE Res. Eng. (August 1991) 337-45.

Goode,P.A. and Thambynayagam, R.K.M.: "Pressure Drawdown and Buildup Analysis of Horizontal Wells in Anisotropic Media," *SPE Form.* Eval. (Dec. 1987) 683-697.

Issaka, M. B.: "Horizontal Well Testing under Thermal and Non-Thermal Situations," M.Sc. Thesis, University of Alberta, Edmonton, Alberta (Nov. 1991) 133 pp.

Issaka, M. B. and Ambastha, A. K.: "Drawdown and Buildup Pressure Derivative Analysis for Horizontal Wells," paper SPE 24323 presented at the Rocky Mountain Reg. Mtg. and Exhibition of SPE of AIME, Casper, WY (May 18-21, 1992a).

Issaka, M. B. and Ambastha, A. K.: "Thermal Well Testing for a Horizontal Well," paper CIM 92-24 presented at the CIM 1992 Annual Technical Conference in Calgary, AB (June 7-10, 1992b).

Joshi, S. D.: "Augmentation of Well Productivity Using Slant and Horizontal Wells," paper SPE 15375 presented at the 61st SPE Annual Technical Conference and Exhibition, New Orlean, Louisiana (October 5-8, 1986).

Kamal, M. M., Buhidma, I. M., Smith, S. A. and Jones, W. R.: " Pressure Transient Analysis for a Well with Multiple Horizontal Sections," paper SPE 26444 presented at the 68th Annual Technical Conference and Exhibition of SPE of AIME, Houston, TX (Oct. 3-6, 1993).

Karcher, B. J., Giger, F. M. and Combe, J.: "Some Practical Formulas to Predict Horizontal Well Behaviour," paper SPE 15430 presented at the 61st Annual Technical Conference and Exhibition of SPE of AIME, New Orleans, LA (Oct. 5-8, 1986).

Kazemi, H.: "Locating a Burning Front by Pressure Transient Measurements," *J. Pet. Tech.* (February 1966) 227-32.

Kuchuk, F. J., Goode, P. A., Wilkinson, D. J. and Thambynayagam, R. K. M.: "Pressure Transient Behaviour of Horizontal Wells With and Without Gas Cap or Aquifer," *SPE Form. Eval.* (March 1991) 86-94.

Messner, G. L. and Williams, R. L.: "Application of Pressure Transient Analysis in Steam Injection Wells," paper SPE 10781 presented at the 1982 California Regional Meeting of SPE of AIME, San Francisco, CA (March 24-26, 1982).

Odeh, A.S. and Babu, D.K.: "Transient Flow Behaviour of Horizontal wells, Pressure Drawdown, and Buildup Analysis," *SPE Form.* Eval. (March 1990) 7-15.

Onyekonwu, M. O., Ramey, H. J., Jr., Brigham, W. E. and Jenkins, R.: "Interpretation of Simulated Falloff Tests," paper SPE 12746 presented at the California Regional Meeting of SPE of AIME, Long Beach, CA (April 11-13, 1984).

Ozkan, E., Raghavan, R. and Joshi, S. D.:"Horizontal Well Pressure Analysis," *SPE Form. Eval.* (Dec. 1989) 567-75.

Peaceman, D. W.: "Further Discussion of Productivity of a Horizontal Well," *SPE Res. Eng.* (Aug. 1990) 437-38.

Peaceman, D.W.: "Representation of a Horizontal Well in Numerical Reservoir Simulation" paper SPE 21217 presented at the 11th SPE Symposium on Reservoir Simulation, Anaheim, CA (Feb. 17-20, 1991).

Satman, A., Eggenschwiler, M., Tang, R. W. and Ramey, H. J., Jr.: "An Analytical Study of Transient Flow in Systems with Radial Discontinuities," paper SPE 9399 presented at the 55th Annual Meeting of SPE of AIME, Dallas, Texas (Sept. 21-24, 1980).

Stehfest, H.: "Algorithm 368, Numerical Inversion of Laplace Transforms," D-5, Communications of ACM (Jan. 1970) Vol. 13, No. 1, 49.

Van Poollen, H. K.: "Transient Tests Find Fire Front in an In-Situ Combustion Project," *Oil & Gas J.* (Feb. 4, 1965) 78-80.

Walsh, J. W., Jr., Ramey, H. J., Jr. and Brigham, W. E.: "Thermal Injection Well Falloff Testing," paper SPE 10227 presented at the 56th Annual Meeting of SPE of AIME, San Antonio, TX (Oct. 5-6, 1981).

Ziegler, V. M.: "Injection-Well Testing in a Light Oil Steamflood, Buena Vista Hills Field, CA " *SPE Prod. Eng.* (Nov. 1990) 394-402.

APPENDIX   A

Program #1:   Pressure Transient Response for a Horizontal Well in Two-Region
Composite Reservoirs

Program # 2:   Pressure Transient Response for a Horizontal Well in Multi-Region
Composite Reservoirs

```
*_____
___

*                    PROGRAM # 1
*
*THE PURPOSE OF THIS PROGRAM IS TO GENERATE PRESSURE   TRANSIENT
*RESPONSE FOR A HORIZONTAL WELL IN A TWO-REGION COMPOSITE
*RESERVOIR.
*_____
___
*
* VARIABLE IDENTIFICATION
*_____
*
* NX          = NUMBER OF GRIDS IN X-DIRECTION
* NY          = NUMBER OF GRIDS IN Y-DIRECTION
* NZ          = NUMBER OF GRIDS IN Z-DIRECTION
* MX,MY,MZ= FIRST GRIDBLOCK NUMBER IN EACH DIRECTION
* LX,LY,LZ   = LAST GRIDBLOCK NUMBER IN EACH DIRECTION
* CMP1        = COMPRESSIBILITY IN THE SWEPT REGION
* CMP2        = COMPRESSIBILITY IN THE UNSWEPT REGION
* VIS1        = VISCOSITY IN THE SWEPT REGION
* VIS2        = VISCOSITY IN THE UNSWEPT REGION
* FVF1        = FORMATION VOLUME FACTOR IN THE SWEPT REGION
* FVF2        = FORMATION VOLUME FACTOR IN THE UNSWEPT REGION
* POR1        = POROSITY IN THE SWEPT REGION
* POR2        = POROSITY IN THE UNSWEPT REGION
* RW          = WELLBORE RADIUS
* PRSIR       = RESERVOIR INITIAL PRESSURE
* PKS!        = RESERVOIR IN THE PREVIOUS TIME STEP
* RT1         = TOTAL PRODUCTION RATE
* APX1        = ABSOLUTE PERMEABILITY IN X-DIRECTION OF THE
*                 SWEPT REGION
* APX2        = ABSOLUTE PERMEABILITY IN X-DIRECTION OF THE
*                 UNSWEPT REGION
* APY1        = ABSOLUTE PERMEABILITY IN Y-DIRECTION OF THE
*                 SWEPT REGION
* APY2        = ABSOLUTE PERMEABILITY IN Y-DIRECTION OF THE
*                 UNSWEPT REGION
* APZ1        = ABSOLUTE PERMEABILITY IN Z-DIRECTION OF THE
*                 SWEPT REGION
* APZ2        = ABSOLUTE PERMEABILITY IN Z-DIRECTION OF THE
*                 UNSWEPT REGION
* SRP         = STEAM RELATIVE PERMEABILITY
* ORP         = OIL RELATIVE PERMEABILITY
* XLGTH       = RESERVOIR LENGTH
* WDTH        = RESERVOIR WIDTH
* THK         = RESERVOIR THICKNESS
* WL          = WELL LENGTH
* AS          = SWEPT REGION LENGTH
* BS          = SWEPT REGION WIDTH
* HS          = SWEPT REGION THICKNESS
* VS          = SWEPT REGION VOLUME
* XO          = X-COORDINATE OF THE WELL W.R.T. OUTER REGION
```

* ZO	= Z-COORDINATE OF THE WELL W.R.T. OUTER REGION
* XSO	= X-COORDINATE OF THE WELL W.R.T. INNER REGION
* ZSO	= Z-COORDINATE OF THE WELL W.R.T. INNER REGION
* Y1	= STARTING POINT OF THE WELL W.R.T. OUTER REGION
* Y2	= ENDING POINT OF THE WELL W.R.T. OUTER REGION
* YS1	= STARTING POINT OF THE WELL W.R.T. INNER REGION
* YS2	= ENDING POINT OF THE WELL W.R.T. INNER REGION
* AD	= DIMENSIONLESS RESERVOIR LENGTH
* BD	= DIMENSIONLESS RESERVOIR WIDTH
* HD	= DIMENSIONLESS RESERVOIR THICKNESS
* ASD	= DIMENSIONLESS SWEPT REGION LENGTH
* BSD	= DIMENSIONLESS SWEPT REGION WIDTH
* HSD	= DIMENSIONLESS SWEPT REGION THICKNESS
* XOD	= DIMENSIONLESS X-COORDINATE OF THE WELL W.R.T.
*	OUTER REGION
* ZOD	= DIMENSIONLESS Z-COORDINATE OF THE WELL W.R.T.
*	OUTER REGION
* XSOD	= DIMENSIONLESS X-COORDINATE OF THE WELL W.R.T.
*	INNER REGION
* ZSOD	= DIMENSIONLESS Z-COORDINATE OF THE WELL W.R.T.
*	INNER REGION
* Y1D	= DIMENSIONLESS STARTI℩G POINT OF THE WELL W.R.T.
*	OUTER REGION
* Y2D	= DIMENSIONLESS ENDING POINT OF THE WELL W.R.T.
*	OUTER REGION
* YS1D	= DIMENSIONLESS STARTING POINT OF THE WELL W.R.T.
*	INNER REGION
* YS2D	= DIMENSIONLESS ENDING POINT OF THE WELL W.R.T.
*	INNER REGION
* LD	= DIMENSIONLESS WELL LENGTH
* D1XD	= SHORTEST DIMENSIONLESS DISTANCE OF THE WELL
*	FROM BOUNDARY W.R.T. X-DIRECTION
* D2XD	= LONGEST DIMENSIONLESS DISTANCE OF THE WELL
*	FROM BOUNDARY W.R.T. X-DIRECTION
* D1YD	= SHORTEST DIMENSIONLESS DISTANCE OF THE WELL
*	FROM BOUNDARY W.R.T. Y-DIRECTION
* D2YD	= LONGEST DIMENSIONLESS DISTANCE OF THE WELL
*	FROM BOUNDARY W.R.T. Y-DIRECTION
* D1ZD	= SHORTEST DIMENSIONLESS DISTANCE OF THE WELL
*	FROM BOUNDARY W.R.T. Z-DIRECTION
* D2ZD	= LONGEST DIMENSIONLESS DISTANCE OF THE WELL
*	FROM BOUNDARY W.R.T. Z-DIRECTION
* EER	= END OF EARLY RADIAL FLOW PERIOD
* SEL	= START OF EARLY LINEAR FLOW PERIOD
* EEL	= END OF EARLY LINEAR FLOW PERIOD
* SLS	= START OF LATE PSEUDO-RADIAL FLOW PERIOD
* ELS	= END OF LATE PSEUDO-RADIAL FLOW PERIOD
* SLL	= START OF LATE LINEAR FLOW PERIOD
* ELL	= END OF LATE LINEAR FLOW PERIOD
* DP	= PRESSURE DROP
* PRS	= BLOCK PRESSURE
* PRF	= WELLBLOCK PRESSURE
* PRIS	= WELLBLOCK PRESSURE DROP
* XMB	= MATERIAL BALANCE

```
* TIM        = TOTAL TIME
* TD         = DIMENSIONLESS TIME
* PD         = DIMENSIONLESS PRESSURE
*_____          *
*
      IMPLICIT REAL*8(A-H,O-Z)
      DIMENSION ARAX(45,45,45),ARAY(45,45,45),ARAZ(45,45,45),
     &    VOLB(45,45,45),DPH(45,45,45),DL(20000),EL(20000),FL(20000),
     &    W(20000),G(20000),DPI(45,45,45),ZK(45,45,45),ZK1(45,45,45),
     &    DX(45),DY(45),DZ(45),QL(20000),UL(20000),PRF1(45,45,45),
     &    CI(45,45,45),Q(45,45,45),PRIS(45,45,45),FVF(45,45,45),
     &    RTE(45,45,45),RADE(45,45,45),PRM(45,45,45),PI(45,45,45),
     &    PRS(45,45,45),PRSI(45,45,45),DP(45,45,45),
     &    PRF(45,45,45),CIX(45,45,45),CIY(45,45,45),CIZ(45,45,45)
      DIMENSION PRMX(45,45,45),PRMY(45,45,45),PRMZ(45,45,45),
     &    TRMX1(45,45,45),TRMX2(45,45,45),TRMY1(45,45,45),
     &    TRMY2(45,45,45),TRMZ1(45,45,45),TRMZ2(45,45,45),
     &    AP(45,45,45),E(45,45,45),Z(45,45,45),B(45,45,45),
     &    D(45,45,45),F(45,45,45),H(45,45,45),S(45,45,45),
     &    POR(45,45,45),CMP(45,45,45),VIS(45,45,45)
*_____
* READING THE VALUES
*_____
      OPEN(5,FILE='h1.d')
      OPEN(8,FILE='h1.o')
*_____
      READ(5,*) NX,NY,NZ
      READ(5,*) MX,MY,MZ
      READ(5,*) LX,LY,LZ
      READ(5,*) NY1,NY2
      READ(5,*) NX1,NZ1
      READ(5,*) GX,GZ,P,KK
      READ(5,*) MB,SHAPE,TOLL
      READ(5,*) CMP11,CMP21
      READ(5,*) VIS11,VIS21
      READ(5,*) FVF1,FVF2
      READ(5,*) POR1,POR2,RW1
      READ(5,*) PRSIB1,RTE11
      READ(5,*) NO,M,N,COUNT
      READ(5,*) TIME1,DELTA1,DELTB1
      READ(5,*) APX1,APY1,APZ1
      READ(5,*) APX2,APY2,APZ2
      READ(5,*) SRP,ORP
      READ(5,*) XLGTH1,WDTH1,THK1,WL1
      READ(5,*) Y11,Y21
      READ(5,*) O1,O2,O3
*_____
* CONVERSION FACTORS
*_____
      FM=3.28084D0
      PP=6894.76D0
      SH=3600
      DM=1.013E15
      DB=543439.6D0
```

```
*
* CONVERTING FROM FIELD UNITS TO SI UNITS
*
      VIS1=VIS11/1000
      VIS2=VIS21/1000
      RW=RW1/FM
      CMP1=CMP11/PP
      CMP2=CMP21/PP
      PRSIB=PRSIB1*PP
      DELTA=DELTA1*SH
      DELTB=DELTB1*SH
      TIME=TIME1*SH
      PRMX1=APX1*SRP/DM
      PRMY1=APY1*SRP/DM
      PRMZ1=APZ1*SRP/DM
      PRMX2=APX2*ORP/DM
      PRMY2=APY2*ORP/DM
      PRMZ2=APZ2*ORP/DM
      RTE1=RTE11/DB
      XLGTH=XLGTH1/FM
      WDTH=WDTH1/FM
      THK=THK1/FM
      WL=WL1/FM
      Y1=Y11/FM
      Y2=Y21/FM
*
*
* UNIFORM GRID
*
      DO 11 I=1,NY
          DY(I)=(WDTH-WL)/(NY-(NY2-NY1+1))
11  CONTINUE
      DO 16 I=NY1,NY2
          DY(I)=WL/(NY2-NY1+1)
16   CONTINUE
*
      IF (GX.EQ.1) THEN
          DO 5 I=1,NX
              DX(I)=XLGTH/NX
5     CONTINUE
      ELSE
*
*
*   GRID REFINING IN X-DIRECTION
*
*
      PX=1
      DO 21 I=1,NX1-1
          PX1=N**I
          PX=PX+2*PX1
21    CONTINUE
      DX(NX1)=XLGTH/PX
      DO 22 I=NX1-1,1,-1
          DX(I)=DX(I+1)*2
```

```
22   CONTINUE
     DO 23 I=NX1+1,NX
        DX(I)=DX(I-1)*2
23   CONTINUE
    ENDIF
*_____
    IF (GZ.EQ.1) THEN
       DO 12 I=1,NZ
          DZ(I)=THK/NZ
12   CONTINUE
    ELSE
*_____
*
*   GRID REFINING IN Z-DIRECTION
*_____
      PZ=1
      DO 51 I=1,NZ1-1
         PZ1=N**I
         PZ=PZ+2*PZ1
51   CONTINUE
       DZ(NZ1)=THK/PZ
       DO 52 I=NZ1-1,1
          DZ(I)=DZ(I+1)*2
52   CONTINUE
       DO 53 I=NZ1+1,NZ
          DZ(I)=DZ(I-1)*2
53   CONTINUE
    ENDIF
*_____
* CALCULATION OF THE SWEPT VOLUME
*_____
      AS=0.0D0
      BS=0.0D0
      HS=0.0D0
      DO 4 I=MX,LX
        AS=AS+FM*DX(I)
 4  CONTINUE
      DO 57 I=MY,LY
        BS=BS+FM*DY(I)
57  CONTINUE
      DO 6 I=MZ,LZ
        HS=HS+FM*DZ(I)
 6  CONTINUE
      VS=AS*BS*HS
*_____
* WELL LOCATION IN X-DIRECTION
*_____
      XOO=0.D0
       IF(NX1.EQ.1) THEN
       XO=(DX(1)/2)*FM
       ELSE
      DO 111 I=1,NX1-1
         XOO=XOO+DX(I)
111 CONTINUE
```

```
      XO=(XOO+DX(NX1)/2)*FM
      ENDIF
*_____
      XSOO=0.D0
      IF(NX1.EQ.MX) THEN
      XSO=(DX(NX1)/2)*FM
      ELSE
      DO 121 I=MX,NX1-1
      XSOO=XSOO+DX(I)
  121 CONTINUE
      XSO=(XSOO+DX(NX1)/2)*FM
      ENDIF
*
*_____
* WELL LOCATION IN Z-DIRECTION
*_____
      ZOO=0.D0
      IF(NZ1.EQ.1) THEN
      ZO=(DZ(1)/2)*FM
      ELSE
      DO 112 I=1,NZ1-1
      ZOO=ZOO+DZ(I)
  112 CONTINUE
      ZO=(ZOO+DZ(NZ1)/2)*FM
      ENDIF
*_____
      ZSOO=0.D0
      IF(NZ1.EQ.MZ) THEN
      ZSO=(DZ(NZ1)/2)*FM
      ELSE
      DO 117 I=MZ,NZ1-1
      ZSOO=ZSOO+DZ(I)
  117 CONTINUE
      ZSO=(ZSOO+DZ(NZ1)/2)*FM
      ENDIF
*_____
      YS1=0.D0
      IF(NY1.EQ.MY) THEN
      YS1=0.D0
      ELSE
      DO 118 I=MY,NY1-1
      YS1=YS1+DY(I)*FM
  118 CONTINUE
      ENDIF
*_____
      YS3=0.D0
      IF(NY2.EQ.LY) THEN
      YS3=0.D0
      ELSE
      DO 119 I=NY2+1,LY
      YS3=YS3+DY(I)*FM
  119 CONTINUE
      YS2=BS-YS3
      ENDIF
```

```
*_____
*
* DIMENSIONLESS VARIABLES
*_____
          XY=SQRT(PRMX1/PRMY1)
          XZ=SQRT(PRMX1/PRMZ1)
          AD=XLGTH/WL
          ASD=AS/WL1
          BD=(WDTH/WL)*XY
          BSD=(BS/WL1)*XY
          HD=(THK/WL)*XZ
          HSD=(HS/WL1)*XZ
          XOD=XO/WL1
          ZOD=(ZO/WL1)*XZ
          XSOD=XSO/WL1
          ZSOD=(ZSO/WL1)*XZ
          Y1D=(Y1/WL)*XY
          Y2D=(Y2/WL)*XY
          XLD=Y2D-Y1D
          YS1D=(YS1/WL1)*XY
          YS2D=(YS2/WL1)*XY
      D1ZD=MIN(ZSOD,(HSD-ZSOD))
      D2ZD=HSD-D1ZD
      D1YD=MIN(YS1D,(BSD-YS2D))
      D2YD=MAX(YS1D,(BSD-YS2D))
      D1XD=MIN(XSOD,(ASD-XSOD))
      D2XD=ASD-D1XD
*_____
          ALPHA=3790.85D0*POR1*VIS11*CMP11*(AS*BS)/(APX1*SRP)
          PD1=0.00708D0*HS*APX1*SRP/(FVF1*VIS11*RTE11)
*_____
* TIME CRITERIA FOR THE RESERVOIR
*_____
      EER2=MIN(0.25D0*D1ZD**2,0.033D0*XLD**2)
      SEL2=0.6D0*D2ZD**2
      EEL2=0.02D0*XLD**2
      SLS2=0.4D0*XLD**2
      ELS2=MIN(0.33D0*(D1YD+XLD/4)**2,0.27*D1XD**2)
      SLL2=MAX(0.88*D2YD**2,0.63*D2ZD**2)
      ELL2=0.162*D1XD**2
*         WRITE(8,1) EER2,SEL2,EEL2,SLS2,ELS2,SLL2,ELL2
*  1        FORMAT(2X,F6.2,2X,F6.2,2X,F6.2,2X,F6.2,2X,F6.2,
*   &          2X,F6.2,2X,F6.2)
*_____
* CALCULATION OF MOBILITY AND STORATIVITY RATIOS
*_____
      RM=(PRMX1*HS/VIS1)/(PRMX2*(THK1-HS)/VIS2)
      SR=(POR1*CMP1*HS)/(POR2*CMP2*(THK1-HS))
*_____
*FORMATING
*_____
         WRITE(8,*)
         IF(P.EQ.1) THEN
         WRITE(8,101)
```

```fortran
101    FORMAT(11X,'DT',16X,'PWF')
  ELSEIF(P.EQ.2) THEN
    WRITE(8,102)
102    FORMAT(11X,'DT',16X,'DP')
  ELSE
    WRITE(8,103)
103    FORMAT(11X,'DTDA',16X,'PWD')
  ENDIF
    WRITE(8,104)
104    FORMAT(7X,'-----------',6X,'-----------')
```
*_____
```fortran
   DO 30 K=1,NZ
   DO 30 J=1,NY
   DO 30 I=1,NX
          PRMX(I,J,K)=PRMX2
          PRMY(I,J,K)=PRMY2
          PRMZ(I,J,K)=PRMZ2
          POR(I,J,K)=POR2
          CMP(I,J,K)=CMP2
          VIS(I,J,K)=VIS2
          FVF(I,J,K)=FVF2
          PI(I,J,K)=10.D0
          RTE(I,J,K)=0.D0
 30 CONTINUE
```
*_____
```fortran
   DO 40 K=MZ,LZ
   DO 40 J=MY,LY
   DO 40 I=MX,LX
          PRMX(I,J,K)=PRMX1
          PRMY(I,J,K)=PRMY1
          PRMZ(I,J,K)=PRMZ1
          POR(I,J,K)=POR1
          CMP(I,J,K)=CMP1
          VIS(I,J,K)=VIS1
          FVF(I,J,K)=FVF1
 40 CONTINUE
```
*_____
```fortran
   DO 820 K=1,NZ
   DO 820 J=1,NY
   DO 820 I=1,NX
      ARAX(I,J,K)=DY(J)*DZ(K)
      ARAY(I,J,K)=DX(I)*DZ(K)
      ARAZ(I,J,K)=DX(I)*DY(J)
      VOLB(I,J,K)=DX(I)*DY(J)*DZ(K)
820 CONTINUE
```
*_____
```fortran
   DO 10 K=1,NZ
   DO 10 J=1,NY
   DO 10 I=1,NX
      IF (I.EQ.1) THEN
            TRMX1(I,J,K)=0.D0
      ELSE
         TRMX1(I,J,K)=2*ARAX(I,J,K)*ARAX(I-1,J,K)*
   &              PRMX(I,J,K)*PRMX(I-1,J,K)/((ARAX(I,J,K)*
```

```
      &                 PRMX(I,J,K)*DX(I-1)+ARAX(I-1,J,K)*
      &                 PRMX(I-1,J,K)*DX(I))*VIS(I-1,J,K))
          ENDIF
 10 CONTINUE
*_____
      DO 31 K=1,NZ
      DO 31 J=1,NY
      DO 31 I=1,NX
          IF (I.EQ.NX) THEN
                 TRMX2(I,J,K)=0.D0
          ELSE
             TRMX2(I,J,K)=2*ARAX(I,J,K)*ARAX(I+1,J,K)*
      &                 PRMX(I,J,K)*PRMX(I+1,J,K)/((ARAX(I,J,K)*
      &                 PRMX(I,J,K)*DX(I+1)+ARAX(I+1,J,K)*
      &                 PRMX(I+1,J,K)*DX(I))*VIS(I,J,K))
          ENDIF
 31 CONTINUE
*_____
      DO 32 K=1,NZ
      DO 32 J=1,NY
      DO 32 I=1,NX
          IF (J.EQ.i) THEN
                 TRMY1(I,J,K)=0.D0
          ELSE
             TRMY1(I,J,K)=2*ARAY(I,J,K)*ARAY(I,J-1,K)*
      &                 PRMY(I,J,K)*PRMY(I,J-1,K)/((ARAY(I,J,K)*
      &                 PRMY(I,J,K)*DY(J-1)+ARAY(I,J-1,K)*
      &                 PRMY(I,J-1,K)*DY(J))*VIS(I,J-1,K))
          ENDIF
 32 CONTINUE
*_____
      DO 33 K=1,NZ
      DO 33 J=1,NY
      DO 33 I=1,NX
          IF (J.EQ.NY) THEN
                 TRMY2(I,J,K)=0.D0
          ELSE
             TRMY2(I,J,K)=2*ARAY(I,J,K)*ARAY(I,J+1,K)*
      &                 PRMY(I,J,K)*PRMY(I,J+1,K)/((ARAY(I,J,K)*
      &                 PRMY(I,J,K)*DY(J+1)+ARAY(I,J+1,K)*
      &                 PRMY(I,J+1,K)*DY(J))*VIS(I,J,K))
          ENDIF
 33 CONTINUE
*_____
      DO 34 K=1,NZ
      DO 34 J=1,NY
      DO 34 I=1,NX
          IF (K.EQ.1) THEN
                 TRMZ1(I,J,K)=0.D0
          ELSE
             TRMZ1(I,J,K)=2*ARAZ(I,J,K)*ARAZ(I,J,K-1)*
      &                 PRMZ(I,J,K)*PRMZ(I,J,K-1)/((ARAZ(I,J,K)*
      &                 PRMZ(I,J,K)*DZ(K-1)+ARAZ(I,J,K-1)*
      &                 PRMZ(I,J,K-1)*DZ(K))*VIS(I,J,K-1))
```

```
        ENDIF
 34 CONTINUE
*_____
    DO 35 K=1,NZ
    DO 35 J=1,NY
    DO 35 I=1,NX
        IF (K.EQ.NZ) THEN
            TRMZ2(I,J,K)=0.D0
        ELSE
            TRMZ2(I,J,K)=2*ARAZ(I,J,K)*ARAZ(I,J,K+1)*
 &                  PRMZ(I,J,K)*PRMZ(I,J,K+1)/((ARAZ(I,J,K)*
 &                  PRMZ(I,J,K)*DZ(K+1)+ARAZ(I,J,K+1)*
 &                  PRMZ(I,J,K+1)*DZ(K))*VIS(I,J,K))
        ENDIF
 35 CONTINUE
*_____
    DO 830 K=1,NZ
    DO 830 J=1,NY
    DO 830 I=1,NX
            Z(I,J,K)=TRMZ1(I,J,K)
            B(I,J,K)=TRMY1(I,J,K)
            D(I,J,K)=TRMX1(I,J,K)
            F(I,J,K)=TRMX2(I,J,K)
            H(I,J,K)=TRMY2(I,J,K)
            S(I,J,K)=TRMZ2(I,J,K)
 830 CONTINUE
*_____
    VT=0.D0
    DO 45 J=NY1,NY2
            VT=VT+VOLB(NX1,J,NZ1)
 45 CONTINUE
*_____
    DO 46 J=NY1,NY2
            RTE(NX1,J,NZ1)=RTE1*VOLB(NX1,J,NZ1)/VT
*
            RADE(NX1,J,NZ1)=0.28D0*DSQRT(DSQRT(PRMZ(NX1,J,NZ1)/
 &              PRMX(NX1,J,NZ1))*(DX(NX1)**2)+
 &              DSQRT(PRMX(NX1,J,NZ1)/
 &              PRMZ(NX1,J,NZ1))*(DZ(NZ1)**2))/
 &              ((PRMZ(NX1,J,NZ1)/PRMX(NX1,J,NZ1))**
 &              0.25D0+(PRMX(NX1,J,NZ1)/PRMZ(NX1,J,NZ1))**
 &              0.25D0)
*
            PI(NX1,J,NZ1)=2*DACOS(-1.D0)*DSQRT(PRMX(NX1,J,NZ1)*
 &              PRMZ(NX1,J,NZ1))*DY(J)/(VIS(NX1,J,NZ1)*
 &              FVF(NX1,J,NZ1)*(DLOG(RADE(NX1,J,NZ1)/RW)))
 46 CONTINUE
*_____
*
        TIM=0.D0
        O=M
    JJ=0
    JJ1=KK
*
```

```fortran
      DO 50 II=1,NO
*
         IF (II.EQ.1) THEN
           DO 60 K=1,NZ
             DO 60 J=1,NY
             DO 60 I=1,NX
               PRSI(I,J,K)=PRSIB
 60        CONTINUE
           DELT=DELTB
         ENDIF
*_____
      DO 73 K=1,NZ
      DO 73 J=1,NY
      DO 73 I=1,NX
         IF (I.EQ.1) THEN
            CIX(I,J,K)=TRMX2(I,J,K)*(PRSI(I+1,J,K)-PRSI(I,J,K))
         ELSEIF (I.EQ.NX) THEN
            CIX(I,J,K)=-TRMX1(I,J,K)*(PRSI(I,J,K)-PRSI(I-1,J,K))
         ELSE
            CIX(I,J,K)=TRMX2(I,J,K)*(PRSI(I+1,J,K)-PRSI(I,J,K))-
     &         TRMX1(I,J,K)*(PRSI(I,J,K)-PRSI(I-1,J,K))
         ENDIF
         IF (J.EQ.1) THEN
            CIY(I,J,K)=TRMY2(I,J,K)*(PRSI(I,J+1,K)-PRSI(I,J,K))
         ELSEIF (J.EQ.NY) THEN
            CIY(I,J,K)=-TRMY1(I,J,K)*(PRSI(I,J,K)-PRSI(I,J-1,K))
         ELSE
            CIY(I,J,K)=TRMY2(I,J,K)*(PRSI(I,J+1,K)-PRSI(I,J,K))-
     &         TRMY1(I,J,K)*(PRSI(I,J,K)-PRSI(I,J-1,K))
         ENDIF
         IF (K.EQ.1) THEN
            CIZ(I,J,K)=TRMZ2(I,J,K)*(PRSI(I,J,K+1)-PRSI(I,J,K))
         ELSEIF (K.EQ.NZ) THEN
            CIZ(I,J,K)=-TRMZ1(I,J,K)*(PRSI(I,J,K)-PRSI(I,J,K-1))
         ELSE
            CIZ(I,J,K)=TRMZ2(I,J,K)*(PRSI(I,J,K+1)-PRSI(I,J,K))-
     &         TRMZ1(I,J,K)*(PRSI(I,J,K)-PRSI(I,J,K-1))
         ENDIF
            CI(I,J,K)=CIX(I,J,K)+CIY(I,J,K)+CIZ(I,J,K)
 73   CONTINUE
*_____
      DO 840 K=1,NZ
      DO 840 J=1,NY
      DO 840 I=1,NX
         AP(I,J,K)=VOLB(I,J,K)*POR(I,J,K)*CMP(I,J,K)/DELT
*
         E(I,J,K)=-(Z(I,J,K)+B(I,J,K)+D(I,J,K)+F(I,J,K)+
     &      H(I,J,K)+S(I,J,K)+AP(I,J,K))
*
         Q(I,J,K)=RTE(I,J,K)*FVF(I,J,K)-CI(I,J,K)
 840  CONTINUE
*_____
*
      DO 93 K=1,NZ
```

```
      DO 93 J=1,NY
      DO 93 I=1,NX
          DPI(I,J,K)=-1.1D0
93 CONTINUE
*  _____
7 DO 90 K=1,NZ
   DO 90 J=1,NY
   DO 89 I=1,NX
          DL(I)=D(I,J,K)
          EL(I)=E(I,J,K)
          FL(I)=F(I,J,K)
          IF(J.EQ.1) THEN
              P1=0.D0
      ELSE
              P1=DPI(I,J-1,K)
          ENDIF
          IF(J.EQ.NY) THEN
              P2=0.D0
      ELSE
              P2=DPI(I,J+1,K)
          ENDIF
          IF(K.EQ.1) THEN
              P3=0.D0
      ELSE
              P3=DPI(I,J,K-1)
          ENDIF
          IF(K.EQ.NZ) THEN
              P4=0.D0
      ELSE
              P4=DPI(I,J,K+1)
          ENDIF
          QL(I)=Q(I,J,K)-B(I,J,K)*P1-H(I,J,K)*
   &              P2-Z(I,J,K)*P3-S(I,J,K)*P4
89 CONTINUE
   W(1)=FL(1)/EL(1)
   DO 600 III=2,NX-1
       W(III)=FL(III)/(EL(III)-DL(III)*W(III-1))
600 CONTINUE
   G(1)=QL(1)/EL(1)
   DO 610 III=2,NX
   G(III)=(QL(III)-DL(III)*G(III-1))/(EL(III)-DL(III)*W(III-1))
610 CONTINUE
       DP(NX,J,K)=G(NX)
   DO 620 III=NX-1,1,-1
       DP(III,J,K)=G(III)-W(III)*DP(III+1,J,K)
620 CONTINUE
90    CONTINUE
   TOL=0.D0
   DO 630 K=1,NZ
   DO 630 J=1,NY
   DO 630 I=1,NX
       DTOL=ABS(DP(I,J,K)-DPI(I,J,K))
     IF(DTOL.GT.TOL) THEN
          TOL=DTOL
```

```
        ENDIF
630 CONTINUE
        IF(TOL.GT.TOLL) THEN
        DO 632 K=1,NZ
        DO 632 J=1,NY
        DO 632 I=1,NX
          DPI(I,J,K)=DP(I,J,K)
 632     CONTINUE
        GO TO 7
     ELSE
   DO 631 K=1,NZ
   DO 631 J=1,NY
   DO 631 I=1,NX
          PRS(I,J,K)=PRSI(I,J,K)+DP(I,J,K)
631 CONTINUE
     ENDIF
*_____
*
* MATERIAL BALANCE
*_____
   IF(MB.EQ.1) THEN
     XDMB=0.D0
     DO 633 K=1,NZ
     DO 633 J=1,NY
     DO 633 I=1,NX
        XDMB=XDMB+CMP(I,J,K)*VOLB(I,J,K)*POR(I,J,K)*DP(I,J,K)
 633  CONTINUE
     XNMB=FVF1*RTE1*DELT
     XMB=XNMB/XDMB
     PRINT*,XMB,TIM1
   ENDIF
*_____
        IF(II.EQ.1) THEN
          TIM=DELT
        ELSE
          TIM=TIM+DELT
        ENDIF
          TIM1=TIM/SH
*_____
          PRF1(O1,O2,O3)=PRS(O1,O2,O3)-RTE(O1,O2,O3)/PI(O1,O2,O3)
          PRF(O1,O2,O3)=PRF1(O1,O2,O3)/PP
          PRIS(O1,O2,O3)=PRSIB1-PRF(O1,O2,O3)
*_____
   IF(P.EQ.1) THEN
     IF(II.EQ.JJ1) THEN
          WRITE(8,9) TIM1,PRF(O1,O2,O3)
 9        FORMAT(2X,F13.5,4X,F15.5)
          JJ1=JJ1+KK
          JJ=JJ+1
     ENDIF
*_____
   ELSEIF(P.EQ.2) THEN
     IF(II.EQ.JJ1) THEN
          WRITE(8,49) TIM1,PRIS(O1,O2,O3)
```

```
49          FORMAT(2X,F13.7,4X,F13.7)
            JJ1=JJ1+KK
            JJ=JJ+1
         ENDIF
*
      ELSE
*_____
*DIMENSIONLESS TIME & PRESSURE
*_____
            TD=TIM1/ALPHA
            PD=PD1*PRIS(O1,O2,O3)
*_____
            IF(II.EQ.JJ1) THEN
               WRITE(8,39) TD,PD
39             FORMAT(2X,F15.9,4X,F15.9)
               JJ1=JJ1+KK
               JJ=JJ+1
            ENDIF
*_____
      ENDIF
*
      IF(II.GT.O) THEN
         DELTA=COUNT*DELTA
         O=O+M
      ENDIF
         IF(TIM1.GT.TIME1) GOTO 13
      DO 650 K=1,NZ
      DO 650 J=1,NY
      DO 650 I=1,NX
         PRSI(I,J,K)=PRS(I,J,K)
650   CONTINUE
         DELT=DELTA
50  CONTINUE
13        WRITE(8,3) JJ
3         FORMAT(5X,I4)
*
     STOP
     END
```

```
*
```

```
*           *                   PROGRAM 2
*
```

*THE PURPOSE OF THIS PROGRAM IS TO GENERATE PRESSURE   TRANSIENT
*RESPONSE FOR A HORIZONTAL WELL IN A MULTI-REGION COMPOSITE
*RESERVOIR.
*

```
*
```

```
*
```

* VARIABLE IDENTIFICATION
*

```
*
```

```
* NX          = NUMBER OF GRIDS IN X-DIRECTION
* NY          = NUMBER OF GRIDS IN Y-DIRECTION
* NZ          = NUMBER OF GRIDS IN Z-DIRECTION
* MX,MY,MZ= FIRST GRIDBLOCK NUMBER IN EACH DIRECTION
* LX,LY,LZ   = LAST GRIDBLOCK NUMBER IN EACH DIRECTION
* CMP21       = COMPRESSIBILITY IN THE UNSWEPT REGION
* VIS21       = VISCOSITY IN THE UNSWEPT REGION
* RW          = WELLBORE RADIUS
* PRSIB       = RESERVOIR INITIAL PRESSURE
* PRSI        = RESERVOIR IN THE PREVIOUS TIME STEP
* RT1         = TOTAL PRODUCTION RATE
* APX21       = ABSOLUTE PERMEABILITY IN X-DIRECTION OF THE
*                 UNSWEPT REGION
* APY21       = ABSOLUTE PERMEABILITY IN Y-DIRECTION OF THE
*                 UNSWEPT REGION
** APZ21      = ABSOLUTE PERMEABILITY IN Z-DIRECTION OF THE
*                 UNSWEPT REGION
* SRP         = STEAM RELATIVE PERMEABILITY
* ORP         = OIL RELATIVE PERMEABILITY
* XLGTH       = RESERVOIR LENGTH
* WDTH        = RESERVOIR WIDTH
* THK         = RESERVOIR THICKNESS
* WL          = WELL LENGTH
* VS          = SWEPT REGION VOLUME
* NREG        = NUMBER OF REGIONS
* DP          = PRESSURE DROP
* PRS         = BLOCK PRESSURE
* PRF         = WELLBLOCK PRESSURE
* PRIS        = WELLBLOCK PRESSURE DROP
* XMB         = MATERIAL BALANCE
* TIM         = TOTAL TIME
* TD          = DIMENSIONLESS TIME
* PD          = DIMENSIONLESS PRESSURE
*
```

```
*
```

```
*
      IMPLICIT REAL*8(A-H,O-Z)
      DIMENSION ARAX(45,45,45),ARAY(45,45,45),ARAZ(45,45,45),
     &   VOLB(45,45,45),DPH(45,45,45),DL(20000),EL(20000),FL(20000),
     &   W(20000),G(20000),DPI(45,45,45),ZK(45,45,45),ZK1(45,45,45),
```

```
&    DX(45),DY(45),DZ(45),QL(20000),UL(20000),PRF1(45,45,45),
&    CI(45,45,45),Q(45,45,45),PRIS(45,45,45),FVF(45,45,45),
&    RTE(45,45,45),RADE(45,45,45),PRM(45,45,45),PI(45,45,45),
&    PRS(45,45,45),PRSI(45,45,45),DP(45,45,45),
&    PRF(45,45,45),CIX(45,45,45),CIY(45,45,45),CIZ(45,45,45)
DIMENSION PRMX(45,45,45),PRMY(45,45,45),PRMZ(45,45,45),
&    TRMX1(45,45,45),TRMX2(45,45,45),TRMY1(45,45,45),
&    TRMY2(45,45,45),TRMZ1(45,45,45),TRMZ2(45,45,45),
&    AP(45,45,45),E(45,45,45),Z(45,45,45),B(45,45,45),
&    D(45,45,45),F(45,45,45),H(45,45,45),S(45,45,45),
&    POR(45,45,45),CMP(45,45,45),VIS(45,45,45),CK(10),
&    MX(10),LX(10),MZ(10),LZ(10),AS(10),BS(10),HS(10),
&    VS(10),VK(10),R(10),PRS1(45,45,45)
*
* READING THE VALUES
*
      OPEN(5,FILE='m3.d')
      OPEN(8,FILE='m3.o')
*
      PRINT *
      READ(5,*) NX,NY,NZ
      READ(5,*) O1,O2,O3
      READ(5,*) MX1,LX1
      READ(5,*) MY,LY
      READ(5,*) MZ1,LZ1
      READ(5,*) NY1,NY2
      READ(5,*) NX1,NZ1
      READ(5,*) NREG,NST,MR,NR
      READ(5,*) RM1,RM2
      READ(5,*) RM3,RM4
      READ(5,*) X11,X21
      READ(5,*) Z11,Z21
      READ(5,*) P,KK
      READ(5,*) MB,TOLL
      READ(5,*) CMP21,VIS21,FVF2
      READ(5,*) POR2,RW1
      READ(5,*) PRSIB1,RTE11
      READ(5,*) NO,M,COUNT
      READ(5,*) TIME1,DELTA1,DELTB1
      READ(5,*) APX2,APY2,APZ2
      READ(5,*) XLGTH1,WDTH1,THK1,WL1
*
* CONVERSION FACTORS
*
      FM=3.28084D0
      PP=6894.76D0
      SH=3600
      DM=1.013E15
      DB=543439.6D0
*
* CONVERTING FROM FIELD UNITS TO SI UNITS
*
      VIS2=VIS21/1000
      RW=RW1/FM
```

```
      X1=X11/FM
      X2=X21/FM
      Z1=Z11/FM
      Z2=Z21/FM
      CMP2=CMP21/PP
      PRSIB=PRSIB1*PP
      DELTA=DELTA1*SH
      DELTB=DELTB1*SH
      TIME=TIME1*SH
      PRMX2=APX2/DM
      PRMY2=APY2/DM
      PRMZ2=APZ2/DM
      RTE1=RTE11/DB
      XLGTH=XLGTH1/FM
      WDTH=WDTH1/FM
      THK=THK1/FM
      WL=WL1/FM
*_____
*FORMATING
*_____
      WRITE(8,*)
      IF(P.EQ.1) THEN
      WRITE(8,101)
 101    FORMAT(11X,'DT',16X,'PWF')
      ELSEIF(P.EQ.2) THEN
      WRITE(8,102)
 102    FORMAT(11X,'DT',16X,'DP')
      ELSE
      WRITE(8,103)
 103    FORMAT(11X,'DTD',16X,'PWD')
      ENDIF
      WRITE(8,104)
 104    FORMAT(7X,'------------',6X,'------------')
*_____
* UNIFORM GRID
*_____
      DO 11 I=1,NY
         DY(I)=(WDTH-WL)/(NY-(NY2-NY1+1))
 11  CONTINUE
      DO 16 I=NY1,NY2
         DY(I)=WL/(NY2-NY1+1)
 16   CONTINUE
*_____
      DO 30 K=1,NZ
      DO 30 J=1,NY
      DO 30 I=1,NX
            PRMX(I,J,K)=PRMX2
            PRMY(I,J,K)=PRMY2
            PRMZ(I,J,K)=PRMZ2
            POR(I,J,K)=POR2
            CMP(I,J,K)=CMP2
            VIS(I,J,K)=VIS2
            FVF(I,J,K)=FVF2
            PI(I,J,K)=10.D0
```

```
              RTE(I,J,K)=0.D0
30  CONTINUE
*_____
    IF(NREG.GE.3) THEN
    MX(NREG)=1
    MZ(NREG)=1
    LX(NREG)=NX
    LZ(NREG)=NZ
    DO 311 I1=NREG-1,1,-1
        MX(I1)=MX(I1+1)+NST
        MZ(I1)=MZ(I1+1)+NST
        LX(I1)=LX(I1+1)-NST
        LZ(I1)=LZ(I1+1)-NST
    IF(I1.EQ.1) THEN
    DO 41 K=MZ(I1),LZ(I1)
    DO 41 J=MY,LY
    DO 41 I=MX(I1),LX(I1)
        VIS(I,J,K)=VIS2/MR
        CMP(I,J,K)=CMP2*NR
41  CONTINUE
        VK(I1)=1
        CK(I1)=1
    ELSE
    DO 40 K=MZ(I1),LZ(I1)
    DO 40 J=MY,LY
    DO 40 I=MX(I1),LX(I1)
        VIS(I,J,K)=(VIS2/MR)*(RM1+(I1-2)*RM2)
        CMP(I,J,K)=CMP2*NR/(RM3+(I1-2)*RM4)
40  CONTINUE
        VK(I1)=RM1+(I1-2)*RM2
        CK(I1)=RM3+(I1-2)*RM4
    ENDIF
311 CONTINUE
    VK(NREG)=VIS(NX,NY,NZ)/VIS(O1,O2,O3)
    CK(NREG)=CMP(O1,O2,O3)/CMP(NX,NY,NZ)
*_____
    DX(NX)=X2/2
    DX(1)=X2/2
    DO 91 I=2,NX 1
    IF(I.GE.MX ).AND.I.LE.LX(1)) THEN
        DX(I)=X1/(LX(1)-MX(1)+1)
    ELSE
        DX(I)=(XLGTH-X2-X1)/(NX-(LX(1)-MX(1)+1+2*NST))
    ENDIF
91  CONTINUE
*_____
    DZ(NZ)=Z2/2
    DZ(1)=Z2/2
    DO 92 I=2,NZ-1
    IF(I.GE.MZ(1).AND.I.LE.LZ(1)) THEN
        DZ(I)=Z1/(LZ(1)-MZ(1)+1)
    ELSE
        DZ(I)=(THK-Z2-Z1)/(NZ-(LZ(1)-MZ(1)+1+2*NST))
    ENDIF
```

```
 92 CONTINUE
*_____
* CALCULATION OF THE SWEPT VOLUME
*_____
    DO 312 I1=1,NREG
      AS(I1)=0.0D0
      BS(I1)=0.0D0
      HS(I1)=0.0D0
      DO 4 I=MX(I1),LX(I1)
        AS(I1)=AS(I1)+FM*DX(I)
 4    CONTINUE
      DO 57 I=MY,LY
        BS(I1)=BS(I1)+FM*DY(I)
 57   CONTINUE
      DO 58 I=MZ(I1),LZ(I1)
        HS(I1)=HS(I1)+FM*DZ(I)
 58   CONTINUE
      VS(I1)=AS(I1)*BS(I1)*HS(I1)
      PRINT*,VK(I1),CK(I1)
312 CONTINUE
    ELSE
      DO 71 K=MZ1,LZ1
      DO 71 J=MY,LY
      DO 71 I=MX1,LX1
        VIS(I,J,K)=VIS2/MR
        CMP(I,J,K)=CMP2*NR
 71   CONTINUE
    ENDIF
*_____
      ALPHA=APX2/(3790.85D0*POR2*(VIS21/MR)*CMP21*NR*
   &       AS(NREG-1)*BS(NREG-1))
      PD1=0.00708*HS(NREG-1)*APX2/(FVF2*(VIS21/MR)*RTE11)
*_____
    DO 820 K=1,NZ
    DO 820 J=1,NY
    DO 820 I=1,NX
      ARAX(I,J,K)=DY(J)*DZ(K)
      ARAY(I,J,K)=DX(I)*DZ(K)
      ARAZ(I,J,K)=DX(I)*DY(J)
        VOLB(I,J,K)=DX(I)*DY(J)*DZ(K)
820 CONTINUE
*_____
    DO 10 K=1,NZ
    DO 10 J=1,NY
    DO 10 I=1,NX
      IF (I.EQ.1) THEN
            TRMX1(I,J,K)=0.D0
      ELSE
        TRMX1(I,J,K)=2*ARAX(I,J,K)*ARAX(I-1,J,K)*
   &          PRMX(I,J,K)*PRMX(I-1,J,K)/((ARAX(I,J,K)*
   &          PRMX(I,J,K)*DX(I-1)+ARAX(I-1,J,K)*
   &          PRMX(I-1,J,K)*DX(I))*VIS(I-1,J,K))
      ENDIF
 10 CONTINUE
```

```
*_____
      DO 31 K=1,NZ
      DO 31 J=1,NY
      DO 31 I=1,NX
         IF (I.EQ.NX) THEN
               TRMX2(I,J,K)=0.D0
         ELSE
            TRMX2(I,J,K)=2*ARAX(I,J,K)*ARAX(I+1,J,K)*
      &               PRMX(I,J,K)*PRMX(I+1,J,K)/((ARAX(I,J,K)*
      &               PRMX(I,J,K)*DX(I+1)+ARAX(I+1,J,K)*
      &               PRMX(I+1,J,K)*DX(I))*VIS(I,J,K))
         ENDIF
   31 CONTINUE
*_____
      DO 32 K=1,NZ
      DO 32 J=1,NY
      DO 32 I=1,NX
         IF (J.EQ.1) THEN
               TRMY1(I,J,K)=0.D0
         ELSE
            TRMY1(I,J,K)=2*ARAY(I,J,K)*ARAY(I,J-1,K)*
      &               PRMY(I,J,K)*PRMY(I,J-1,K)/((ARAY(I,J,K)*
      &               PRMY(I,J,K)*DY(J-1)+ARAY(I,J-1,K)*
      &               PRMY(I,J-1,K)*DY(J))*VIS(I,J-1,K))
         ENDIF
   32 CONTINUE
*_____
      DO 33 K=1,NZ
      DO 33 J=1,NY
      DO 33 I=1,NX
         IF (J.EQ.NY) THEN
               TRMY2(I,J,K)=0.D0
         ELSE
            TRMY2(I,J,K)=2*ARAY(I,J,K)*ARAY(I,J+1,K)*
      &               PRMY(I,J,K)*PRMY(I,J+1,K)/((ARAY(I,J,K)*
      &               PRMY(I,J,K)*DY(J+1)+ARAY(I,J+1,K)*
      &               PRMY(I,J+1,K)*DY(J))*VIS(I,J,K))
         ENDIF
   33 CONTINUE
*_____
      DO 34 K=1,NZ
      DO 34 J=1,NY
      DO 34 I=1,NX
         IF (K.EQ.1) THEN
               TRMZ1(I,J,K)=0.D0
         ELSE
            TRMZ1(I,J,K)=2*ARAZ(I,J,K)*ARAZ(I,J,K-1)*
      &               PRMZ(I,J,K)*PRMZ(I,J,K-1)/((ARAZ(I,J,K)*
      &               PRMZ(I,J,K)*DZ(K-1)+ARAZ(I,J,K-1)*
      &               PRMZ(I,J,K-1)*DZ(K))*VIS(I,J,K-1))
         ENDIF
   34 CONTINUE
*_____
      DO 35 K=1,NZ
```

```
      DO 35 J=1,NY
      DO 35 I=1,NX
         IF (K.EQ.NZ) THEN
               TRMZ2(I,J,K)=0.D0
         ELSE
            TRMZ2(I,J,K)=2*ARAZ(I,J,K)*ARAZ(I,J,K+1)*
     &               PRMZ(I,J,K)*PRMZ(I,J,K+1)/((ARAZ(I,J,K)*
     &               PRMZ(I,J,K)*DZ(K+1)+ARAZ(I,J,K+1)*
     &               PRMZ(I,J,K+1)*DZ(K))*VIS(I,J,K))
         ENDIF
   35 CONTINUE
*_____
      DO 830 K=1,NZ
      DO 830 J=1,NY
      DO 830 I=1,NX
            Z(I,J,K)=TRMZ1(I,J,K)
            B(I,J,K)=TRMY1(I,J,K)
            D(I,J,K)=TRMX1(I,J,K)
            F(I,J,K)=TRMX2(I,J,K)
            H(I,J,K)=TRMY2(I,J,K)
            S(I,J,K)=TRMZ2(I,J,K)
  830 CONTINUE
*_____
*_____
      VT=0.D0
      DO 45 J=NY1,NY2
         VT=VT+VOLB(NX1,J,NZ1)
   45 CONTINUE
*_____
      DO 46 J=NY1,NY2
         RTE(NX1,J,NZ1)=RTE1*VOLB(NX1,J,NZ1)/VT
*
         RADE(NX1,J,NZ1)=0.28D0*DSQRT(DSQRT(PRMZ(NX1,J,NZ1)/
     &         PRMX(NX1,J,NZ1))*(DX(NX1)**2)+
     &         DSQRT(PRMX(NX1,J,NZ1)/
     &         PRMZ(NX1,J,NZ1))*(DZ(NZ1)**2))/
     &         ((PRMZ(NX1,J,NZ1)/PRMX(NX1,J,NZ1))**
     &         0.25D0+(PRMX(NX1,J,NZ1)/PRMZ(NX1,J,NZ1))**
     &         0.25D0)
*
         PI(NX1,J,NZ1)=2*DACOS(-1.D0)*DSQRT(PRMX(NX1,J,NZ1)*
     &         PRMZ(NX1,J,NZ1))*DY(J)/(VIS(NX1,J,NZ1)*
     &         FVF(NX1,J,NZ1)*(DLOG(RADE(NX1,J,NZ1)/RW)))
   46 CONTINUE
*_____
*
      TIM=0.D0
      O=M
      JJ=0
      JJ1=KK
*
      DO 50 II=1,NO
*
         IF (II.EQ.1) THEN
```

```
              DO 60 K=1,NZ
                DO 60 J=1,NY
                  DO 60 I=1,NX
                    PRSI(I,J,K)=PRSIB
   60         CONTINUE
              DELT=DELTB
              ENDIF
*_____
      DO 73 K=1,NZ
      DO 73 J=1,NY
      DO 73 I=1,NX
              IF (I.EQ.1) THEN
                  CIX(I,J,K)=TRMX2(I,J,K)*(PRSI(I+1,J,K)-PRSI(I,J,K))
              ELSEIF (I.EQ.NX) THEN
                  CIX(I,J,K)=-TRMX1(I,J,K)*(PRSI(I,J,K)-PRSI(I-1,J,K))
              ELSE
                  CIX(I,J,K)=TRMX2(I,J,K)*(PRSI(I+1,J,K)-PRSI(I,J,K))-
     &              TRMX1(I,J,K)*(PRSI(I,J,K)-PRSI(I-1,J,K))
              ENDIF
              IF (J.EQ.1) THEN
                  CIY(I,J,K)=TRMY2(I,J,K)*(PRSI(I,J+1,K)-PRSI(I,J,K))
              ELSEIF (J.EQ.NY) THEN
                  CIY(I,J,K)=-TRMY1(I,J,K)*(PRSI(I,J,K)-PRSI(I,J-1,K))
              ELSE
                  CIY(I,J,K)=TRMY2(I,J,K)*(PRSI(I,J+1,K)-PRSI(I,J,K))-
     &              TRMY1(I,J,K)*(PRSI(I,J,K)-PRSI(I,J-1,K))
              ENDIF
              IF (K.EQ.1) THEN
                  CIZ(I,J,K)=TRMZ2(I,J,K)*(PRSI(I,J,K+1)-PRSI(I,J,K))
              ELSEIF (K.EQ.NZ) THEN
                  CIZ(I,J,K)=-TRMZ1(I,J,K)*(PRSI(I,J,K)-PRSI(I,J,K-1))
              ELSE
                  CIZ(I,J,K)=TRMZ2(I,J,K)*(PRSI(I,J,K+1)-PRSI(I,J,K))-
     &              TRMZ1(I,J,K)*(PRSI(I,J,K)-PRSI(I,J,K-1))
              ENDIF
              CI(I,J,K)=CIX(I,J,K)+CIY(I,J,K)+CIZ(I,J,K)
   73 CONTINUE
*_____
      DO 840 K=1,NZ
      DO 840 J=1,NY
      DO 840 I=1,NX
              AP(I,J,K)=VOLB(I,J,K)*POR(I,J,K)*CMP(I,J,K)/DELT
*
              E(I,J,K)=-(Z(I,J,K)+B(I,J,K)+D(I,J,K)+F(I,J,K)+
     &              H(I,J,K)+S(I,J,K)+AP(I,J,K))
*
              Q(I,J,K)=RTE(I,J,K)*FVF(I,J,K)-CI(I,J,K)
  840 CONTINUE
*_____
*
      DO 93 K=1,NZ
      DO 93 J=1,NY
      DO 93 I=1,NX
              DPI(I,J,K)=-1.1D0
```

```
 93 CONTINUE
*_____
  7 DO 90 K=1,NZ
    DO 90 J=1,NY
      DO 89 I=1,NX
            DL(I)=D(I,J,K)
            EL(I)=E(I,J,K)
            FL(I)=F(I,J,K)
            IF(J.EQ.1) THEN
                  P1=0.D0
          ELSE
                  P1=DPI(I,J-1,K)
          ENDIF
            IF(J.EQ.NY) THEN
                  P2=0.D0
          ELSE
                  P2=DPI(I,J+1,K)
          ENDIF
            IF(K.EQ.1) THEN
                  P3=0.D0
          ELSE
                  P3=DPI(I,J,K-1)
          ENDIF
            IF(K.EQ.NZ) THEN
                  P4=0.D0
          ELSE
                  P4=DPI(I,J,K+1)
          ENDIF
                  QL(I)=Q(I,J,K)-B(I,J,K)*P1-H(I,J,K)*
     &                  P2-Z(I,J,K)*P3-S(I,J,K)*P4
 89 CONTINUE
    W(1)=FL(1)/EL(1)
    DO 600 III=2,NX-1
        W(III)=FL(III)/(EL(III)-DL(III)*W(III-1))
600 CONTINUE
    G(1)=QL(1)/EL(1)
    DO 610 III=2,NX
    G(III)=(QL(III)-DL(III)*G(III-1))/(EL(III)-DL(III)*W(III-1))
610 CONTINUE
        DP(NX,J,K)=G(NX)
    DO 620 III=NX-1,1,-1
        DP(III,J,K)=G(III)-W(III)*DP(III+1,J,K)
620 CONTINUE
90    CONTINUE
    TOL=0.D0
    DO 630 K=1,NZ
    DO 630 J=1,NY
    DO 630 I=1,NX
        DTOL=ABS(DP(I,J,K)-DPI(I,J,K))
      IF(DTOL.GT.TOL) THEN
          TOL=DTOL
      ENDIF
630 CONTINUE
        IF(TOL.GT.TOLL) THEN
```

```fortran
      DO 632 K=1,NZ
      DO 632 J=1,NY
      DO 632 I=1,NX
         DPI(I,J,K)=DP(I,J,K)
632      CONTINUE
      GO TO 7
      ELSE
      DO 631 K=1,NZ
      DO 631 J=1,NY
      DO 631 I=1,NX
         PRS(I,J,K)=PRSI(I,J,K)+DP(I,J,K)
631 CONTINUE
      ENDIF
*_____
* MATERIAL BALANCE
*_____
      IF(MB.EQ.1) THEN
      XDMB=0.D0
      DO 633 K=1,NZ
      DO 633 J=1,NY
      DO 633 I=1,NX
         XDMB=XDMB+CMP(I,J,K)*VOLB(I,J,K)*POR(I,J,K)*DP(I,J,K)
633   CONTINUE
      XNMB=FVF2*RTE1*DELT
      XMB=XNMB/XDMB
      PRINT*,XMB,TIM1
      ENDIF
*_____
      IF(II.EQ.1) THEN
      TIM=DELT
      ELSE
      TIM=TIM+DELT
      ENDIF
      TIM1=TIM/SH
*_____
      PRF1(O1,O2,O3)=PRS(O1,O2,O3)-RTE(O1,O2,O3)/PI(O1,O2,O3)
      PRF(O1,O2,O3)=PRF1(O1,O2,O3)/PP
      PRIS(O1,O2,O3)=PRSIB1-PRF(O1,O2,O3)
*_____
      IF(P.EQ.1) THEN
      IF(II.EQ.JJ1) THEN
         WRITE(8,9) TIM1,PRF(O1,O2,O3)
9        FORMAT(2X,F13.5,4X,F15.5)
      JJ1=JJ1+KK
      JJ=JJ+1
      ENDIF
*_____
      ELSEIF(P.EQ.2) THEN
      IF(II.EQ.JJ1) THEN
         WRITE(8,49) TIM1,PRIS(O1,O2,O3)
49       FORMAT(2X,F13.7,4X,F9.3)
      JJ1=JJ1+KK
      JJ=JJ+1
      ENDIF
```

```
*_____
      ELSE
*_____
*DIMENSIONLESS TIME & PRESSURE
*_____
            TD=TIM1*ALPHA
            PD=PD1*PRIS(O1,O2,O3)
*_____
            IF(II.EQ.JJ1) THEN
                WRITE(8,39) TD,PD
   39           FORMAT(2X,F15.5,4X,F15.9)
            JJ1=JJ1+KK
            JJ=JJ+1
            ENDIF
*_____
      ENDIF
*
      IF(II.GT.O) THEN
          DELTA=COUNT*DELTA
          O=O+M
      ENDIF
          IF(TIM1.GT.TIME1) GOTO 13
      DO 650 K=1,NZ
      DO 650 J=1,NY
      DO 650 I=1,NX
          PRSI(I,J,K)=PRS(I,J,K)
  650   CONTINUE
          DELT=DELTA
   50 CONTINUE
   13     WRITE(8,3) JJ
    3     FORMAT(5X,I4)
*_____
      STOP
      END
```

APPENDIX B

Transient Pressure Response for a Two-Region Composite Reservoir with a Horizontal Well

Input Data

as_D	= 2.0	k_{x1}	= 200.0
bs_D	= 2.0	k_{y1}	= 200.0
hs_D	= 4.0	k_{z1}	= 20.0
a_D	= 4.0	k_{x2}	= 20.0
b_D	= 2.0	k_{y2}	= 20.0
h_D	= 6.0	k_{z2}	= 2.00
L_D	= 1.0	L/b	= 0.50

Output

Δt, Hrs	t_D	Δp, Psia	p_{wD}	$dp_{wD}/d\ln t_D$	dp_{wD}/dt_D
0.03500	0.0030776	117.78	2.8531	0.69959	233.98
0.03600	0.0031655	118.55	2.8724	0.69952	227.27
0.03700	0.0032534	119.30	2.8911	0.69976	221.02
0.03800	0.0033414	120.03	2.9093	0.69972	215.10
0.03900	0.0034293	120.73	2.9270	0.69953	209.38
0.04000	0.0035172	121.42	2.9443	0.69951	204.00
0.04100	0.0036052	122.09	2.9610	0.69911	198.78
0.04200	0.0036931	122.74	2.9773	0.69866	193.80
0.04300	0.0037810	123.38	2.9932	0.69805	189.02
0.04400	0.0038690	124.00	3.0087	0.69744	184.46
0.04500	0.0039569	124.60	3.0238	0.69712	180.18
0.04600	0.0040448	125.19	3.0386	0.69630	175.97
0.04700	0.0041328	125.77	3.0530	0.69571	171.99
0.04800	0.0042207	126.33	3.0670	0.69508	168.18
0.04900	0.0043086	126.88	3.0808	0.69445	164.52
0.05000	0.0043966	127.42	3.0942	0.69380	161.01
0.05100	0.0044845	127.95	3.1073	0.69293	157.59
0.05200	0.0045724	128.46	3.1202	0.69232	154.40

0.05300	0.0046603	128.97	3.1328	0.69169	151.29
0.05400	0.0047483	129.46	3.1451	0.69080	148.24
0.05500	0.0048362	129.95	3.1571	0.69010	145.35
0.05600	0.0049241	130.42	3.1689	0.68927	142.53
0.05700	0.0050121	130.88	3.1805	0.68864	139.85
0.05800	0.0051000	131.34	3.1918	0.68780	137.23
0.05900	0.0051879	131.79	3.2030	0.68691	134.69
0.06000	0.0052759	132.23	3.2139	0.68622	132.27
0.06100	0.0053638	132.66	3.2246	0.68542	129.91
0.06200	0.0054517	133.08	3.2351	0.68461	127.63
0.06300	0.0055397	133.50	3.2454	0.68377	125.42
0.06400	0.0056276	133.90	3.2555	0.68291	123.27
0.06500	0.0057155	134.30	3.2655	0.68224	121.22
0.06600	0.0058034	134.70	3.2752	0.68131	119.19
0.06700	0.0058914	135.09	3.2848	0.68050	117.27
0.06800	0.0059793	135.47	3.2943	0.67971	115.38
0.06900	0.0060672	135.84	3.3036	0.67889	113.55
0.07000	0.0061552	136.21	3.3127	0.67808	111.77
0.07100	0.0062431	136.57	3.3217	0.67719	110.02
0.07200	0.0063310	136.93	3.3305	0.67642	108.35
0.07300	0.0064190	137.28	3.3392	0.67566	106.72
0.07400	0.0065069	137.63	3.3478	0.67474	105.12
0.07500	0.0065948	137.97	3.3562	0.67397	103.58
0.07600	0.0066828	138.30	3.3645	0.67313	102.07
0.07700	0.0067707	138.63	3.3727	0.67239	100.61
0.07800	0.0068586	138.96	3.3808	0.67155	99.180
0.07900	0.0069466	139.28	3.3887	0.67067	97.780
0.08000	0.0070345	139.59	3.3965	0.66994	96.436
0.08100	0.0071224	139.91	3.4042	0.66915	95.131
0.08200	0.0072103	140.21	3.4119	0.66833	93.840
0.08300	0.0072983	140.52	3.4194	0.66754	92.585
0.08400	0.0073862	140.82	3.4268	0.66671	91.355
0.08500	0.0074741	141.11	3.4341	0.66602	90.174
0.08600	0.0075621	141.40	3.4413	0.66518	88.999
0.08700	0.0076500	141.69	3.4484	0.66440	87.860
0.08800	0.0077379	141.97	3.4554	0.66365	86.752
0.08900	0.0078259	142.25	3.4623	0.66288	85.665
0.09000	0.0079138	142.53	3.4691	0.66213	84.607
0.09100	0.0080017	142.80	3.4759	0.66134	83.566
0.09200	0.0080897	143.07	3.4825	0.66061	82.556
0.09300	0.0081776	143.34	3.4891	0.65991	81.571
0.09400	0.0082655	143.60	3.4956	0.65909	80.593

APPENDIX C

Development of an Expression for the Constant Value of the Dimensionless Cartesian Pressure Derivative During the Pseudosteady-state Period

This appendix presents the development of an expression to demonstrate the relationship between the dimensionless Cartesian pressure derivative response and the dimensionless time based on the swept region area for the pseudosteady-state flow regime corresponding to the swept region.

Depending on the geometry of any closed reservoir, the dimensionless Cartesiar pressure derivative versus dimensionless time, on a log-log scale, has a constant value for the pseudosteady-state flow period corresponding to the swept region. For closed circular reservoirs, this value happens to be 2π. By using the basic definition of compressibility and the definitions used for the dimensionless variables in Chapter 4, a constant value for the Cartesian pressure derivative during the pseudosteady-state flow period in a closed rectangular reservoir can be calculated as follows:

$$c_t = -\frac{1}{v}\frac{dv}{dp} \qquad\qquad (C\text{-}1)$$

where

$$v = \phi A_s h_s \qquad\qquad (C\text{-}2)$$

and

$$dv = \beta q dt \qquad\qquad (C\text{-}3)$$

By rearranging Equations 4.28 and 4.29:

$$dt = \frac{3790.85\phi\mu c_t A_s}{k_{xl}} t_{DA} \tag{C-4}$$

By rearranging Equation 4.30:

$$dp = \frac{\mu\beta q}{0.00708\ k_{xl}h_s} p_{wD} \tag{C-5}$$

By rearranging Equation (C-1):

$$c_t v dp = -dv \tag{C-6}$$

To account properly for the units, q should be converted to ft^3/hr from STB/day. Therefore, Equation (C-3) becomes:

$$dv = \beta q(STB/D)*\frac{5.614ft^3/D}{STB/D}*\frac{D}{24\ Hrs} = 0.234\ \beta q dt \tag{C-7}$$

Substituting Equations (C-5) and (C-7) into Equation (C-6) and simplifying;

$$p_{wD} = (3790.85)*(0.00708)*\frac{(5.614)}{24} t_{DA} \tag{C-8}$$

and

$$p_{wD} = 6.28\ t_{DA} = 2\pi t_{DA} \tag{C-9}$$